

T-4377

THE PREPARATION, CHARACTERIZATION AND TESTING OF CATALYSTS
FOR USE IN THE HYDROTREATMENT OF MODEL LIGNIN FEEDSTOCKS

by

Xianghong Zhao

ARTHUR LAKES LIBRARY
COLORADO SCHOOL OF MINES
GOLDEN, CO 80401

ProQuest Number: 10796560

All rights reserved

INFORMATION TO ALL USERS

The quality of this reproduction is dependent upon the quality of the copy submitted.

In the unlikely event that the author did not send a complete manuscript and there are missing pages, these will be noted. Also, if material had to be removed, a note will indicate the deletion.



ProQuest 10796560

Published by ProQuest LLC (2019). Copyright of the Dissertation is held by the Author.

All rights reserved.

This work is protected against unauthorized copying under Title 17, United States Code
Microform Edition © ProQuest LLC.

ProQuest LLC.
789 East Eisenhower Parkway
P.O. Box 1346
Ann Arbor, MI 48106 – 1346

T-4377

A thesis submitted to the Faculty and the Board of Trustees of the Colorado School of Mines in partial fulfillment of the requirements for the degree of Doctor of Philosophy in Applied Chemistry.

Golden, Colorado

Date Aug. 27, 1993

Signed: Xianghong Zhao
Xianghōng Zhao

Approved: Scott W. Cowley
Dr. Scott W. Cowley
Thesis Advisor

Golden, Colorado

Date Aug. 27, 1993

Approved: Stephen R. Daniel
Dr. Stephen R. Daniel
Department Head
Chemistry and Geochemistry

ABSTRACT

Three kinds of catalyst, Pt/SiO₂-Al₂O₃, Pt/AlPO₄-Al₂O₃ and Ni/SiO₂-Al₂O₃ were prepared and tested. The results show that model lignin compounds and a mixture of model lignin compounds were successfully converted into phenolic products using a Pt/SiO₂-Al₂O₃ catalyst. Phosphate or silica provide a good acidity function, which is necessary for dealkylation. High reaction temperatures also assists dealkylation. Platinum has a good hydrogenation function which reduces transalkylation. Low pressures reduce deoxygenation. Pt/SiO₂-Al₂O₃ catalyst shows the best phenol yields and lowest transalkylation products. The SiO₂-Al₂O₃ supported platinum (Pt/SiO₂-Al₂O₃) catalyst is a potential hydrotreating catalyst for low molecular weight lignin-derived feedstock.

The catalysts and supports were characterized by X-ray diffraction (XRD). The coke content of various catalysts tested in this study was measured by thermal gravimetric analysis (TGA).

TABLE OF CONTENTS

ABSTRACT	iii
LIST OF TABLES	vii
LIST OF FIGURES	x
ACKNOWLEDGMENTS	xiii
DEDICATION	xv
Chapter 1 INTRODUCTION	1
1.1 Background	1
Chapter 2 LITERATURE REVIEW	4
2.1 Conversion of Lignin to Phenolics	4
2.2 Model Lignin Compound Studies	6
2.3 Catalysts	9
2.3.1 Molybdenum Sulfide Catalysts	10
2.3.2 Hydrocracking Catalysts	10
2.4 Lignin Depolymerization Reaction	11
2.4.1 Methods	12
2.4.2 Products	13
Chaper 3 STATEMENT OF PROBLEM	15
Chapter 4 EXPERIMENTAL	19
4.1 Materials	19
4.1.1 Solids and Liquids	19
4.1.2 Gases	23
4.1.3 Catalysts	24

4.2 Support Preparation	24
4.2.1 Silica-Alumina Support	24
4.2.2 Aluminophosphate Support	25
4.3 Support Incipient Wetting Volume Determination	28
4.4 Catalyst Preparation	29
4.4.1 Platinum/Silica-Alumina Catalyst	30
4.5 Support and Catalyst Characterization	31
4.5.1 Total Surface Area	32
4.5.2 Composition and Crystallinity	32
4.5.3 Catalyst Reduction	33
4.5.4 Surface Carbonaceous Residue (Coke) Content	34
4.5.5 Total Surface Area	35
4.6 Catalyst Evaluation System	36
4.6.1 Catalyst Bed	39
4.7 System Calibrations	40
4.8 Catalyst Testing	40
4.8.1 Feedstocks	40
4.8.2 Reaction Conditions	42
4.8.3 Catalyst Testing Procedure	42
4.9 Product Analysis	46
4.9.1 Gas Chromatography	46
4.9.2 Calibration of Gas Chromatograph	47
4.9.3 GC Retention time	48
4.9.4 Gas Chromatography/Mass Spectrometry	48
4.10 Solvent for a Model Lignin Feedstock	49
 Chapter 5 EXPERIMENTAL RESULTS AND DISCUSSION	 50
5.1 Evaluation of Catalysts	50
5.2 Reactor Calibration Tests	50
5.2.1 Activity and Selectivity of α -Alumina	54
5.2.2 Activity and Selectivity of Quartz	54
5.3 Effect of Preparation on Pt/ AlPO_4 - Al_2O_3 Activity	56
5.4 Effect of Quartz vs α -alumina on Catalyst Activity and Selectivity	57
5.5 Effect of Temperature on 4-Propylphenol Conversion Over Pt/ SiO_2 - Al_2O_3	59
5.6 Results of Replicate Runs	72
5.7 Activity and Selectivity of Catalyst Supports	72

5.7.1 AlPO ₄ -Al ₂ O ₃ Support	72
5.7.2 SiO ₂ -Al ₂ O ₃ Support	74
5.8 Effect of Temperature and Pressure on Toluene Conversion . . .	78
5.9 Effect of Solvent on Product Distribution	80
5.10 Subtracting the Product Due to Toluene	81
5.11 Effect of Temperature on 4-Propylguaiaacol Conversion	83
5.12 Effect of Temperature on Syringol Conversion	96
5.13 4-Propylphenol Conversion Over Ni/SiO ₂ -Al ₂ O ₃	98
5.14 Activity, Selectivity and Durability of Catalysts	105
5.14.1 Activity, Selectivity, and Durability of Pt/SiO ₂ -Al ₂ O ₃ . . .	106
5.14.2 Activity, Selectivity, and Durability of Pt/AlPO ₄ -Al ₂ O ₃ . .	108
5.14.3 Activity, Selectivity, and Durability of Ni/SiO ₂ -Al ₂ O ₃ . . .	108
5.14.4 Comparison of the Catalyst Activity and Selectivity . . .	110
5.15 Activity and Selectivity of Pt/SiO ₂ -Al ₂ O ₃ for Model Compound Mixtures	110
5.16 Blending Ability of Products	113
5.17 Support and Catalyst Characterization	115
5.17.1 XRD Analysis	115
5.17.2 Surface Carbonaceous Residue (Coke) Content	132
5.18 Preparation and Characterization of More Realistic Lignin Feedstock	137
Chapter 6 CONCLUSIONS	139
6.1 Catalysts	139
6.2 Physical and Chemical Properties of Catalysts	140
Chapter 7 RECOMMENDATIONS FOR FUTURE STUDIES	143
REFERENCES CITED	146
APPENDIX A	153
APPENDIX B	182
APPENDIX C	185
APPENDIX D	190

LIST OF TABLES

Table 1.	GC calibration chemicals	20
Table 2.	Reactants and solvents	21
Table 3.	Solvents for lignin studies	22
Table 4.	Catalyst synthesis chemicals	22
Table 5.	Total surface area of supports	36
Table 6.	Run conditions	51
Table 7.	Run conditions	52
Table 8.	Run conditions	53
Table 9.	Catalysts characterized by XRD	117
Table 10.	XRD results and calculated average catalyst particle diameters	129
Table 11.	Apparent surface coke content on the tested catalysts	134
Table A-1.	Activity and selectivity of α -Al ₂ O ₃ for conversion of 4-propylphenol to phenol	154
Table A-2.	Effect of temperature on liquid products distribution for 4-propylphenol conversion over pure quartz	155
Table A-3.	Catalysts used with preparation conditions	156
Table A-4.	Effect of catalyst on product distribution	157
Table A-5.	Comparison of the effect of quartz and α -Al ₂ O ₃ on liquid	

	product distribution for 4-propylphenol conversion over Pt/AlPO ₄ -Al ₂ O ₃	158
Table A-6.	Effect of temperature and pressure on liquid product distribution for 4-propylphenol conversion over Pt/SiO ₂ -Al ₂ O ₃	159
Table A-7.	Duplicate runs to test experimental reproducibility at fixed temperature and pressure	160
Table A-8.	Duplicate runs to test experimental reproducibility at fixed temperature and pressure	161
Table A-9.	Effect of temperature on liquid product distribution for 4-propylphenol conversion over AlPO ₄ -Al ₂ O ₃ blank support . . .	162
Table A-10.	Effect of temperature on liquid product distribution for 4-propylphenol conversion over SiO ₂ -Al ₂ O ₃ blank support	163
Table A-11.	Effect of temperature and pressure on liquid product distribution of pure toluene over Pt/SiO ₂ -Al ₂ O ₃	164
Table A-12.	Effect of temperature and pressure on liquid product distribution for pure toluene over Pt/SiO ₂ -Al ₂ O ₃	165
Table A-13.	Effect of pressure and time on liquid product distribution for pure toluene over Pt/SiO ₂ -Al ₂ O ₃	166
Table A-14.	Effect of temperature and pressure on liquid product distribution for 4-propylphenol conversion over Pt/SiO ₂ -Al ₂ O ₃	167
Table A-15.	Effect of temperature and pressure on liquid product distribution for 4-propylphenol conversion over Pt/SiO ₂ -Al ₂ O ₃ (The estimated contribution of toluene products is subtracted)	168
Table A-16.	Effect of temperature on liquid product distribution 4-propylguaiacol over Pt/SiO ₂ -Al ₂ O ₃ at 200 psig	169

Table A-17.	Effect of temperature on liquid product distribution 4-propylguaiacol over Pt/SiO ₂ -Al ₂ O ₃ at 300 psig	170
Table A-18.	Effect of temperature and pressure on liquid product distribution for syringol over Pt/SiO ₂ -Al ₂ O ₃	171
Table A-19.	Effect of temperature on liquid product distribution for syringol over Pt/SiO ₂ -Al ₂ O ₃	172
Table A-20.	Liquid product distribution for 4-propylphenol over Ni/SiO ₂ -Al ₂ O ₃	173
Table A-21.	Comparison of selectivity and activity of the platinum catalysts and the nickel catalyst	174
Table A-22.	Liquid product distribution for mixture of 4-propylguaiacol and syringol over Pt/SiO ₂ -Al ₂ O ₃	175
Table A-23.	Comparison of PE Sigma-3B GC TCD relative response weight factors to references	176
Table A-24.	Retention times (PE Sigma-3B)	177
Table A-25.	Retention times (PE Sigma-3B)	178
Table A-26.	Retention times (PE Sigma-3B)	179
Table A-27.	PE Sigma-3B GC Operation conditions	180
Table A-28.	HP-5890 GC Run parameters	181
Table A-29.	MSD Acquisition parameters	181
Table D-1.	Properties of the solvents and the solubility of ROSL	195
Table D-2.	Properties of the solvents and the solubility of Repap SEL	196
Table D-3.	Results of ROSL Soxhlet extraction by different solvents	196

T-4377

Table D-4. Assignments of absorption bands in the infrared spectra of lignins	200
--	-----

LIST OF FIGURES

Figure 1.	A representative section of the molecular structure of soft wood lignin	5
Figure 2.	Model lignin compounds	8
Figure 3.	Illustration of desired reactions	17
Figure 4.	Schematic of catalyst activity evaluation system	38
Figure 5.	Schematic of reactor tube	41
Figure 6.	Comparison of activity and selectivity of α -alumina and quartz for 4-propylphenol conversion	55
Figure 7.	Comparison of the effects of α -alumina and quartz on catalyst activity and selectivity	58
Figure 8.	Product types of 4-propylphenol as a function of temperature	61
Figure 9.	Reaction types of 4-propylphenol as a function of temperature	62
Figure 10.	Reaction scheme for 4-propylphenol conversion	64
Figure 11.	Heterogeneous surface dealkylation mechanism by acid function	65
Figure 12.	Heterogeneous surface transalkylation mechanism by acid function	68
Figure 13.	Heterogeneous surface hydrogenation mechanism (1) by metal function	69

Figure 14.	Heterogeneous surface hydrogenation mechanism (2) by metal function	70
Figure 15.	Heterogeneous surface hydrogenation mechanism (3) by metal function	71
Figure 16.	Possible surface structures of $\text{AlPO}_4\text{-Al}_2\text{O}_3$ support	73
Figure 17.	Possible surface structure of $\text{SiO}_2\text{-Al}_2\text{O}_3$ support	75
Figure 18.	Comparison of activity, selectivity, dealkylation and transalkylation reactions of supports	77
Figure 19.	Comparison of activity and selectivity of $\text{Pt/SiO}_2\text{-Al}_2\text{O}_3$ for toluene and hexane as a solvent in 4-PP conversion	82
Figure 20.	Comparison of the measured product distribution to the distribution corrected for estimated toluene product	84
Figure 21.	Product types of 4-propylguaiacol as a function of temperature	86
Figure 22.	Reaction types of 4-propylguaiacol as a function of temperature	87
Figure 23.	Possible reaction scheme for 4-propylguaiacol conversion	89
Figure 24.	Possible catalyst support demethylation mechanism on an acid site	90
Figure 25.	Possible mechanism of metal surface hydrogenolysis for demethylation of 4-propylguaiacol	91
Figure 26.	Possible catalyst support alkylation mechanism involving a surface methoxy group	92
Figure 27.	Possible transalkylation mechanism involving a catalyst support acid site	93

Figure 28.	Possible metal surface hydrogenolysis mechanism for the selective dehydroxylation of catacol	95
Figure 29.	Effect of pressure on syringol product distribution	99
Figure 30.	Effect of temperature on catalyst function during syringol conversion	100
Figure 31.	Possible reaction scheme for syringol conversion	101
Figure 32.	Comparison of activity and selectivity of Ni/SiO ₂ -Al ₂ O ₃ catalyst with Pt/SiO ₂ -Al ₂ O ₃ catalyst for 4-propylphenol conversion	103
Figure 33.	Possible reaction sequence of nickel aluminate formation . . .	104
Figure 34.	Comparison of activity and selectivity of Pt/SiO ₂ -Al ₂ O ₃ catalyst for 4PP, 4PG and SYR conversion	107
Figure 35.	Comparison of activity and selectivity of catalysts for 4-propylphenol conversion	111
Figure 36.	The mixture of model lignin compounds product as a function of time	114
Figure 37.	XRD pattern of platinum metal reference	120
Figure 38.	XRD patterns of nickel oxide and nickel metal references . . .	121
Figure 39.	XRD patterns of commercial SiO ₂ -Al ₂ O ₃ and prepared AlPO ₄ -Al ₂ O ₃ supports	122
Figure 40.	XRD patterns of (a) 0.3 wt% Pt/SiO ₂ -Al ₂ O ₃ and (b) reduced 0.3 wt% Pt/SiO ₂ -Al ₂ O ₃ catalysts	123
Figure 41.	XRD patterns for (a) calcined 0.3 wt% Pt/AlPO ₄ -Al ₂ O ₃ and (b) reduced 0.3 wt% Pt/AlPO ₄ -Al ₂ O ₃ catalysts	126
Figure 42.	XRD patterns for (a) calcined 1.2 wt% Pt/AlPO ₄ -Al ₂ O ₃ , (b)	

	calcined 0.3 wt% Pt/AlPO ₄ -Al ₂ O ₃ and (c) calcined 0.3 wt% Pt/SiO ₂ -Al ₂ O ₃	127
Figure 43.	XRD patterns for 15 wt% Ni/SiO ₂ -Al ₂ O ₃ and reduced 15 wt% Ni/SiO ₂ -Al ₂ O ₃ catalysts	130
Figure 44.	Thermal analysis of tested catalyst (a) DTA and (b) TGA . . .	133
Figure C-1.	Schematic of two-stage catalytic reactor system	186
Figure C-2.	Structural formulae of the products (1)	187
Figure C-3.	Structural formulae of the products (2)	188
Figure C-4.	Structural formulae of the products (3)	189
Figure D-1.	Effect of solvent properties on ROSL solubility.	194
Figure D-2.	IR-spectra of the steam exploded lignin	201
Figure D-3.	IR-spectra of the repap organosolve lignin	202
Figure D-4.	IR-spectra of the repap organosolve lignin residue after extraction by (a) 2-heptanone, (b) acetone, and (c) toluene .	203
Figure D-5.	IR-spectra of the solid repap organosolve lignin (a) extracted by acetone with acetone then evaporated, and (b) extracted by THF with THF then evaporated	204
Figure D-6.	IR-spectra of (a) acetone, (b) THF, and (c) toluene	205

ACKNOWLEDGMENTS

I would like to gratefully thank my advisor Dr. Scott W. Cowley, for the years of his guidance, patience, and confidence throughout my studies. I greatly appreciated his providing me with the opportunity to undertake the project. Without his help and understanding, I could not have accomplished this work.

I would like to thank my tutors Ken Cooper and Ruth Cooper, for not only teaching me English since I came to the United States four years ago, but helping me in technical report writing and being good friends. Without their kindness, I could not have accomplished the school work.

I would like to thank the other members of my thesis committee, Dr. Dean Dickerhoof, Dr. George Lucas, Dr. Robert Baldwin and Dr. Jean Bell for advice and patience particularly during the writing of this thesis.

I would like to thank all my teachers for their dedicated teaching. Without them I would not be able to enter the kingdom of knowledge.

I would like to thank the National Renewable Energy Laboratory for the financial support and I also would like to thank Dr. Dave Johnson at NREL for

his advice and help in accomplishing this project.

I would like to thank Mrs. Dee A. Erickson for calibrating the system.

I would like to thank Dr. Hengyen Xia and Mrs. Yuzen Yan for helping me take care of my son George while I was writing this thesis. Without their kindness I could not have completed this thesis this soon.

Finally, I especially thank my lovely son George Zhao Deng for having been a good boy while I was writing this thesis and my dear husband XiaoJun Deng, for his love, understanding and help.

DEDICATION

This work is dedicated to my parents in appreciation of their love and understanding.

Chapter 1

INTRODUCTION

1.1 Background

Transportation fuels are almost totally derived from petroleum, but the amount of petroleum is limited in the earth. Also petroleum-derived transportation fuels are the source for up to 2/3 of the atmospheric carbon monoxide and 30 to 50 % of smog-causing emissions (*Wyman, 1990*). Many high altitude cities such as Denver experience excessive levels of carbon monoxide due to incomplete combustion of carbon-containing fuels. The basic motor-fuel combustion problems are associated with air quality and public health.

Modern technology can produce clean fuels including methanol, ethanol, and reformulated gasoline. Methanol and ethanol are clean burning liquid fuels that can be readily substituted for gasoline in our transportation sector. The safety and economic problems of methanol and ethanol used as

fuels for transportation are still under investigation.

Reformulation of gasoline is mainly for the purpose of reducing tailpipe emissions. Reformulated gasoline is a gasoline blended with oxygenated compounds. These oxygenates can help gasoline burn cleaner by increasing its oxygen content and raising its octane number. Fleet tests of reformulated gasoline show statistically significant reductions in emissions of hydrocarbons (HC), CO and NO_x. The reformulated gasoline will be required in order for this fuel to conform with federal and state government clean fuel standards in the future. Gasolines will be required to have a high octane, a high oxygen content, low volatility, a low aromatic content and produce reduced CO emissions. Ethyl tertiary butyl ether (ETBE) has high octane, low volatility, and is considered to be ideally suited as an oxygenated octane booster.

Methanol and ethanol can be produced from several carbohydrate-containing feedstocks including sugar, corn starch, and cellulosic biomass. The cost of feedstock is an important factor in determining the selling prices of methanol and ethanol. Cellulosic biomass has long been studied since it is much less expensive than corn or sugar, because it has no competing value as food.

Cellulosic biomass is a complex mixture of carbohydrate polymers from plant cell walls known as cellulose and hemicellulose, plus lignin and a small amount of other extractive compounds. Lignin is the third largest component

in cellulosic biomass after cellulose and hemicellulose.

Lignin has a high energy content and can be used as a boiler fuel, but it is potentially more valuable as oxygenate feedstock. Lignin is a complex and heterogeneous phenolic polymer that can be broken down to form a mixture of monomeric phenolic compounds and hydrocarbons. The phenolic fraction can be reacted with alcohols to form methyl or ethyl aryl ether; these are good oxygenated octane boosters. Also the methyl and ethyl aryl ether made by lignin and alcohols are less expensive than ETBE. The conversion of lignin into a high octane oxygenated blending agent for gasoline is an interesting prospect, and promises to produce a valuable product from a relatively abundant and inexpensive source.

The purpose of this project is to develop a catalyst which will facilitate the conversion of lignin to monomeric phenolic compounds.

Chapter 2

LITERATURE REVIEW

2.1 Conversion of Lignin to Phenolics

Lignin is a complex and heterogeneous phenolic polymer (**Figure 1**) and one of the major components of wood (*Kirk, et al. 1987*). A number of publications have dealt with the depolymerization of lignin to obtain monomeric compounds (*Goheen, 1971; Goldstein, 1975; Chum, 1987*). Lignin can be broken down by several methods such as pyrolysis, hydrolysis, and biodegradation to form a mixture of monomeric phenolic compounds and hydrocarbons. However, most investigators have found that, although lignin yields a variety of phenols, no particular component is significantly predominant (*Elder, 1980*). Researchers such as *Panasyuk, et al. (1970)* discovered that, among the phenols from softwood lignin, guaiacol is dominant, whereas cresols are predominant in annual plants. Actually, pure phenol itself was obtained in only small quantities. Even in the improved

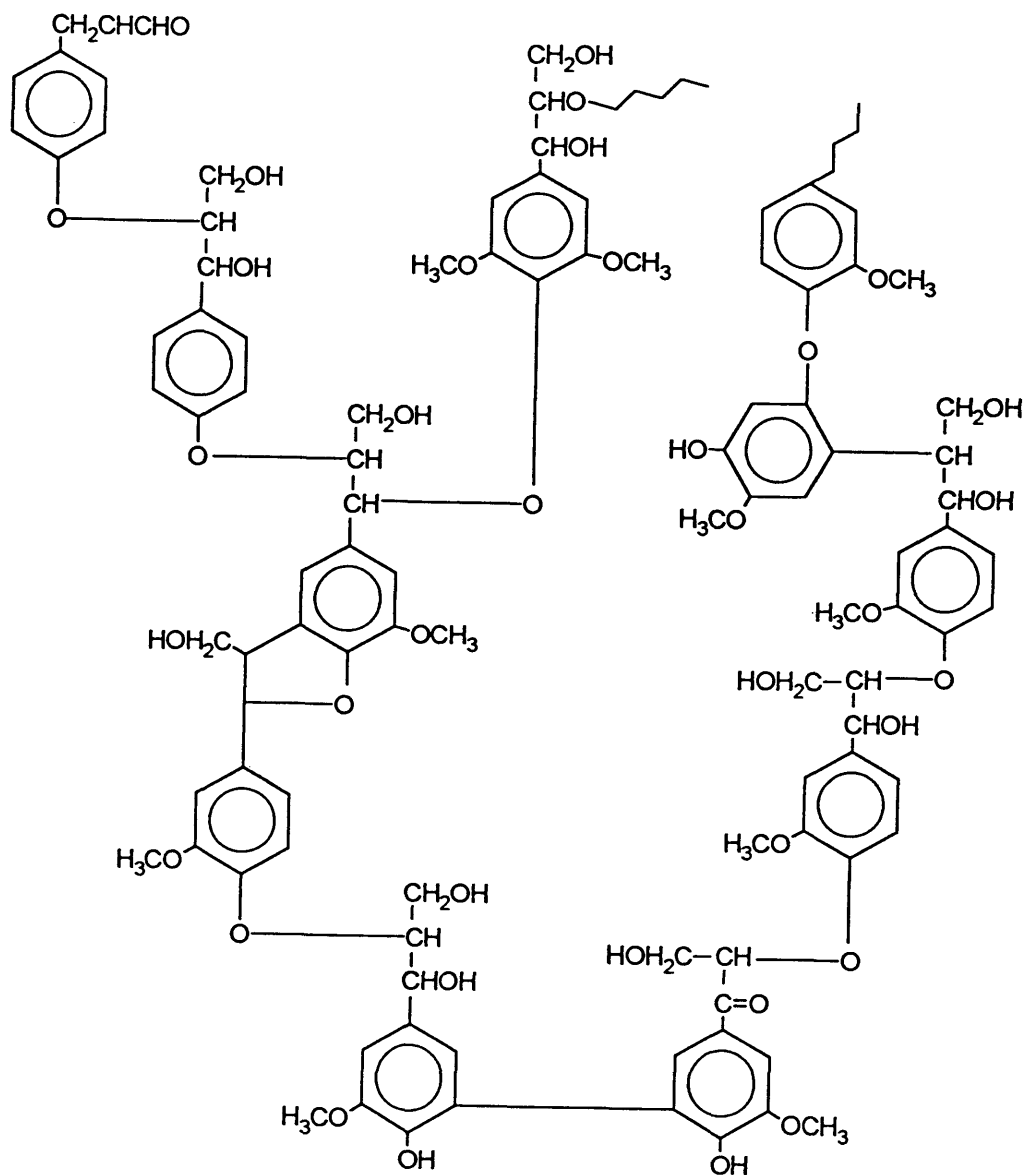


Figure 1. A representative section of the molecular structure of soft wood lignin (Owen and Thomas, 1989).

Noguchi process, the best yields were 3% phenol, 4% o-cresol, and 6% m/p-cresols in a total monophenol yield of 21%. There were at least 10 to 15 different phenolic compounds in the product (*Goldstein, et al., 1975*).

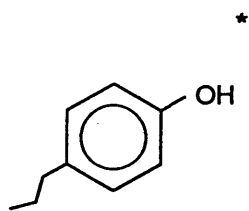
Acid is commonly employed to separate the reaction products derived from lignin depolymerization into liquid and solid phases. It precipitates the unreacted lignin and converts the phenolate salts in solution to phenols. These phenolic compounds are then isolated from the liquid phase by extraction with a selective solvent (*Pepper and Hagerman, 1951; Pepper and Fleming, 1978*).

2.2 Model Lignin Compound Studies

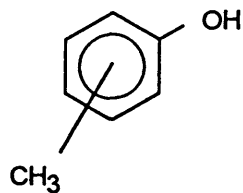
A number of structural formulas of lignin have been proposed (*Brauns, 1948; Freudenberg, 1939; 1965*). The highest formulation contains 18 structural units which are interlaced in a fashion corresponding to the biochemical growth of the naturally occurring lignin molecule.

Raw lignin degradation has been studied in the classical organic tradition for many years, but the refractory nature of the starting materials prevented the production of significant amounts of the oligomeric degradation products. Lignin typically contains aromatic rings linked together with both oxygen and carbon bridges. The mass spectra of pyrolyzed lignin show compounds such as alkyl-substituted phenols, cresols, guaiacols, catechols, and dimethoxy phenols (**Figure 2**) (*Hurff and Klein, 1983*). These represent the more stable components present in lignin, and are commonly called model lignin compounds.

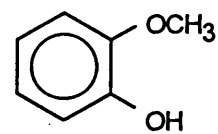
The development of new catalysts using a complex feedstock such as lignin presents enormous problems. The surface reaction network is complex and competing reactions often obscure important information about the role of a given catalyst function. The proper selection of model compounds which contain the functional groups to be studied in the conversion process can overcome most of these problems. For this reason, model oxygenated compounds have been studied at the Colorado School of Mines and the National Renewable Energy Laboratory in order to more effectively develop an improved catalyst system (*Edelman, 1988; Maholland, 1987; Ratcliff, 1988; Erickson, 1990*).



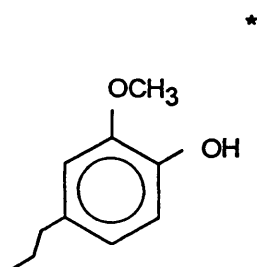
4-Propylphenol



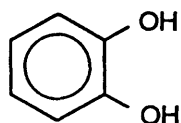
Cresol



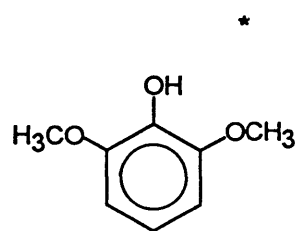
Guaiacol



4-Propylguaiacol



Catachol



Syringol

* Used in this study

Figure 2. Model lignin compounds.

2.3 Catalysts

The importance of the hydrotreating process in the refining of petroleum and coal liquids is well recognized (*Ohtsuka, 1977*). The catalysts used in this process generally consist of molybdenum supported on γ -alumina with various promoters such as cobalt and nickel (*Stanislaus, et al. 1989; Grange, 1980*). The catalyst possesses three functions, namely acidity, hydrogenolysis and hydrogenation; these occur at different sites. The chemical composition and preparation of such catalysts have a significant effect on performance (*Thakur, 1985; Houalla, 1983*). The nature of the acidic sites and the relationship between the acid properties and the performance of these catalyst systems have been the subject of a number of studies (*Chen, et al. 1992; Ware and Wei, 1985; Muralidar, et al. 1984*). These catalysts contain Bronsted and Lewis acid sites (*Ramirez, et al. 1987; Valyon, et al. 1984; Ratnasamy and Knozinger, 1978*). The acidic properties of the hydrotreating catalysts have an important influence on the performance. The acid sites of the support increase the stability (less coke) and promote dealkylation (*Assafi and Duprez, 1992*). Also a mixed oxide with a perovskite-type oxide chemical formula of ABO_3 such as $LaCoO_3$, becomes an important catalyst in hydrocarbon hydrogenation and hydrogenolysis (*Ichimura, et al. 1992*).

2.3.1 Molybdenum Sulfide Catalysts

Conventional catalysts for petroleum refining are molybdenum-based. Commonly used catalysts are nickel (or cobalt) with molybdenum on supports of alumina or silica (*Boorman, 1985; Furimsky, 1983; Kallury, 1985*). They contain the hydrogenolysis and hydrogenation functions required, but lack the acid function required for the dealkylation step. Studies using Mo and Ni-Mo on acidic aluminophosphate supports showed a marked improvement in the phenol yield (*Maholland, 1987; Ratcliff, et al., 1988; Erickson, et al., 1990*). In petroleum crude oil, the amount of sulfur normally present in the feedstock is sufficient to maintain the active sulfided surface. In lignin, however, there is very little sulfur present. Therefore, the catalyst requires the presence of an organosulfur compound in the feedstock in order to maintain the catalyst in an active state. The low sulfur content in lignin makes it ideal for catalytic conversion using noble metal catalysts such as platinum and palladium. These metals are so sensitive to sulfur that they have not been extensively studied for use in hydroprocessing of petroleum.

2.3.2 Hydrocracking Catalysts

Since high molecular-weight lignin is a problem during the hydrotreatment, the lignin must be depolymerized to yield single ring products

before the deoxygenation occurs. The single ring products can access the active sites that are present on the catalyst surface which promote deoxygenation.

Hydrocracking processes are generally used in the petroleum refining industry for the cracking of heavy residua to produce gasoline. They consist of two stages, a hydrotreatment stage and a hydrocracking stage. Originally, catalytic hydrocracking involved the use of silica-alumina as a catalyst with metal (*Pines, 1981*). This is considered to be a solid acid, and the reactions occurring on this catalyst involve carbonium ions. For example, Ni/W on silica-alumina catalysts (sulfided) (*Thompson and Mathews, 1989*) are the most common hydrocracking catalysts for the petroleum refining industry. Cracking by dealkylation normally occurs on acid sites on the catalyst support. Acid-catalyzed cracking of alkyl aromatics often is assumed to occur by complete cleavage of the side chain from the aromatic ring (*Venuto and Mabib, 1979*).

2.4 Lignin Depolymerization Reaction

Low molecular weight fractions have been obtained by chemical and thermal degradation of the lignin (*Thring et al., 1991; Funaoka et al., 1990*). However, the low molecular fragments tend to repolymerize into less tractable

higher molecular weight products. The chemical process development and product characterization was considered too complex and time consuming for this project.

In previous work at the Colorado School of Mines, the catalytic behavior of a complex hydrocarbon mixture was successfully modeled by a mixture of selected model compounds (*Frerichs, 1984*). In several studies, the monomer units obtained from the depolymerization of lignin have been identified (*Funaoka et al., 1990; Thring et al., 1990; Davoudzadeh, 1985; Pepper, 1978*). It is proposed that the catalysts can be successfully evaluated using a model lignin feedstock containing the appropriate proportions of model compounds.

2.4.1 Methods

Various lignins from both softwoods and hardwoods have been subjected to pyrolysis (*Avni and Coughlin, 1985; Elder and Soltes, 1980*), alkali fusion (*Freudenberg, 1939; Clark and Green 1968*), hydrogenation (*Train and Klein, 1991*), hydrolysis (*Agblevor and Boocock, 1989*) and biodegradation (*Hammel and Moen, 1991; Tai and Terazawa, et al. 1990*). Although yields of phenols as high as 50% (*Goldstein, 1975*) of the lignin have been reported, commercial production has not taken place, mainly because the products are complex mixtures with many components. Reforming the complex mixture by catalytic processing to yield simpler, more marketable compounds could lead

to commercial practice.

2.4.2 Products

The low molecular weight products obtained from lignin degradation are phenol, cresol, ethylphenol, propylphenol, xylenol, catechol, guaiacol and syringol et al (*Goldstein, 1975*). A successful catalyst must be able to convert products of this type to phenol. Therefore, these compounds can serve as good models to test a potential catalyst's behavior.

Among the major pyrolysis products identified from loblolly pine lignin were guaiacol, 4-methylguaiacol, 4-vinylguaiacol, vanillin, coniferaldehyde, and coniferyl alcohol (*Obst, 1983*). White oak lignin pyrolysis products also included guaiacol, 4-methylguaiacol, and vanillin and additionally, 2, 6-dimethoxyphenol, 4-methyl-2,6-dimethoxyphenol, syringaldehyde, and sinapaldehyde (*Obst, 1983*). By identification of these pyrolysis products from either wood or milled wood lignin it is possible to classify lignins as either guaiacol-type or syringol/guaiacol-type. In other studies by *Dr. Kuroda and Dr. Inoue (1990)*, the main pyrolysis products were the nine guaiacol derivatives.

In a study by *Clark and Green (1968)* Kraft lignin was cooked in solutions of sodium hydroxide and sodium sulfide. The principal products identified were guaiacol, catechol, methyl- and ethyl-guaiacols and methyl- and ethyl-catechols, phenol and p-cresol.

Hybrid poplar lignin alkaline hydrolysis was studied by *Agblevor and Boocock (1989)*. The major products are phenol, guaiacol, methyl-4-methoxybenzoate, 2,6-dimethoxyphenol, vanillin, methyl-4-hydroxybenzoate, methyl vanillate, 4-hydroxy-3-methoxy phenyl, 3,4,5-trimethoxybenzaldehyde and syringoldehyde.

Biodepolymerization of synthetic lignin was studied by *Wariishi et al. (1991)*. 3,5-dimethoxy-1,4-benzoquinone, 3,5-dimethoxy-1,4-hydroquinone and syringolaldehyde were identified as degradation products of the syringol and syringol-guaiacol lignins.

Chaper 3

STATEMENT OF PROBLEM

Lignins derived from biomass are a potential source of fuel, particularly if the lignin feed stock can be converted into low-molecular weight phenolics and hydrocarbons. The purpose of this project is to develop a catalyst which will facilitate the conversion of lignin into low-molecular weight phenolics and hydrocarbons. The phenolics can be converted into methy aryl ethers by reacting them with methanol in the presence of a base catalyst. Such a fuel would have the chemical and physical properties necessary to make it compatible with gasoline.

Lignins consist of aromatic rings which contain hydrogen, methoxy and alkyl substituents. Ideally, the lignin will be converted to a mixture containing primarily monomeric phenols in one step.

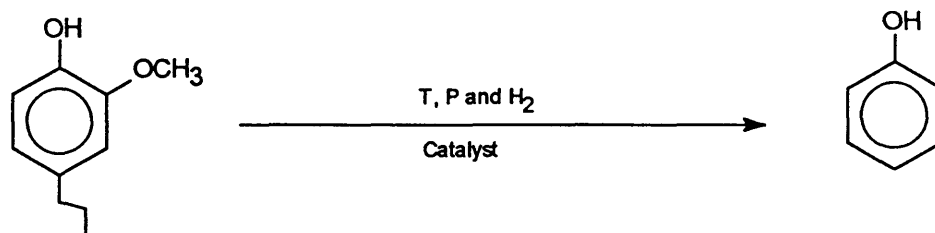
The production of phenolics and hydrocarbons from lignin feedstocks will require a multifunctional catalyst capable of reducing this complex structure to a simple phenolic product. That is, the catalyst must contain a

hydrogenolysis function to cleave C-O bonds, an acid function to facilitate dealkylation of alkylaromatics, and a hydrogenation function to prevent the transalkylation of alkenes to other aromatic rings. The desired reactions are shown in **Figure 3**.

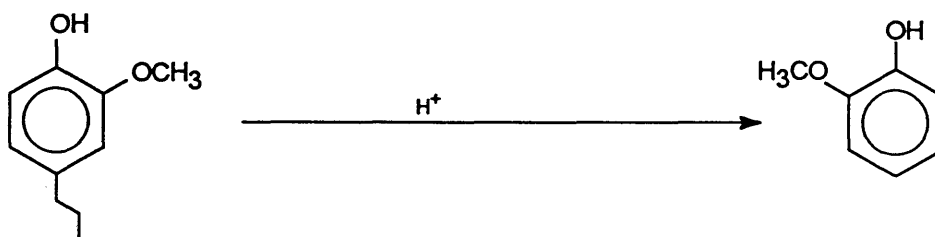
To convert lignin into the desired product, it is also necessary to develop a catalyst which will depolymerize and partially deoxygenate the lignin. It is advantageous to leave some of the oxygen, because it will enhance the production of desirable products. The current objective for lignin hydrodeoxygenation (HDO) is the removal of all the oxygen in excess of one atom per ring, leaving low molecular-weight phenols.

Conventional hydrotreating catalysts such as Mo/Al₂O₃ and Ni-Mo/Al₂O₃ contain the hydrogenolysis and hydrogenation functions required, but lack the strong acid function required for the dealkylation step. Studies using Mo and Ni-Mo on acidic aluminophosphate supports showed a marked improvement in the phenol yield (*Maholland, 1987; Ratcliff, et al., 1988; Erickson, 1990*). However, these catalysts produced a substantial yield of the dialkylphenols (transalkylation). Although these catalysts contain some hydrogenation activity, it is insufficient to prevent the transalkylation reaction.

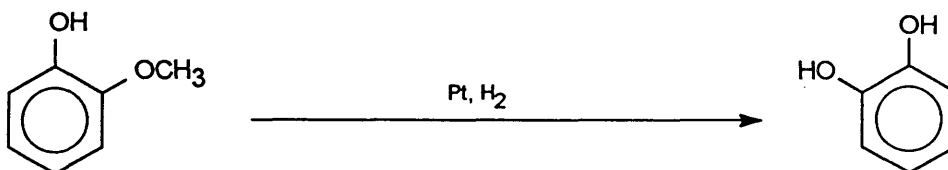
Overall reaction (only the desired product is shown):



Dealkylation:



Hydrogenolysis:



Deoxygenation:

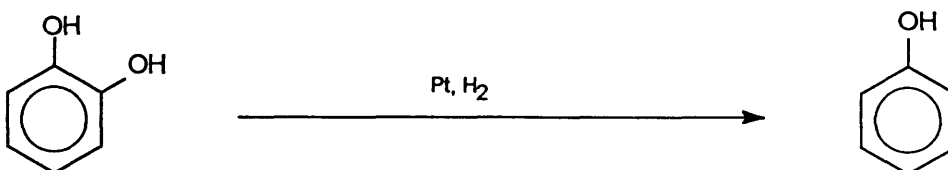


Figure 3. Illustration of desired reactions.

In addition, these catalysts require the presence of hydrogen sulfide in the feedstock in order to maintain the catalyst in an active state. Since lignin feedstocks are very low in sulfur content, it is possible to consider catalysts which do not require H₂S and are not normally used in hydrotreating processes.

In order to more effectively develop an improved catalyst system, the fundamental studies of this project will be started with model lignin compounds that contain the same structure as lignin repeating units. The model lignin compounds studies will facilitate the lignin feed stock studies.

Chapter 4

EXPERIMENTAL

4.1 Materials

4.1.1 Solids and Liquids

The chemicals required for this research project can be divided into four groups; (1) GC calibration chemicals (**Table 1**), (2) reactants and solvents (**Table 2**), (3) lignin solvents (**Table 3**) and (4) catalyst synthesis chemicals (**Table 4**). Unless otherwise specified the chemicals were used as received without further purification.

Table 1. GC calibration chemicals

Chemical	Formula	Purity (wt%)	B.P. (°C)	Supplier
n-Hexane	C ₆ H ₁₄	99+	69	Fisher Chemical Co.
Heptane	C ₇ H ₁₆	99+	98	Baker Resi-Analyzed
Cyclohexane	C ₆ H ₁₂	99+	83	Fisher Chemical Co.
Methylcyclohexane	C ₇ H ₁₄	99	101	Eastman Kodak Co.
Ethylcyclohexane	C ₈ H ₁₆	99+	131	Eastman Kodak Co.
Benzene	C ₆ H ₆	99.9	80	Mallinckrodt, Inc.
Propylcyclohexane	C ₉ H ₁₈	99	155	Aldrich Chemical Co., Inc.
Toluene	C ₇ H ₈	99+	111	Mallinckrodt, Inc.
Ethylbenzene	C ₈ H ₁₀	99	135	Eastman Kodak Co.
Propylbenzene	C ₉ H ₁₂	98	159	Aldrich Chemical Co., Inc.
Phenol	C ₆ H ₆ O	99+	182	Aldrich Chemical Co., Inc.
2-Propylphenol	C ₉ H ₁₂ O	98	225	Aldrich Chemical Co., Inc.
4-Propylphenol	C ₉ H ₁₂ O	99	232	Aldrich Chemical Co., Inc.
4-Propylguaiacol	C ₁₀ H ₁₄ O ₂	97+	129*	Frinton Laboratories
Syringol	C ₈ H ₁₀ O ₃	99	261	Aldrich Chemical Co., Inc.

* The boiling points were obtained at 760 mm Hg, except 4-propylguaiacol, whose boiling point of 129°C was obtained at 15 mm Hg.

Table 2. Reactants and solvents

Chemical	Formula	Purity (wt.%)	B. .P (°C)	Supplier
4-Propylphenol	$C_9H_{11}OH$	99	232	Aldrich Chemical Co.
4-Propylguaiacol	$C_{10}H_{14}O_2$	97+	129*	Frinton Labratories
2,6-Dimethoxyphenol	$C_8H_{10}O_3$	99	261	Aldrich Chemical Co.
Hexane	C_6H_{14}	99	69	Fisher Chemical Co.
Toluene	C_7H_8	99	111	Mallinckrodt, Inc.

* The boiling points were obtained at 760 mm Hg, except 4-propylguaiacol, whose boiling point of 129°C was obtained at 15 mm Hg.

Table 3. Solvents for lignin studies

Chemical	Formula	Purity (wt.%)	B. P.(°C) (760 mm Hg)	Supplier
Acetone	C_3H_6O	99+	56	Mallinckrodt, Inc.
Toluene	C_7H_8	99+	111	Chemical Sales Co.
Tetrahydrofuran	C_4H_8O	99.9+	66	Mallinckrodt, Inc.

Table 4. Catalyst synthesis chemicals

Chemical	Formula	Purity (wt.%)	Supplier
Aluminum Nitrate	$Al(NO_3)_3 \cdot 9H_2O$	100	Mallinckrodt, Inc.
Phosphoric Acid	H_3PO_4	85	EM Science
Ammonium Hydroxide	NH_4OH	30	EM Science

4.1.2 Gases

The list below details the use and purity of the bottled gases which were employed in this research.

a. Reactor System

- * Ultra high purity grade hydrogen (99.999%)
- * High purity grade helium (99.995%)

b. Sigma-3B Gas Chromatography

- * Ultra high purity grade helium (99.999%)

c. HP-5890 GC/HP-5970 MSD

- * Ultra high purity grade helium (99.999%)

4.1.3 Catalysts

All catalysts were synthesized in this laboratory. Phosphate was incorporated into the catalyst primarily by the alumina-phosphate coprecipitation method. The active metals then were impregnated onto the support by the incipient wetness technique. In order to eliminate the metal concentrations from being a variable in this study, the laboratory catalysts were prepared having metal loadings identical to the catalysts made by *Erickson (1990)*. The procedures used to prepare the supports and the catalysts are described below.

4.2 Support Preparation

4.2.1 Silica-Alumina Support

The silica-alumina pellets were bought from Davison Chemical Co.. The following procedure was utilized for the silica-alumina support preparation:

1. The silica-alumina pellets were ground using a mortar and pestle, then screened to a size of 20/40 mesh.
2. This support material was stored in crucibles and transferred to a

muffle furnace. The temperature was raised to 500°C over a period of four hours. The material was calcined at 500°C for 18 hours, then removed from the furnace and allowed to cool to room temperature. The catalyst was transferred to a glass jar and stored in a desiccator which contained no desiccant.

4.2.2 Aluminophosphate Support

The aluminophosphate ($\text{AlPO}_4\text{-Al}_2\text{O}_3$) support was made by the alumina-phosphate coprecipitation method in the laboratory. The procedure used for the preparation of supports with a P:Al ratio of 0.8 (indicated as [0.8P:Al]) is given as follows:

1. Preparation of Acid Solution:

800 grams of aluminum nitrate ($\text{Al}(\text{NO}_3)_3 \cdot 9 \text{H}_2\text{O}$) was dissolved in 8 liters of deionized water. 196.8 grams of 85% phosphoric acid (H_3PO_4) was added to the solution. This is called the acid solution.

2. Preparation of Basic Solution:

900 ml of (30%) NH_4OH was dissolved in 900 ml of deionized water. This is called the basic solution.

3. Formation of Hydrogel:

- a. The acid solution was poured into a 2000 ml separatory funnel.
The basic solution was transferred into a 1000 ml buret.
- b. 4000 ml of deionized water with the pH adjusted by 30% NH_4OH to 9.0 was added to a 5 gallon plastic receptacle.
- c. The acid solution was added to the plastic receptacle at a rate of approximately 400 ml/minute and the basic solution was added at the rate necessary to maintain the pH of the solution at 9.0.
The resulting hydrogel was agitated with a heavy duty mixer.
- d. The funnel and buret were continuously refilled until one of the solutions was depleted. The hydrogel was stirred for an additional hour.
- e. The hydrogel was transferred to a Buchner funnel which was connected to a water aspirator. The hydrogel was filtered until most of the water had been removed. When the surface of the hydrogel cake appeared dry, 500 ml of 30% NH_4OH adjusted pH = 9.0 deionized water was added to the funnel to wash the hydrogel. Each funnel was washed six times with 500 ml of deionized water containing NH_4OH at a pH of 9.0.
- f. The funnels were disconnected from the aspirator after the last

500 ml had been added and the cake remained in the funnel for at least a half hour.

4. Calcination of Hydrogel:

- a. The hydrogel cakes were removed to several large glass dishes, transferred to the oven and dried at 65°C overnight in an air flow to prevent water condensation.
- b. Next morning the temperature was raised to 120°C. The dry hydrogel cakes continued to dry at 120°C for 24 hours.
- c. The dried cakes were transferred to ceramic evaporating dishes and placed in a muffle furnace. The temperature was raised to 500°C over five hours. The cakes were calcined at 500°C for 18 hours.
- d. The cakes were then removed from the furnace and allowed to cool to room temperature. They were transferred to a glass jar and stored in a desiccator which contained no desiccant.

5. Grinding of Cakes:

- a. The cakes were ground using a mortar and pestle to a size of 20/40 mesh, to form the [0.8P:Al] support.

4.3 Support Incipient Wetting Volume Determination

The support incipient wetting volume is the amount of water just necessary to fill the pore volume of the support and wet all the support particles. This was needed to prepare the salt solution which would be used in the support impregnation step to form the catalyst.

Since the green color of the adsorbed copper nitrate can be used to visually determine the volume of solution required to evenly coat each particle of the support, the wetting volume of each support was determined with a copper nitrate solution $[\text{Cu}(\text{NO}_3)_2]$. The following procedure was used for determination of the support incipient wetting volume.

1. 1.0 g of the support material was put into a 250 ml round-bottom three-neck flask.
2. One neck of the flask was connected to a water aspirator. A 10 ml teflon stopcock buret with a rubber stopper in the bottom was placed in the center neck. The teflon stopcock was used to control the flow volume to be added to the support. The remaining neck was fitted with a glass stopper. 5 ml of the copper nitrate solution was added to the buret attached to the

center neck of the three necked flask. The flask was evacuated for 5 minutes with a water aspirator.

3. Under the vacuum, the required volume of copper nitrate solution was added to the support by opening the teflon stopcock. The flask was shaken vigorously while adding sufficient solution to obtain a uniformly wetted support, as indicated by a uniform green color on the support particles.
4. The volume of solution added to the support and weight of the support were recorded. The test was run three times. The volume of the solution was divided by the weight of the support. The averaged value was used as the standard incipient wetting volume.

4.4 Catalyst Preparation

The supported metal catalysts were used, because the large support surface area gives better dispersion of the metals and the support surface may exhibit its own catalytic function. The impregnation method requires the least equipment of all methods, since the filtering, washing, and forming steps

are eliminated. It is the preferred process for preparing supported noble metal catalysts in which the noble metal is highly dispersed on the support. A range of 0.3 to 1.2 wt% platinum metal and 15 wt% nickel metal were used in this study. The support material was impregnated with various concentrations of PtCl_4 solutions and $\text{Ni}(\text{NO}_3)_2$ solution.

4.4.1 Platinum/Silica-Alumina Catalyst

The following procedure was used to impregnate the silica-alumina support with 0.3 wt% Pt using an aqueous solution of PtCl_4 :

1. Exactly 0.0577 grams of PtCl_4 was dissolved in 10.0 ml of deionized water.
2. Approximately 5 grams of the (20/40 mesh) support was put into a round-bottom three-neck flask.
3. One neck of the flask was connected to an aspirator, and the central neck was attached to a 10 ml buret. The buret was opened using a teflon stopcock. The third neck was closed off with a glass stopper.
4. With the stopcock closed, 4.5 ml of the PtCl_4 solution was added to the buret.
5. The aspirator was turned on to evacuate the flask for 5-10

minutes to about 24 torr.

6. The PtCl_4 solution was added to the support in two stages with equal volumes by opening the teflon stopcock of the buret. Each time when the stopcock was closed, the flask was shaken by hand vigorously for 30 seconds.
7. The stopcock was closed, when the buret was just emptied. The flask was shaken by hand vigorously for about 5 minutes to evenly distribute the solution among the support particles.
8. The wet catalyst was dried at 120°C for 24 hours. Then the dried impregnated catalyst was calcined at 500°C for 24 hours in a muffle furnace. The temperature was raised to 500°C in about 5 hours.

4.5 Support and Catalyst Characterization

The characterization of a support or a supported metal catalyst is the qualitative and quantitative measure of those physical and chemical properties of the support and the catalyst assumed to be responsible for its performance in a given reaction. Two analytical methods were applied in this research. The supports and the catalysts were analyzed to determine total surface area

by the Brunauer-Emmett-Teller (BET) method, and the crystallinity by X-ray diffraction (XRD).

4.5.1 Total Surface Area

Total surface area is one of the most fundamentally important physical properties in catalysis. The total surface areas of the supports and catalysts were determined by the Brunauer-Emmett-Teller (BET) method on a Micromeritics Accusorb 2100E surface area analyzer. Nitrogen was used as the adsorbate. Multipoint measurements were made and sample surface areas were replicated 3 times and the results averaged. This work was reported by *Erickson (1990)*.

4.5.2 Composition and Crystallinity

X-ray diffraction (XRD), in particular X-ray powder diffraction, has been used extensively to identify and characterize materials used as catalysts in the petroleum refining and petrochemical industries (*Rohrbaugh and Wu, 1989*). Many of the catalytic materials are crystalline; i. e., the atoms are in three-dimensional periodic arrays. Every atom in a crystalline solid contributes to the observed XRD pattern, thus making a fingerprint of the material.

Common catalytic materials can be identified using tabulations of reference patterns. The minimum limit of detection is approximately 5 weight

percent for compounds and 1 weight percent for elements. The diffraction data obtained for catalytic material can tell many things about these materials, such as what crystalline materials are present and the average crystallite size on a supported-metal catalyst. The average crystallite size can be determined from the broadening of an X-ray diffraction peak.

The composition and crystallinity of several supports and catalysts were determined using a Rigaku powder X-ray diffractometer. The samples were prepared by grinding to a fine powder in a mortar. A current of 55 mA and a potential of 60 KV was used. The X-ray source was a copper K_{α} target. The scans were performed between 2θ values of 10° and 100° at a scan rate of 3 degrees per minute. For compound identification, peak locations and intensities were compared to known diffraction data for selected metals and metal oxides.

4.5.3 Catalyst Reduction

In order to characterize the catalysts in a freshly reduced state like that obtained at the beginning of a catalyst test sequence, it was necessary to reduce the catalysts in a separate experiment without testing them. The catalysts were reduced at 450°C with hydrogen at atmospheric pressure for two hours, then the oven was turned off and allowed to cool to room temperature with hydrogen. A helium purge followed for about five minutes

with a flow rate of approximately 100 ml/min., then the metal surfaces were passivated by introducing air. The air flow started at 1-2 ml/min., and was increased every 3 min. by about 1 ml/min. to prevent any large exotherms which could result in oxidation of the metal subsurface. When the concentration of air in helium was about 10%, the flow through the catalyst continued at this air/helium concentration for another ten minutes. The catalyst was removed from the catalyst bed and stored in a glass jar, then characterized by XRD.

4.5.4 Surface Carbonaceous Residue (Coke) Content

Thermogravimetry is a valuable tool to determine weight change. It is perhaps most useful when it complements differential thermal analysis studies. Virtually all weight-change processes absorb or release energy and are thus measurable by differential thermal analysis (DTA).

The surface coke content of selected tested catalysts was determined by thermal gravimetric analysis (TGA). The tested catalysts were heated in the oven at about 110 °C for 12 hours to remove the moisture from the surface just before the thermal analysis. The heated catalysts were removed from the oven then stored in a glass jar without a desiccant.

The thermal analysis temperature program for the SSC 5200H series thermal analysis system is listed below:

Initial temperature (°C)	100
Final temperature (°C)	750
Rate of temperature increase (°C/min.)	10
Gas	Air
Gas flow rate (ml/min.)	300

When the temperature increased, the surface coke content was converted to the volatile gases CO₂ and H₂O, resulting in a weight loss in the catalyst and a temperature increase (exothermic reaction) during combustion of the the coke.

4.5.5 Total Surface Area

The BET total surface area of the AlPO₄-Al₂O₃ supports was measured previously by *Maholland (1987)* and *Erickson (1990)*. The results are in good agreement with each other. Since the same method and procedure were employed for making the AlPO₄-Al₂O₃ support in the present study, the BET total surface area of the AlPO₄-Al₂O₃ support in this study was taken as measured by *Erickson (1990)*.

The total surface area of the $\text{SiO}_2\text{-Al}_2\text{O}_3$ support in this study was provided by Davison Chemical Corporation. The $\text{SiO}_2\text{-Al}_2\text{O}_3$ support surface area was much higher than that of the $\text{AlPO}_4\text{-Al}_2\text{O}_3$ support. The results are shown in **Table 5**.

Table 5. Total surface area of supports

<u>Support</u>	<u>Total surface area (m²/gm)</u>
$\text{AlPO}_4\text{-Al}_2\text{O}_3$	134
$\text{SiO}_2\text{-Al}_2\text{O}_3$	375

4.6 Catalyst Evaluation System

The central part of the catalyst evaluation system was a continuous down-flow, vapor phase, and fixed-bed tubular microreactor, see **Figure 4**.

The liquid feed-stock was stored in a buret, which was surrounded by an ice water jacket pumped by a submersible pump to minimize evaporation of the volatile components. The liquid feed-stocks were meter-pumped into the preheated mixing tee with a Milton Roy Minipump high pressure liquid pump. The hydrogen gas was metered separately and fed to the preheated mixing tee at the same time. The liquid feed-stock was vaporized and mixed with the hydrogen, then the mixture flowed through a heated line to the reactor tube. The mixture entered the reactor tube, which was heated by a Lindberg tube furnace, and flowed down through the catalyst bed. A needle valve downstream of the reactor was used to control the total pressure and flow rate of the system.

The liquid reaction products were condensed in a 250 ml steel condenser which was surrounded by a coiled copper tubing containing circulating ice water. The condensation products were collected during the run and placed in capped 5 ml serum bottles and analyzed by a HP Sigma-3B gas chromatograph equipped with a thermal conductivity detector. The column used for the analysis was a 10 feet long 1/8" O.D. stainless steel tube packed with Supelco 10% SP-1000 on 80/100 mesh Supelcoport. The product identities were confirmed using an HP 5890 GC/MS.

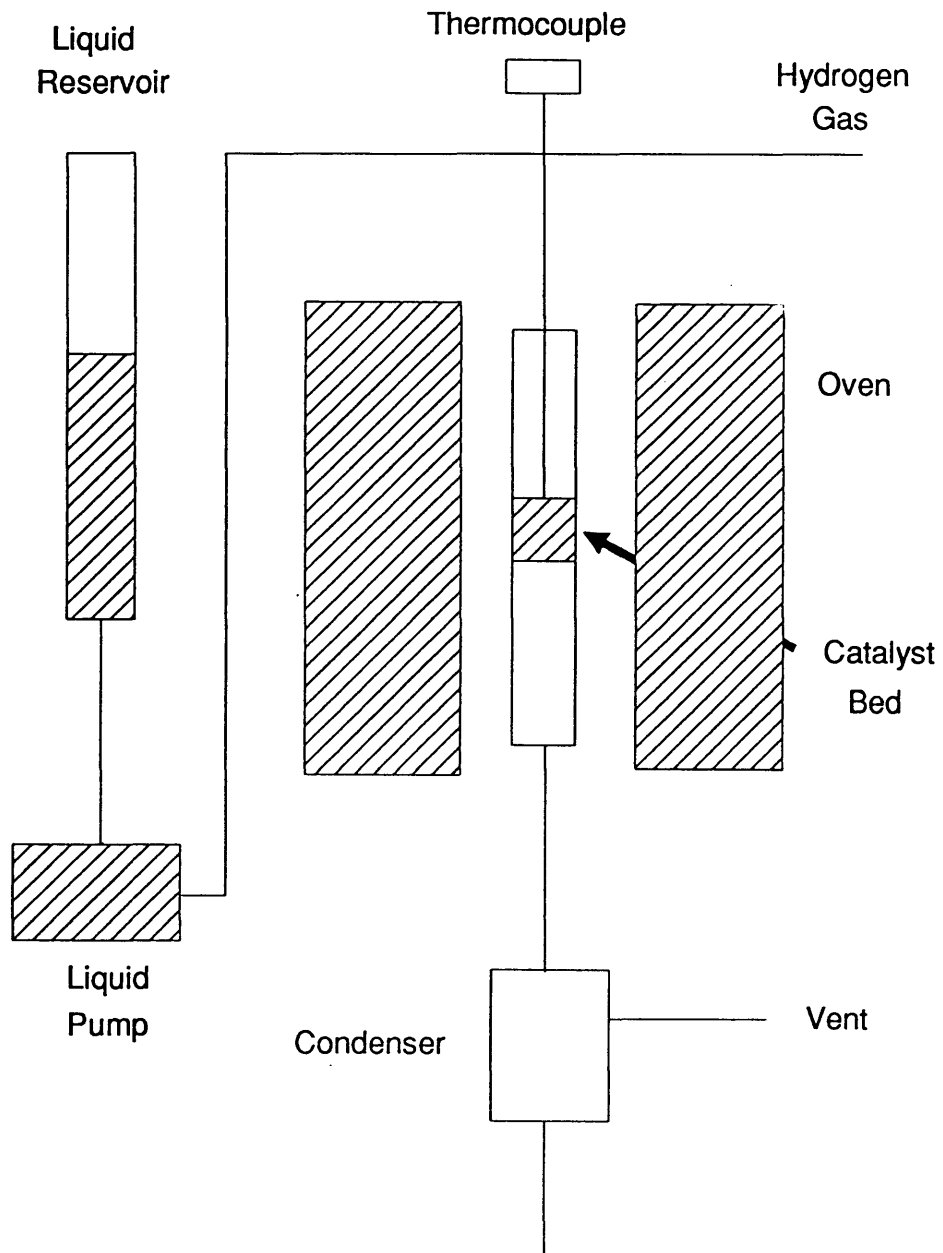


Figure 4. Schematic of catalyst activity evaluation system.

4.6.1 Catalyst Bed

The central component of this reactor system consisted of a 1/2" O.D., 0.402" I.D. and 21" total length 316 stainless steel tube with a stainless steel wire screen at the center. In the reactor tube, the catalyst bed occupied the central 1/4" of the isothermal zone. The catalyst bed configuration is shown in **Figure 5**. The concentration of the catalyst bed was 0.20 grams 20/40 mesh catalyst diluted in a 1:5 weight ratio with inert 10/15 mesh quartz chips (the quartz chips were made from quartz waste). The diluted catalyst layer was sandwiched with 1 gram of quartz in the bottom and 2 grams of quartz on the top. The three layers are supported by a steel mesh covered with a plug of pyrex wool used to prevent elutriation of the solids. The reactor tube was heated in a Lindberg tube furnace. The furnace was controlled by an Athena Controls model 400-B temperature controller. Type-K thermocouples were placed at the entrance of the reactor system and at the center of the catalyst bed. Temperatures were scanned using an Omega 10 position selector switch and monitored on an Omega Model 199 digital temperature indicator.

4.7 System Calibrations

To ensure accuracy, the two major pieces of equipment were calibrated by a previous student (*Erickson, 1990*).

4.8 Catalyst Testing

4.8.1 Feedstocks

The model compounds tested for this study were 4-propylphenol (4PP), 4-propylguaiacol (4PG) and syringol (SYR), see **Figure 2**. The 4PP contains both hydroxy and alkene substituents for evaluating the activity of deoxygenation and dealkylation functions of the catalyst. The ideal catalyst will dealkylate but not deoxygenate 4PP to yield primarily phenol. The 4PG contains an additional methoxy group compared to 4PP. The ideal catalyst will remove the propyl side chain and one of the oxygen groups to yield phenol. The syringol contains two methoxy groups and one hydroxy group but no alkyl group. The ideal catalyst should remove both methoxy groups to yield phenol. The feed mixture contained 10 wt% of 4PP, 4PG or SYR in hexane or toluene and 5 wt% of 4PG with 5 wt% of SYR in toluene.

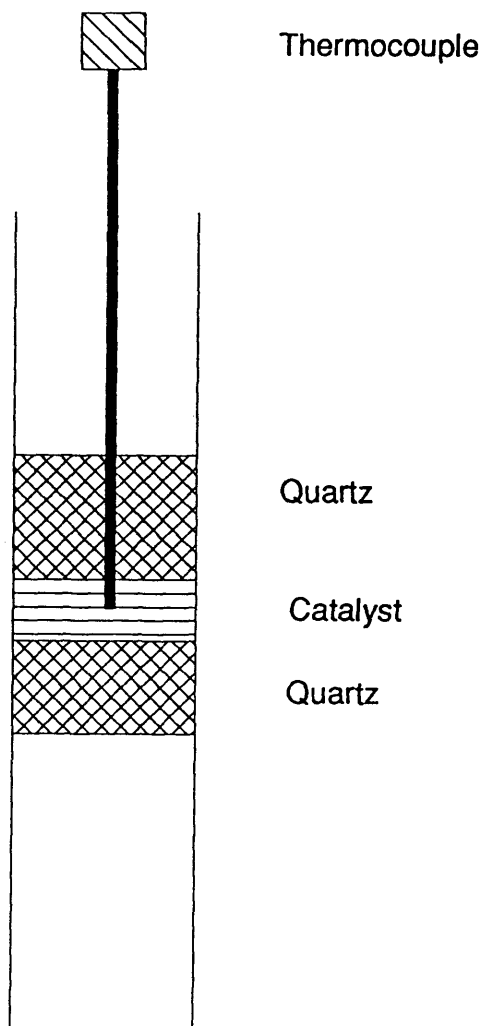


Figure 5. Schematic of reactor tube.

4.8.2 Reaction Conditions

A standard condition of 350°C, 500 psig, and space velocity of 1 g-feed/hr/g-catalyst was used for the first tests of each new catalyst in order to compare their performance. The influence of the temperature and the pressure on the feedstock catalytic conversions were also studied. Temperatures ranged from 350°C to 450°C and pressure from 200 psig to 500 psig.

4.8.3 Catalyst Testing Procedure

The following procedure was used to test the catalysts for this study:

1. Catalyst Bed Preparation

- a. A 5/8" diameter stainless steel wire screen was inserted into the reactor tube using a 3/8" o.d. wooden dowel. The screen was positioned approximately 4 cm below the center of the experimentally determined isothermal zone of the reactor tube in order to assure that the catalyst was at the center of the isothermal region.
- b. Approximately 1 gram of quartz was gently placed on top of the screen. A quantity of 0.2 g catalyst was weighed out and mixed

with approximately 1 gram of the 10 mesh quartz to produce a diluted catalyst. The diluted catalyst was placed into the reactor tube to form the catalyst bed.

- c. Approximately 2 grams of quartz was added to the top of the reactor tube.

2. System Setup and Leak Testing

- a. The catalyst containing reactor tube was gently attached to the reactor system by quick-connect swagelock connectors located at both ends of the reactor tube. The on/off valves downstream of the reactor were closed. The on/off valves upstream of the reactor were opened.
- b. Helium was added into the reactor system until the pressure reached 600 psig. The gas inlet valve of the helium was then closed. The system was allowed to remain pressurized for over five hours.
- c. If loss of pressure indicated leaks, the leaks were corrected. The pressure in the system was checked again after five hours to confirm that the system was not leaking. The experiment was then resumed. The reactor was depressurized by opening the on/off valve and the needle valve downstream from the reactor.

3. Experiment

- a. After the helium was released, the on/off valve downstream of the reactor was closed. The system was repressurized to 500 psig with hydrogen. The system pressure was maintained at 500 psig and the hydrogen outlet flow was controlled to approximately 50 ml/min on the hydrogen mass flow meter with the needle valve downstream of the reactor.
- b. All the heating tapes on the gas inlet were turned on. The temperature of the catalyst bed was raised to 450°C over a one hour period. The catalyst was reduced in hydrogen at 450°C for two hours.
- c. The temperature of the catalyst bed was then reduced to 350°C and the hydrogen flow was lowered to 20 ml/min.
- d. The feedstock was added to the jacketed buret. A submersible pump was turned on to circulate cooling water through the jacketed feed buret and the steel condenser. The submersible water pump was immersed in an insulated container filled with ice water.
- e. The Milton Roy Minipump was turned on when the reactor system conditions had stabilized at 350°C, 500 psig, and gas flow of approximately 20 ml/min.. The liquid flow rate was

maintained at 3.5 ml/hr.

- f. The actual liquid flow rate was monitored and recorded by the change of the buret level and the minipump reset when necessary. The system pressure and outlet gas flow rate were maintained by periodically adjusting the hydrogen gas flow valve.
- g. Liquid samples were collected at half-hour intervals. Samples were saved after the system reached a steady state, usually several hours after the liquid flow was started.
- h. The reaction was allowed to continue at the desired conditions until steady state was attained, as evidenced by the analysis of the products by gas chromatography.

4. Shutting off the System

- a. After the experiment was finished, power to the liquid pump, the submersible water pump, and the heating tapes was shut off.
- b. The needle valve downstream from the reactor was opened to depressurize the reactor. When the pressure reached approximately 50 psig, a slow flow of helium (approximately 10 ml/min.) was turned on to flush the system. The helium was left flowing through the system overnight.
- c. The reactor tube was removed the following day. The catalyst

bed was pushed out from the bottom and the particles were examined for signs of discoloration and coking.

4.9 Product Analysis

The primary analytical technique for determining the reactant conversion and product distribution was gas chromatography (GC). This was supplemented with combined gas chromatography/mass spectrometry. These methods helped to elucidate the chemical changes which the reactants underwent.

4.9.1 Gas Chromatography

Liquid product samples were analyzed on a Perkin-Elmer (PE) Sigma-3B gas chromatograph using a thermal conductivity detector and helium as the carrier gas. The GC was equipped with a 10 foot packed column containing 10% SP-1000 on 80/100 mesh Supelcoport packing. The SP-1000 liquid phase is a nitroterephthalic acid modified polyethylene glycol and is moderately polar. Separation in this column is a function of both the polarity and the boiling point of the compound. All identifiable reaction products were separated effectively in this column.

4.9.2 Calibration of Gas Chromatograph

Calibration of the thermal conductivity detector (TCD) in the gas chromatograph (GC) was performed for liquid reactants and products. The relative weight response factors (RRF) for 18 compounds are presented in **Table A-23**. The compounds of dipropylphenols (1), (2) and (3) in **Table A-23** are isomers, which were labeled by a previous student (*Erickson, 1990*).

The RRF's for the PE Sigma-3B GC were used, compared to a previous calibration using an HP-5840A GC (*Erickson, 1990*) and to literature values (*Dietz, 1967*). There is good agreement between the RRF values for the hydrocarbon products, but there is a significant difference for the oxygenated reactants and products. The phenol RRF value (0.87) is close to that obtained for oxygenated compounds of similar molecular weight, such as cyclohexanol (0.89).

The RRF values followed by a question mark are estimates based on literature and laboratory data for similar compounds. The use of estimated RRF values was necessary because reference samples were not available. The equations to calculate the weight factor, RRF and mole% of products are listed in **Appendix B**.

4.9.3 GC Retention times

Retention times for the reactants and products during the experiments were determined by GC with a comparison to standards and using a computer library search to compare unknowns to reference mass spectra (GC/MS). The retention times of PE Sigma-3B GC for various compounds using the column as above are shown in **Tables A-24, A-25 and A-26**. The operating conditions for the GC are shown in **Table A-27**.

4.9.4 Gas Chromatography/Mass Spectrometry

A Hewlett-Packard 5890 gas chromatography / 5970 Mass Selective Detector (GC/MS) was used for confirm the product identification based on the above GC analysis. The HP-5890 GC was equipped with a 15 meter long, high performance crosslinked methyl silicone capillary column. The HP-5970 quadrupole mass spectrometer used an electron impact ionization source and had a total ion current (TIC) detector.

The identification of a specific peak on the TIC chromatogram was made by use of the NBS mass spectral database (MSD). This database contains 38,971 compounds and is stored on the internal hard disc of the GC/MS system computer.

The GC run parameters and the MS acquisition parameters are listed in **Table A-28 and Table A-29**.

4.10 Solvent for a Model Lignin Feedstock

Hexane was previously used as the solvent for 4-propylphenol and 4-propylguaiacol (*Erickson, 1990*). Hexane was selected because it was relatively inert under the conditions selected. However, it was not suitable for a more realistic lignin feedstock such as syringol (the solubility of syringol in hexane was lower than 10 wt%). In addition, other studies in the Surface and Catalyst Laboratory of CSM indicate that hexane causes excessive catalyst coking on platinum metal (*Frerichs, 1984 and Hadsell, 1985*).

Since lignin has significantly more oxygen than the model compounds studied, syringol was selected to test the catalyst deoxygenation capability. Therefore a solvent which has the potential to dissolve syringol was needed. This solvent must not interfere with the product distribution or the catalyst activity. Several potential solvents were evaluated and toluene was selected as the best candidate.

Chapter 5

EXPERIMENTAL RESULTS AND DISCUSSION

5.1 Evaluation of Catalysts

In order to evaluate each new catalyst, over 30 individual tests were completed. The total experimental run time was over 250 hours. The experimental conditions for each run are shown in **Tables 6, 7 and 8**.

5.2 Reactor Calibration Tests

The catalyst bed was initially sandwiched between layers of α -alumina (*Erickson, 1990*) in order to obtain a uniform flow. Initial catalyst testing was done using α -alumina as the "inert" sandwich material for comparison with a previous study. However, as tests were conducted using lignin type model compounds it became clear that α -alumina was not inert as first assumed.

Table 6. Run conditions

<u>Run #</u>	<u>Catalyst</u>	<u>Temp.</u> <u>(°C)</u>	<u>Press.</u> <u>(psig)</u>	<u>Feed</u> <u>Material</u>	<u>Time</u> <u>(hr)</u>
01-02-90	XZ-05A	350-425	250-350	4-PP/H	33.0
01-16-90	XZ-01	350	500	4-PP/H	3.0
01-30-90	XZ-03A	350-450	500	4-PP/H	11.0
03-14-90	XZ-01A	350	500	4-PP/H	3.0
03-07-90	XZ-02A	350	500	4-PP/H	3.0
04-10-90	XZ-07B	350	500	4-PP/H	3.0
05-11-90	XZ-09A	350	500	4-PP/H	3.0
05-15-90	XZ-10A	350	500	4-PP/H	3.0
05-21-90	XZ-01A	350	500	4-PP/H	3.0
05-21-90	XZ-01A	350-400	250-500	4-PP/H	22.0
06-04-90	DE-01A	350	500	4-PP/H	3.0
06-05-90	XZ-01A	350	500	4-PP/H	3.0
06-06-90	XZ-01A	350	500	4-PP/H	3.0
06-07-90	XZ-01A	350	500	4-PP/H	3.0
06-11-90	XZ-13D	350	500	4-PP/H	3.0

Table 7. Run conditions

<u>Run #</u>	<u>Catalyst</u>	<u>Temp.</u> <u>(°C)</u>	<u>Press.</u> <u>(psig)</u>	<u>Feed</u> <u>Material</u>	<u>Time</u> <u>(hr)</u>
06-11-90	XZ-13D	350	500	4-PP/H	3.0
06-15-90	XZ-16D	350	500	4-PP/H	3.0
06-18-90	XZ-15D	350	500	4-PP/H	3.0
06-19-90	XZ-03A	350	500	4-PP/H	3.0
06-21-90	α -Al ₂ O ₃	350-450	500	4-PP/H	6.0
06-20-90	0.8P:Al	350-450	500	4-PP/H	6.5
07-30-90	Quartz	350-450	500	4-PP/H	6.0
08-20-90	XZ-026A	350	500	4-PP/H	3.0
08-23-90	DE-01A	350	500	4-PP/H	3.0
08-25-90	SiO ₂ -Al ₂ O ₃	350-450	500	4-PP/H	6.0
08-27-90	XZ-2D	350	500	4-PP/H	3.0
08-28-90	XZ-20D	350-450	200-500	4-PP/H	12.5
08-31-90	XZ-20D	350-450	200-500	4-PP/T	12.5
09-04-90	XZ-20D	350-450	200-500	Toluene	6.5
09-07-90	XZ-20D	350-450	200	SYR/T	9.0

Table 8. Run conditions

<u>Run #</u>	<u>Catalyst</u>	<u>Temp.</u> <u>(°C)</u>	<u>Press.</u> <u>(psig)</u>	<u>Feed</u> <u>Material</u>	<u>Time</u> <u>(hr)</u>
10-25-90	XZ-28	350	500	4-PP/H	3.0
11-12-90	XZ-28	350-450	200-500	Toluene	12.5
11-19-90	XZ-28	450	200-350	Toluene	9.0
03-07-91	XZ-28	400-450	300-500	SYR/T	8.0
03-11-91	XZ-28	400-450	200	SYR/T	6.0
03-13-91	XZ-28	400-450	200	4-PG/T	6.0
03-17-91	XZ-28	400-450	300	4-PG/T	6.0
09-05-92	XZ-29	350	500	4-PP/H	3.0
04-23-93	XZ-28	450	300	Mix/T	3.5

Definitions:

4-PP/H = 10 wt% 4-propylphenol + 90 wt% hexane

4-PP/T = 10 wt% 4-propylphenol + 90 wt% toluene

4-PG/H = 10 wt% 4-propylguaiacol + 90 wt% hexane

SYR/T = 10 wt% syringol + 90 wt% hexane

Mix/T = 5 wt% 4-propylguaiacol + 5 wt% syringol + 90 wt% toluene

Toluene = 100 % toluene, XZ = Xianghong Zhao, DE = Dee Erickson

The α -alumina was replaced with more inert quartz material. Calibration tests to evaluate the activity of the reactor tube system in the absence of a catalyst were conducted using both α -alumina and quartz particles placed in the catalyst bed.

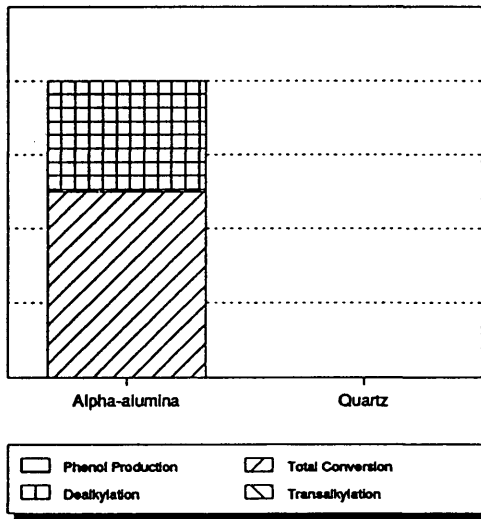
5.2.1 Activity and Selectivity of α -Alumina

The results of 4-propylphenol conversion over the α -alumina are shown in **Appendix A, Table A-1**. At 350°C and 500 psig, 5 mole% methylcyclohexane and 8 mole% dipropylbenzene were produced. No phenol or dipropylphenol was produced. At 450°C and 500 psig, significant amounts of propylcyclohexane, phenol and dialkylphenols were produced. Although α -alumina has been successfully used as an inert catalyst bed support material in other studies, it is too reactive for consideration in this work.

5.2.2 Activity and Selectivity of Quartz

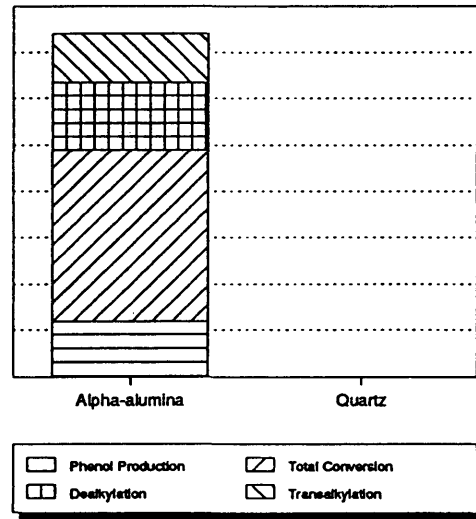
Alpha-alumina was replaced by quartz chips and tested for 4-propylphenol conversion at the same conditions. Quartz was shown to have no activity (**Appendix A, Table A-2**). Comparison of the activity and the selectivity of α -alumina and quartz for 4-propylphenol conversion is shown in **Figure 6**. This data shows quartz remains inert over the range of reaction conditions planned for catalyst evaluation.

Activity and selectivity of alpha-alumina and quartz for 4-propylphenol conversion



Temp=350 C, Pressure=500 psig
Figure 6 (Table A-1 and A-2)

Activity and selectivity of alpha-alumina and quartz for 4-propylphenol conversion



Temp=450 C, Pressure=500 psig
Figure 6 (Table A-1 and A-2)

Figure 6. Comparison of activity and selectivity of α -alumina and quartz for 4-propylphenol conversion.

5.3 Effect of Preparation on Pt/AlPO₄-Al₂O₃ Activity

In order to compare this study to a previous study (*Erickson, 1990*), several Pt/AlPO₄-Al₂O₃ catalysts were prepared and tested using the six different AlPO₄-Al₂O₃ supports which had been made at different times. The details of their preparation are summarized in **Appendix A, Table A-3**. The relative activity and selectivity for each catalyst is given in **Appendix A, Table A-4**.

The replication of the AlPO₄-Al₂O₃ support preparation was difficult in this study. The catalyst preparation and pretreatment has a marked effect on the final behavior of the catalyst. The preparation appears to be especially sensitive to the impregnation volume and calcination temperature used. The optimum preparation conditions appear to be 0.9 ml-solution/g-support for impregnation of the platinum solution and a calcining temperature of 500°C for 24 hours.

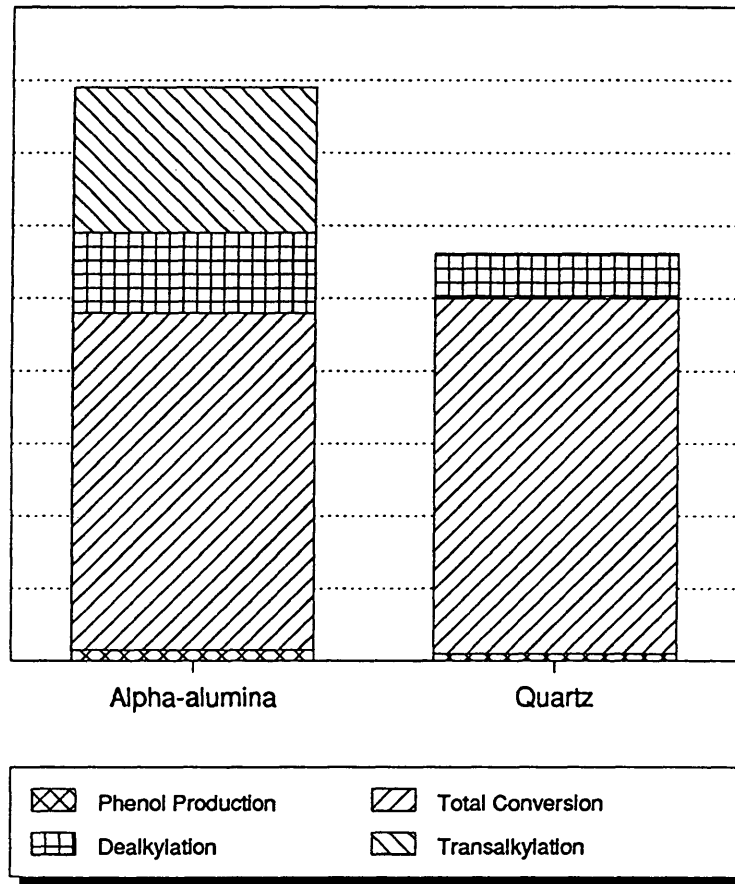
It was not possible to prepare a catalyst which duplicated the performance of a catalyst (DE-01A) reported in a previous study, but it was possible to prepare a series of catalysts (XZ-01A, XZ-16D, and XZ-15D) with almost identical behavior.

5.4 Effect of Quartz vs α -alumina on Catalyst Activity and Selectivity

The initial catalyst tests in this study were made using layers of α -alumina above and below the catalyst bed in order to compare results with those reported earlier (*Erickson, 1990*). The entire catalyst bed contained approximately 90 volume % α -alumina, the remainder being catalyst. The catalyst was 0.3 wt% platinum supported on $\text{AlPO}_4\text{-Al}_2\text{O}_3$ ($\text{Pt/AlPO}_4\text{-Al}_2\text{O}_3$) with a P:Al atomic ratio of 0.8 (0.8P:Al).

As previously stated, reactor calibration tests for the activity of α -alumina showed a small but unacceptable deoxygenation activity, while quartz was completely inert to the lignin model compounds tested. Subsequent tests were made using the same catalysts but quartz was used in place of the α -alumina (**Appendix A, Table A-5**). The overall activity decreased but the selectivity of phenol production increased as α -alumina was replaced by quartz. For example, at 350°C and 500 psig, the total activity (4-propylphenol conversion) was 96 mole% using the α -alumina layers, and 87 mole% using quartz layers. The total selectivity for phenol production was 1 mole% using the α -alumina layers and 3 mole% using quartz layers. Comparison of the effects of α -alumina and quartz on catalyst activity and selectivity is shown in **Figure 7**.

Effects of alpha-alumina and quartz
on liquid product distribution



Temp.= 350 C, Pressure=500 psig, 4PP
Fig-7 (Table A-5)

Figure 7. Comparison of the effects of α -alumina and quartz on catalyst activity and selectivity.

5.5 Effect of Temperature on 4-Propylphenol Conversion Over Pt/SiO₂-Al₂O₃

The metal function of each catalyst was evaluated and the test results were compared to those obtained for the catalyst without the metal present. It was concluded that the metal function of the supported catalyst is primarily responsible for the hydrogenation and hydrogenolysis, as expected.

In order to evaluate the lifetime of the catalyst, a standard set of reaction conditions was selected: 500 psig and 350°C. For each test, the initial and final reaction conditions were the same, so that the initial and final activity for all catalysts could be compared. From this, the amount of catalyst deactivation could be determined.

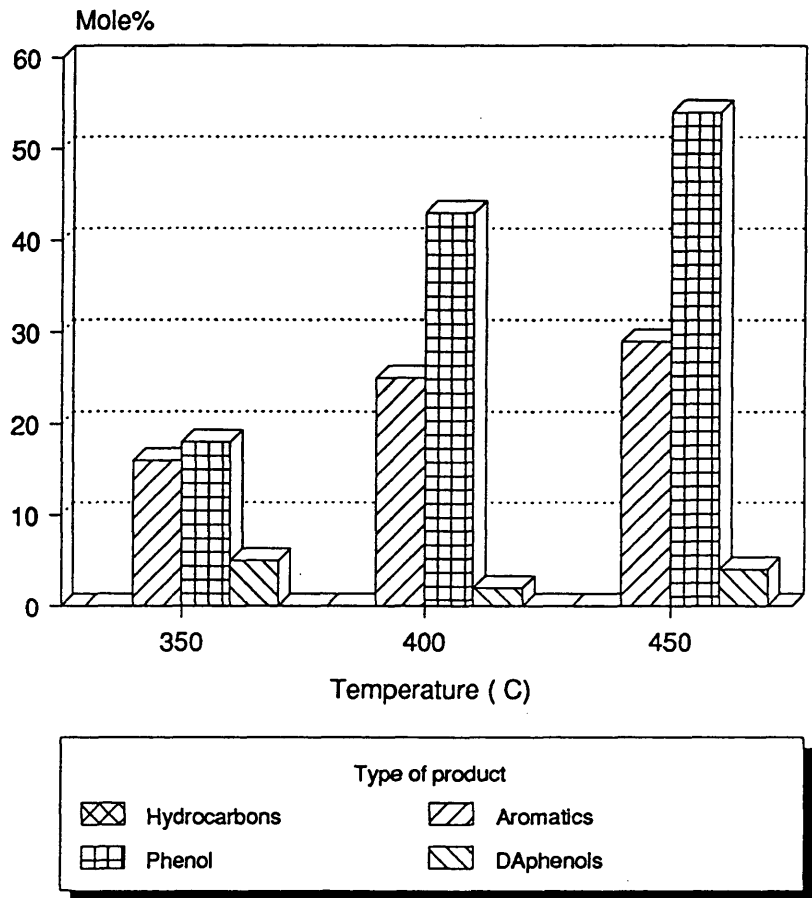
A 0.3 wt % Pt/SiO₂-Al₂O₃ catalyst (designated as XZ-20D) was prepared. A feedstock of 10 wt % 4-propylphenol in hexane was passed over the catalyst, designated as Run-08-28-90. The catalyst was shown to have good activity and selectivity for phenol production. Details of the experiment are give in **Appendix A, Table A-6**.

At the initial standard conditions of 350°C, 500 psig hydrogen and 3 hours experimental time, the 4-propylphenol conversion was 93 mole %, and the major products were hydrocarbon and aromatic compounds. Deoxygenation of the model compound was over 90 mole% under these

conditions. High hydrogen pressure is known to favor the saturation of aromatic rings. Once the ring is saturated, the C-O bond is much weaker due to loss in resonance overlap with the aromatic ring, and the rate of C-O bond cleavage is dramatically increased. The reaction pressure was reduced from 500 psig to 200 psig in an attempt to eliminate saturation of the aromatic rings. Unfortunately, catalyst coking is favored at lower hydrogen pressures. Keeping the temperature constant and lowering the hydrogen pressure resulted in a marked increase in the aromatic hydrocarbon and phenol content with a corresponding decrease in the total conversion (**Appendix A, Table A-6**). Increasing the temperature to 400°C and maintaining the pressure at 200 psig hydrogen resulted in a further increase in the aromatic and phenol content (**Figure 8**). This trend continued as the temperature was increased to 450°C.

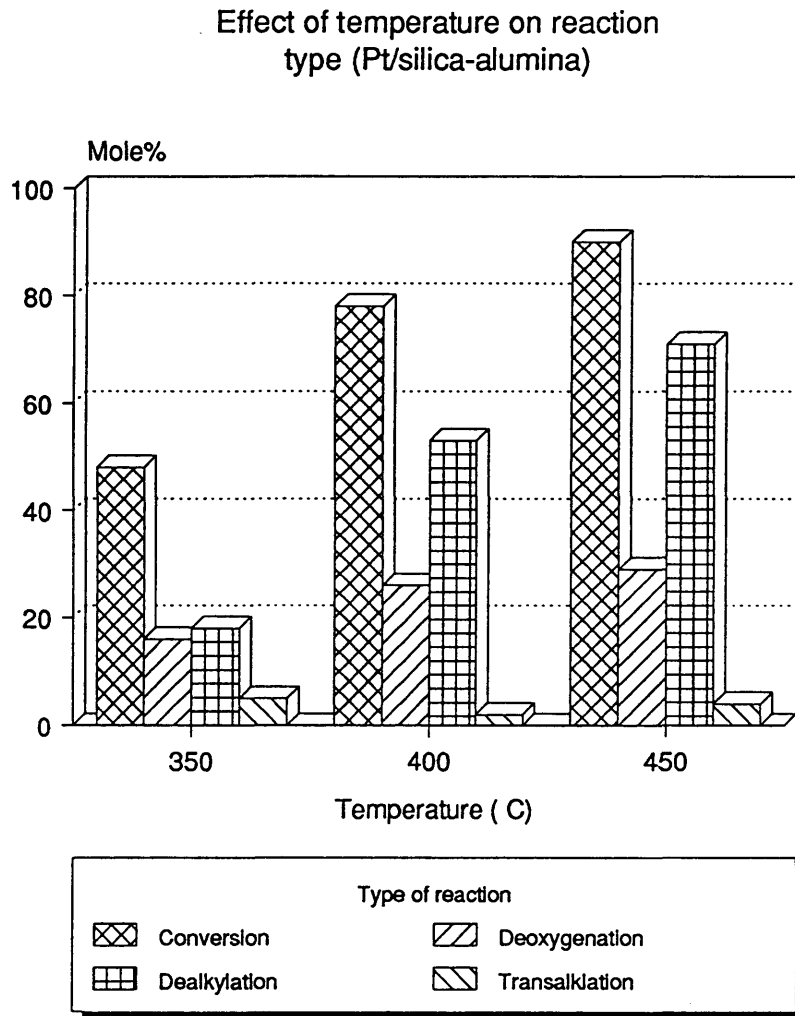
In general the conversion and dealkylation reactions showed an increase as the temperature was increased, while total deoxygenation showed a smaller increase (**Figure 9**). These were precisely the results desired for maximum phenol conversion. This catalyst was as active as the 0.3 Pt/AlPO₄-Al₃O₂, producing as much as 54 mole% phenol, but with a much smaller transalkylation rate, resulting in only 4 mole % of the transalkylation products. This catalyst has good potential as a lignin hydrotreating catalyst.

Effect of temperature on product distribution (Pt/silica-alumina)



4-propylphenol, Pressure = 200 psig
Fig-8 (Table A-6)

Figure 8. Product types of 4-propylphenol as a function of temperature.



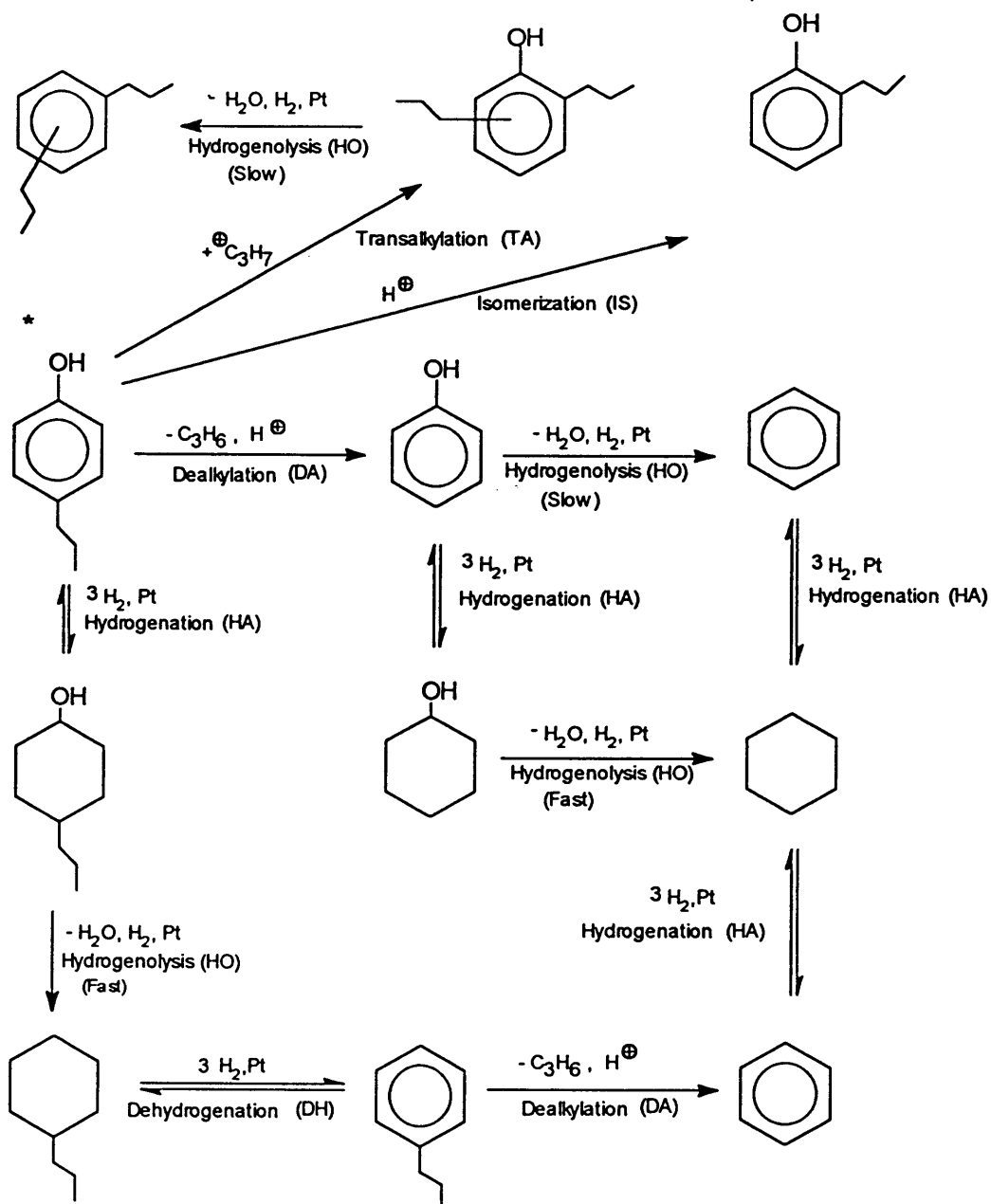
4-propylphenol, Pressure = 200 psig
Fig-9 (Table A-6)

Figure 9. Reaction types of 4-propylphenol as a function of temperature.

In order to check the durability of the catalyst the initial reaction run conditions of 350°C and 500 psig were repeated. The apparent loss of activity was indicative of coking, which means the catalyst will need to be periodically regenerated during any long term operation. The surface carbon content was 3.4% after the 12.5 hour experimental time period.

The mass balance of each test was determined by the percentage of liquid recovery as shown in **Appendix A**. The range of the liquid recovery was between 84 and 99 mole%. To determine the carbon balance of the each test, the carbon in the reactant was set equal to the carbon in the products plus the carbon in the surface coke. The surface coke content was determined by the TGA. The average coke content was between 0.02 and 0.04 g. Therefore, the comparison of activity of the catalysts should have no significant error.

Based on the observed products the following reaction sequence for 4-propylphenol can be proposed (**Figure 10**). The type of catalyst function is shown in each step, where H⁺ represents a surface proton provided by the SiO₂-Al₂O₃ support. The mechanism for the dealkylation reaction most likely involves an electrophilic substitution reaction similar to that observed in homogeneous reaction systems (*March, 1985*). A proposed surface dealkylation mechanism is shown in **Figure 11**.



* 4-Propylphenol

Figure 10. Reaction scheme for 4-propylphenol conversion.

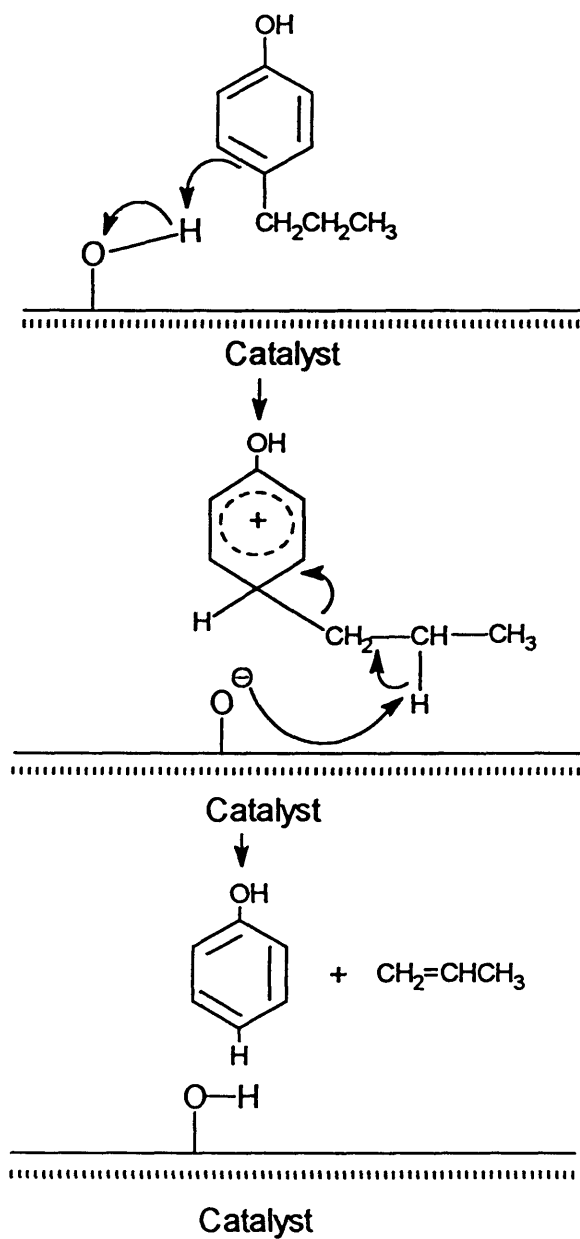


Figure 11. Heterogeneous surface dealkylation mechanism by acid function.

A surface proton on the support undergoes electrophilic attack on the aromatic ring of 4-propylphenol to form an adsorbed σ -complex. The aromatic ring is restored when $C_3H_7^{\oplus}$ is eliminated. The acidic catalyst surface is regenerated when a proton is transferred from the surface $C_3H_7^{\oplus}$ species and propene is produced. Propene is then rapidly hydrogenated to propane over the platinum metal. The production of propane reduces the amount of adsorbed propene and in turn reduces the amount of $C_3H_7^{\oplus}$ surface species.

The dealkylation product, $C_3H_7^{\oplus}$ carbonium, becomes an electrophile for attack on other aromatic rings resulting in the transalkylation reaction **(Figure 12)**.

A proposed heterogeneous surface hydrogenation mechanism is shown in **Figures 13, 14** and **15**. A benzene ring is adsorbed on the surface of platinum metal to form a π -complex, it then changes to form a σ -complex. This is followed by associative adsorption on the platinum metal as shown in **Figure 13**. The associatively adsorbed benzene ring then reacts with the chemically adsorbed hydrogen atom on the platinum surface, and the product is desorbed from the metal surface.

In the second sequence (**Figure 14**), the product formed in the first sequence is associatively adsorbed on the surface of the platinum metal and reacts with the chemically adsorbed hydrogen atom. It is then desorbed from the metal surface. This process is much faster than the first one which opened the aromatic ring.

In the third sequence (**Figure 15**) the product from the second sequence then is associatively adsorbed on the surface of the platinum metal and reacts with the chemically adsorbed hydrogen atom again. Then it is desorbed from the metal surface and terminates the hydrogenation reaction.

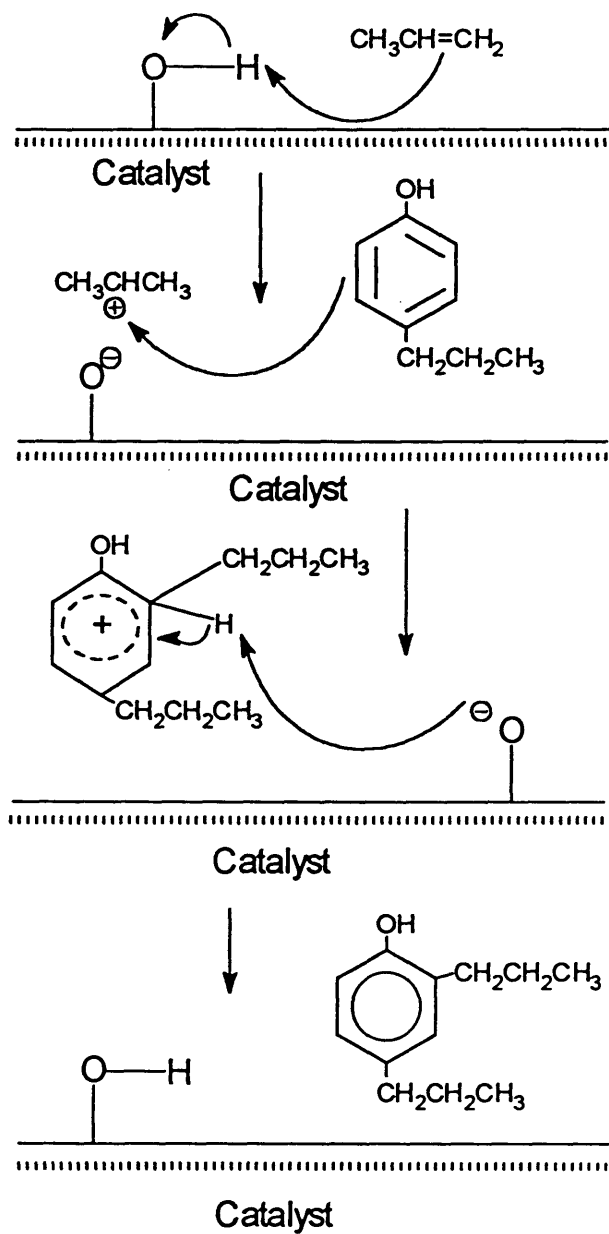


Figure 12. Heterogeneous surface transalkylation mechanism by acid function.

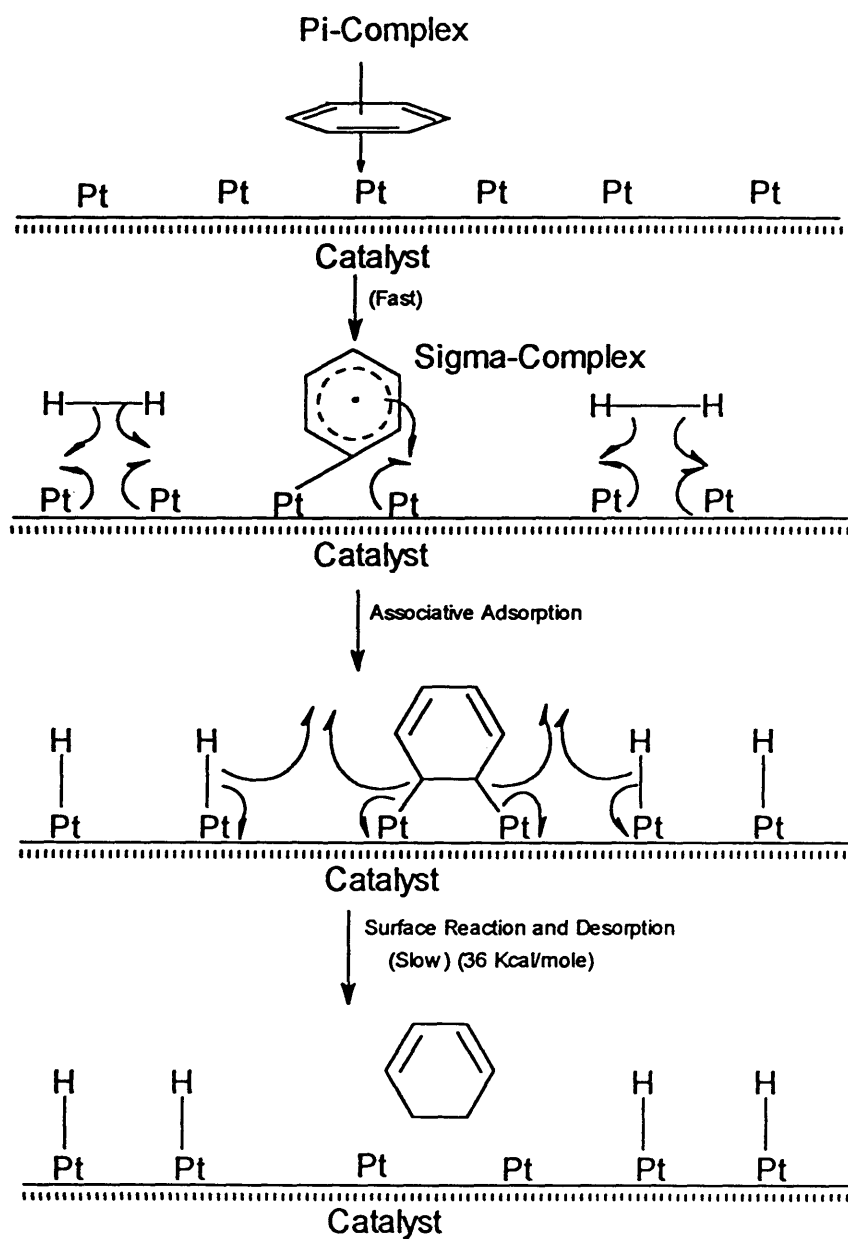


Figure 13. Heterogeneous surface hydrogenation mechanism (1) by metal function.

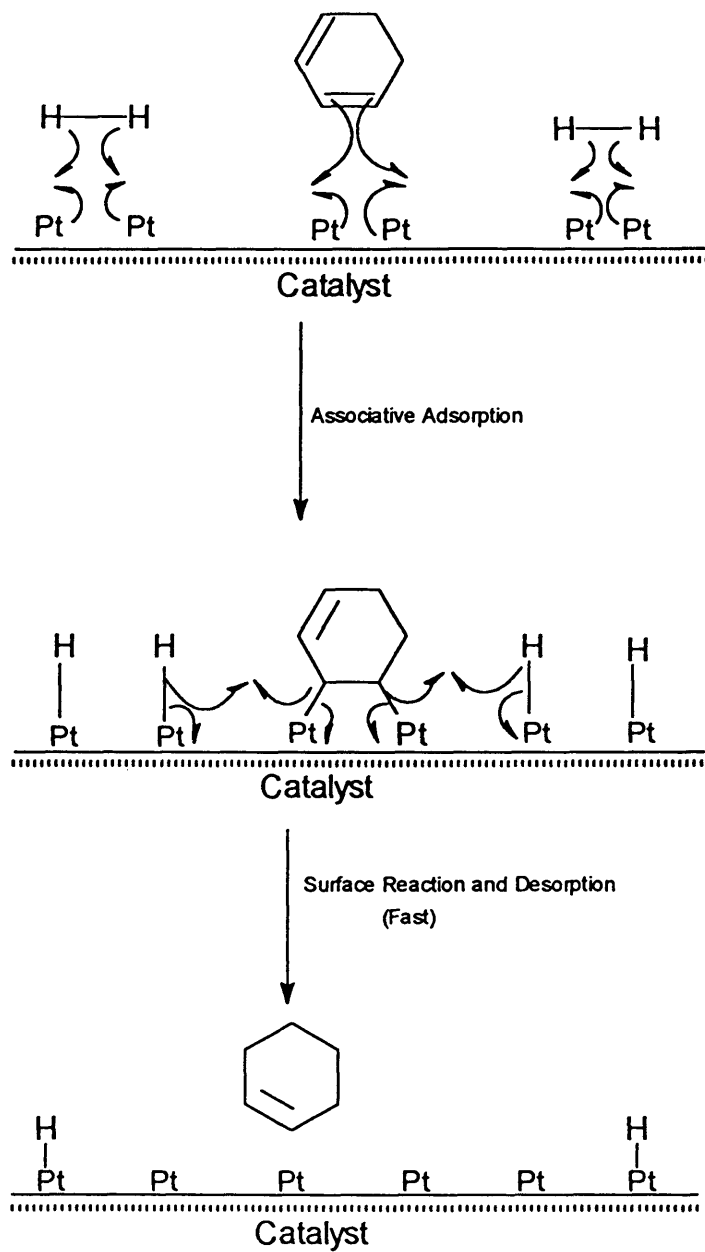


Figure 14. Heterogeneous surface hydrogenation mechanism (2) by metal function.

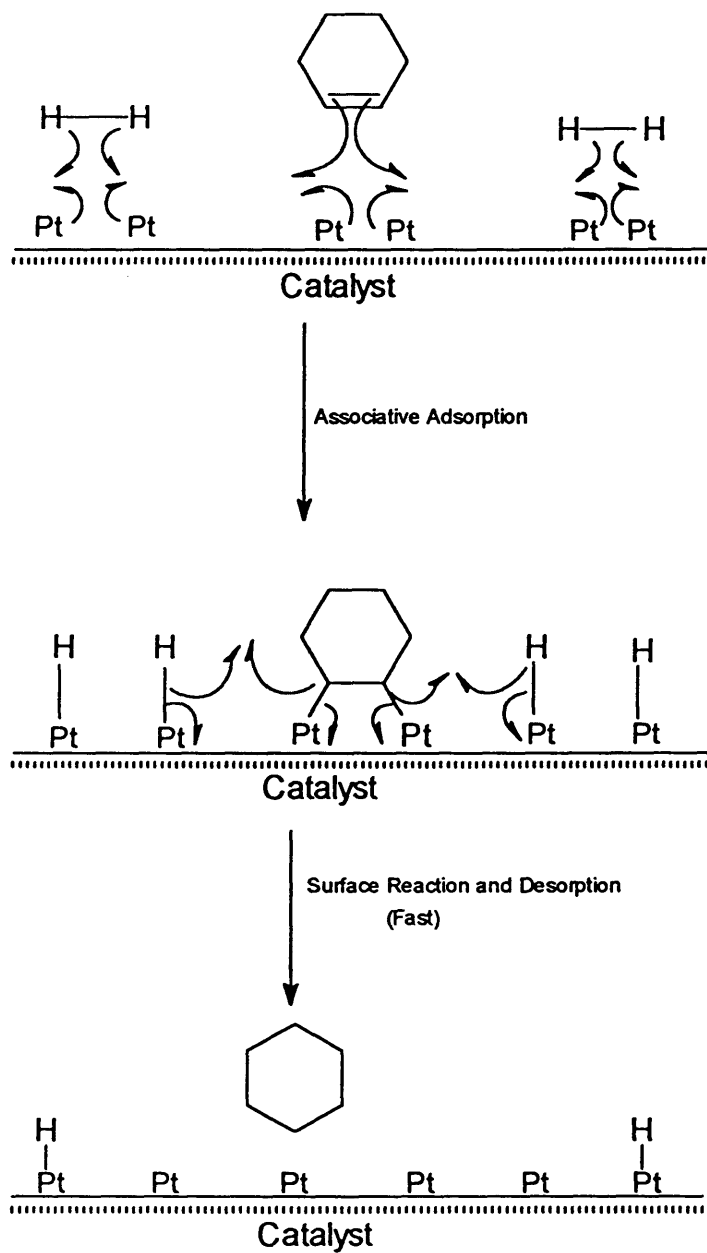


Figure 15. Heterogeneous surface hydrogenation mechanism (3) by metal function.

5.6 Results of Replicate Runs

Using the same catalyst and conditions, five replicate tests were made. The product distributions were nearly identical in each case, as shown in **Appendix A, Tables A-7 and A-8**. This indicates that the variance of the product distributions from run to run is small compared to changes in reaction conditions or catalyst formulation.

5.7 Activity and Selectivity of Catalyst Supports

In order to evaluate the function of each catalyst component, the support material without platinum metal was tested and the results were compared to those obtained for catalyst with the metal present. These results were consistent with the acid function of the support being primarily responsible for the dealkylation reaction as was expected.

5.7.1 $\text{AlPO}_4\text{-Al}_2\text{O}_3$ Support

An $\text{AlPO}_4\text{-Al}_2\text{O}_3$ support (**Figure 16**) with a P:Al ratio of 0.8 was tested prior to adding any platinum metal. This support is strongly acidic and

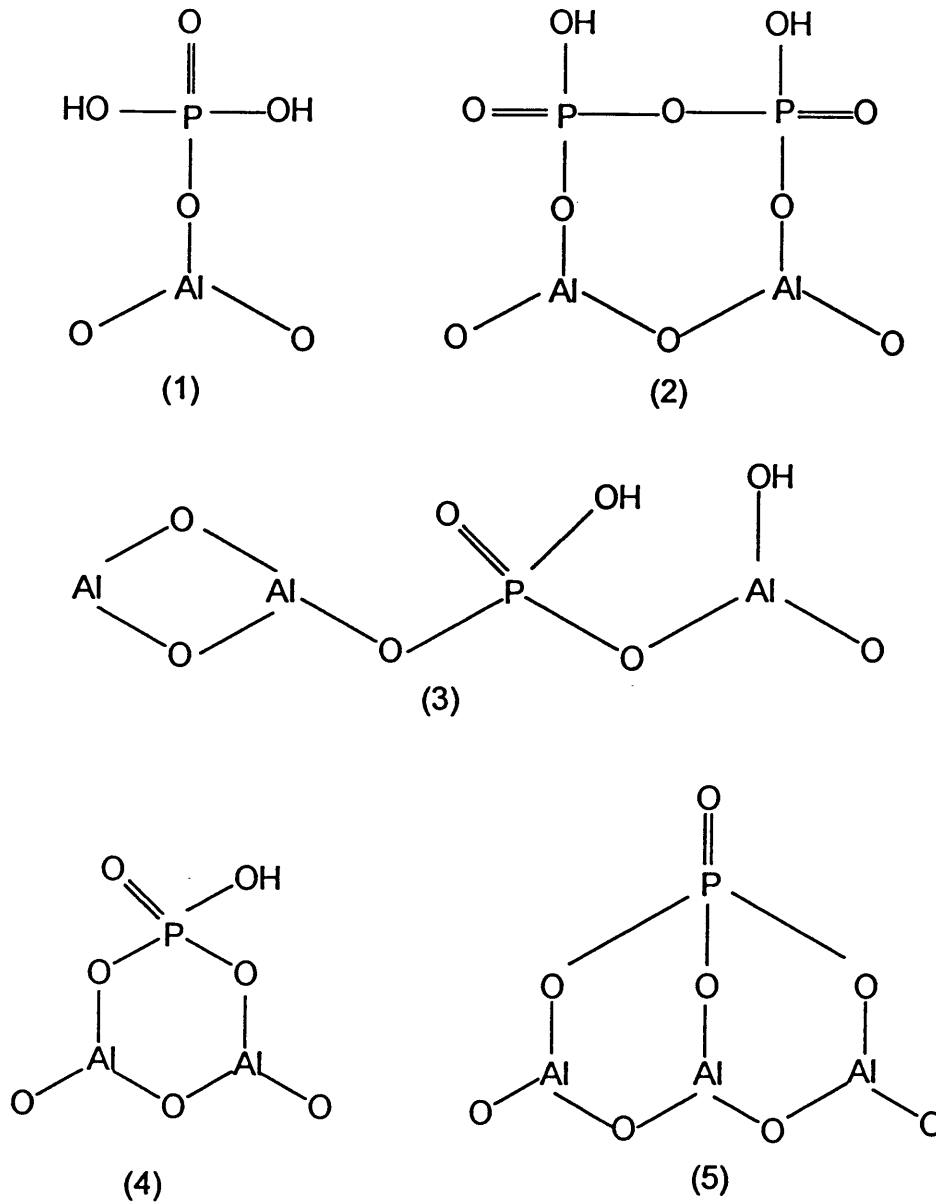


Figure 16. Possible surface structures of $\text{AlPO}_4\text{-Al}_2\text{O}_3$ support.

provides the dealkylation function required for the conversion of alkylated phenols such as propylphenol and propylguaiacol into phenols. The $\text{AlPO}_4\text{-Al}_2\text{O}_3$ support showed a good dealkylation activity but the transalkylation activity was unacceptably high. As an example, transalkylation (TA) involves the conversion of 2 molecules of 4-propylguaiacol into guaiacol and dipropylguaiacol. Dialkyl products are undesirable because the boiling point of their methylether derivatives are unacceptably high for blending into gasoline. At 350°C, 500 psig hydrogen and 3.5 hours, the unreacted 4-propylphenol was 33 mole% and the dipropylphenols yield was 24 mole%. At 450°C, 500 psig hydrogen and 6.5 hours, the unreacted 4-propylphenol was 13 mole% and dipropylphenols yield was 20 mole%. The detailed results are given in **Appendix A, Table A-9**.

5.7.2 $\text{SiO}_2\text{-Al}_2\text{O}_3$ Support

Although the $\text{AlPO}_4\text{-Al}_2\text{O}_3$ support demonstrated excellent activity for the dealkylation reaction, it exhibits an unacceptably high transalkylation activity. In addition, it appears to be very sensitive to the method of preparation, making it hard to duplicate the platinum impregnation step. Therefore, $\text{SiO}_2\text{-Al}_2\text{O}_3$ (**Figure 17**), also known to possess Bronsted acidity, was considered as a potential support material.

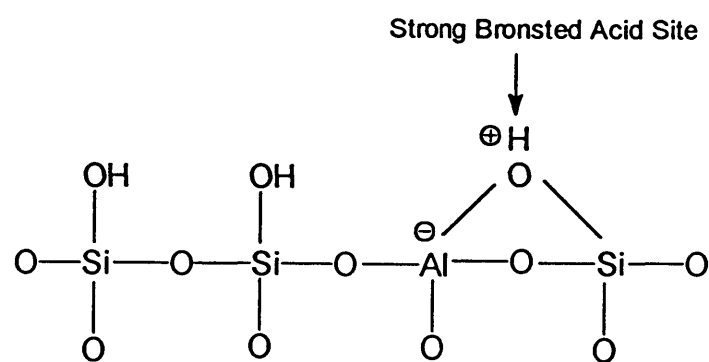
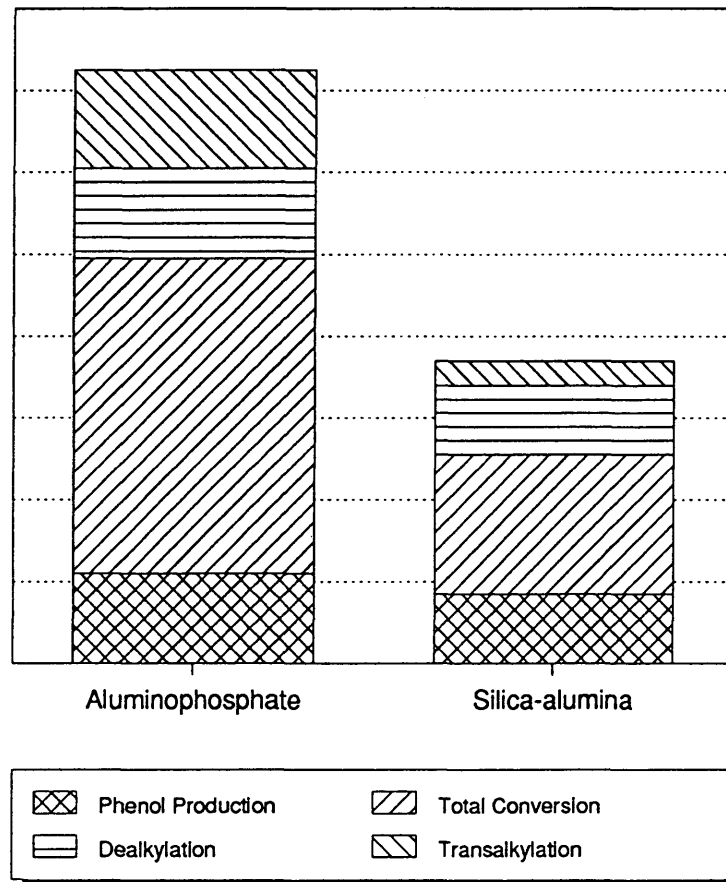


Figure 17. Possible surface structure of $\text{SiO}_2\text{-Al}_2\text{O}_3$ support.

A $\text{SiO}_2\text{-Al}_2\text{O}_3$ support without platinum metal was placed in the space normally occupied by catalyst and sandwiched between the quartz layers. The $\text{SiO}_2\text{-Al}_2\text{O}_3$ support was very selective for phenol production at 450°C , which is similar to the $\text{AlPO}_4\text{-Al}_2\text{O}_3$ blank support. However, the $\text{SiO}_2\text{-Al}_2\text{O}_3$ exhibited a much lower transalkylation activity as evidenced by the presence of little or no dipropylphenol in the product. The results are presented in **Appendix A, Table A-10**. At 350°C , 500 psig hydrogen and 3 hours, the unconverted 4-propylphenol was 66 mole % and the yield of dealkylation products was 17 mole %. At 450°C , 500 psig hydrogen and 6 hours, the unconverted 4-propylphenol was 47 mole % and the yield of dealkylation products was 53 mole %. Comparison of the activity, selectivity, dealkylation and transalkylation reactions of the supports is shown in **Figure 18**.

The product distribution slowly changes with time, suggesting that the support was deactivating. Examination of the catalyst at the conclusion of the experiment (approximately 6 hours later), showed it was severely coked as evidenced by the black color. Coking under these conditions is expected, especially in the absence of a metal hydrogenation function.

Activity and selectivity of
Aluminophosphate and silica-alumina



Temp=350 C, Pressure=500 psig, 4PP
Fig-18 (Table A-9 and A-10)

Figure 18. Comparison of activity, selectivity, dealkylation and transalkylation reactions of supports.

5.8 Effect of Temperature and Pressure on Toluene Conversion

The catalytic reactivity of pure toluene over the XZ-0.3PtSiO₂-Al₂O₃-20D catalyst was studied and designated as Run-09-04-90. The results are given in **Appendix A, Table A-11**.

At 350°C, 500 psig hydrogen and 3.5 hours, 77 mole% of the toluene was converted to hydrocarbon products. The major products were methylcyclohexane (50 mole %) and cyclohexane (27 mole %). Increasing the temperature and dropping the pressure to 450°C and 200 psig reduced the conversion of toluene to 1 mole %. The catalyst did not show the excessive signs of coking observed in previous studies. The results of these studies show that toluene is a good solvent candidate at 450°C and 200 psig of hydrogen.

Pure toluene was also tested under the standard temperature sequence used previously, in order to establish an acceptable range of temperatures and pressures for its use. The results of the reactivity of toluene over 0.3 wt% Pt/SiO₂-Al₂O₃ catalyst are presented in **Appendix A, Tables A-12 and A-13**.

Run-11-12-90 was conducted using the standard test sequence, that is, the test was begun and ended using the test conditions of 350°C and 500 psig to observe changes in catalyst activity during the test. The catalyst performance was observed using a constant reactor pressure of 200 psig and temperatures of 350, 400, and 450°C. The results are given in **Appendix A, Table A-12**. At 350°C, 200 psig hydrogen and 3.5 hours, the unreacted toluene was 26 mole%; at 450°C, 200 psig hydrogen and 11 hours, the unreacted toluene was 98 mole %. These results suggest that toluene does undergo significant reaction at low pressure (200 psig) and low temperature (350°C) as well as at the standard conditions. However, its reactivity at 200 psig decreases rapidly as the temperature is increased to 450°C. The best temperature and pressure ranges were determined to be 400-450°C and 200-300 psig.

The next test sequence was designed to establish the best reaction pressure for this solvent. In Run-11-19-90 the temperature was maintained at 450°C and the pressure was decreased from 350 to 200 psig. At 450°C, 350 psig hydrogen and 3 hours, the unreacted toluene was 91 mole %. At 450°C, 200 psig hydrogen and 9 hours, the unreacted toluene was 99 mole%. The results are given in **Appendix A, Table A-13**. Decreasing the hydrogen pressure decreases the reactivity of toluene.

These results suggest that lower temperatures and higher pressures resulted in excessive ring saturation, which caused a substantial loss of phenol production due to C-O bond hydrogenolysis. Toluene can successfully be used as a solvent for model lignin compounds, in the temperature range of 400 to 450°C, and pressure range of 200 to 300 psig hydrogen.

5.9 Effect of Solvent on Product Distribution

In order to compare toluene with earlier results obtained using hexane as a solvent, a feedstock of 10 wt% 4-propylphenol/toluene was tested with the 0.3 wt% Pt/SiO₂-Al₂O₃ catalyst and the results are given in **Appendix A, Table A-14**. Comparison of the activity and the selectivity of the catalyst using toluene vs hexane as a solvent is shown in **Figure 19**. The selectivity for phenol using toluene and hexane solvents is 63 and 54 mole% respectively. The improvement in phenol production when toluene is used as a solvent is likely due to toluene adsorption on the Pt metal hydrogenolysis site which inhibits phenol adsorption on these sites and thus prevents further reaction.

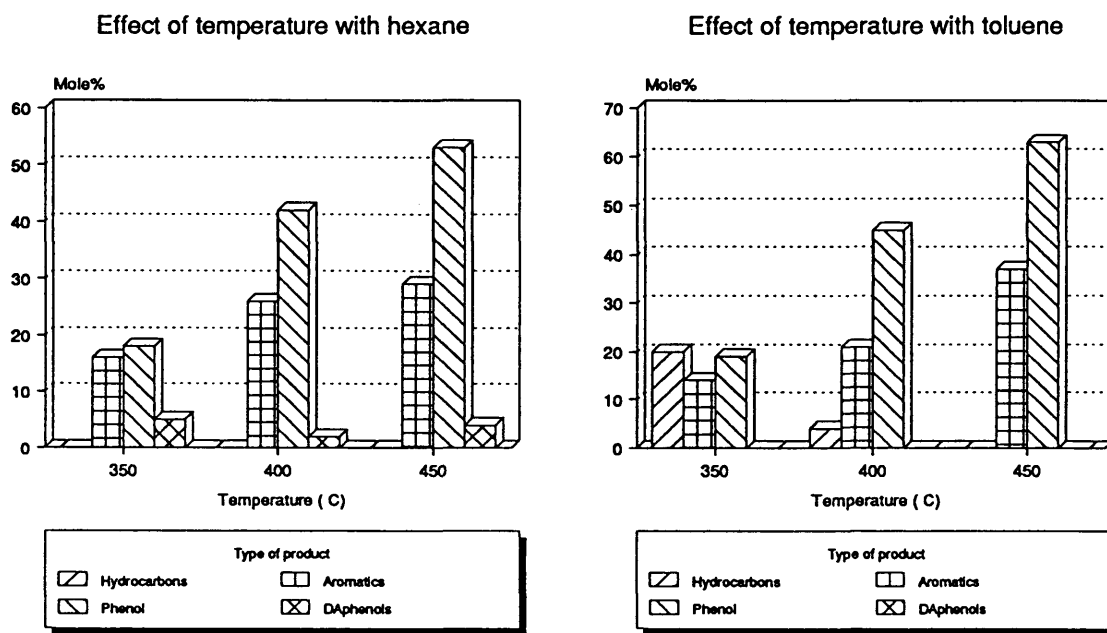
In addition, at 450°C and 200 psig, the activity was 100 mole% conversion of 4-propylphenol using toluene as the solvent as compared to only 90 mole% for hexane.

Most importantly, deactivation due to coking is markedly reduced when toluene is used as a solvent. The surface coke content was 12% with toluene as a solvent, and 18% with hexane as a solvent after 12.5 hours experimental time (**Table 11**). This was in agreement with studies conducted by *Frerichs (1984)* and *Hadsell (1985)* where toluene and hexane were used as model naphtha reforming compounds.

The platinum on the $\text{SiO}_2\text{-Al}_2\text{O}_3$ support demonstrated excellent activity, selectivity for phenol production, very low transalkylation activity, and better resistance to coking when toluene was the solvent instead of hexane.

5.10 Subtracting the Product Due to Toluene

Since some of the toluene and 4-propylphenol products are the same, the product distribution was corrected by subtracting the amount estimated to be due to toluene, using the pure toluene studies as a reference (**Appendix A, Table A-15**).



4-propylphenol, Pressure = 200 psig,
Fig-19-1 (Table A-6)

4-propylphenol, Pressure = 200 psig,
Fig-19-2 (Table A-14)

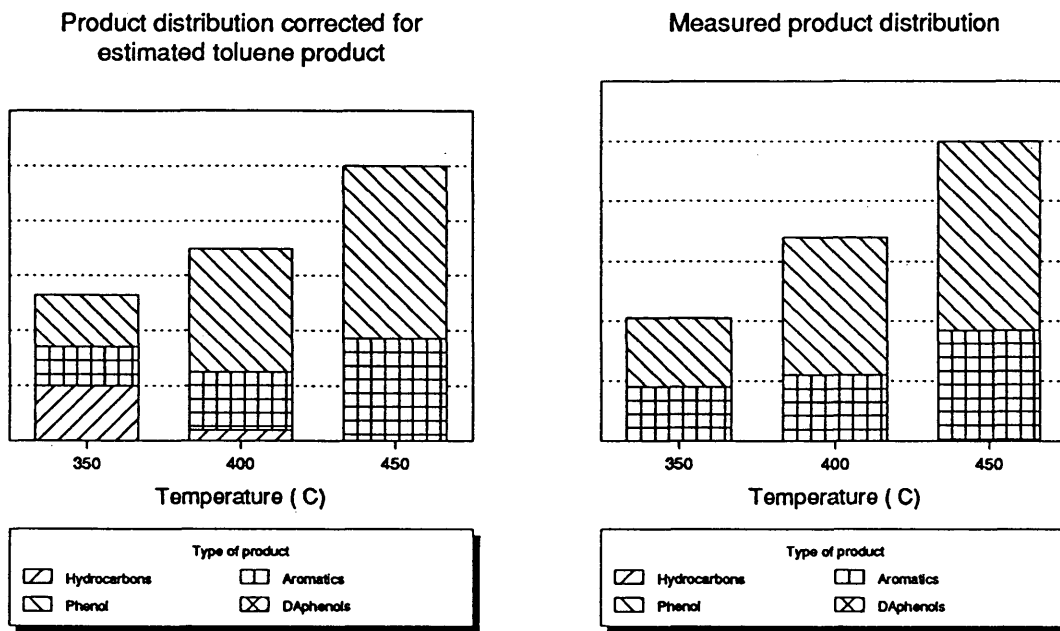
Figure 19. Comparison of activity and selectivity of Pt/SiO₂-Al₂O₃ for toluene and hexane as a solvent in 4-PP conversion.

Comparison of the measured product distribution (**Table A-14**) with the distribution corrected for the estimated toluene products (**Table A-15**) is shown in **Figure 20**.

At 350°C and 500 psig the toluene contribution was very significant, and contributed a serious error to the analysis. When the hydrogen pressure was decreased to 200 psig and the temperature was maintained at 350°C, the contribution of toluene was decreased. At 450°C and 200 psig hydrogen pressure the toluene contribution contributed very little error to the analysis. The overall results suggest that toluene is an acceptable solvent at 400 to 450°C.

5.11 Effect of Temperature on 4-Propylguaiacol Conversion

In order to evaluate the demethoxylation ability of the catalyst, a feedstock of 10 wt% 4-propylguaiacol (2-methoxy-4-propylphenol) in toluene was passed over the 0.3 wt% Pt/SiO₂-Al₂O₃ catalyst at two different pressures. The distribution of major products is shown in **Appendix A, Table A-16** and **Table A-17**. Results of both of the experiments showed a good catalyst activity and excellent selectivity for phenol production.



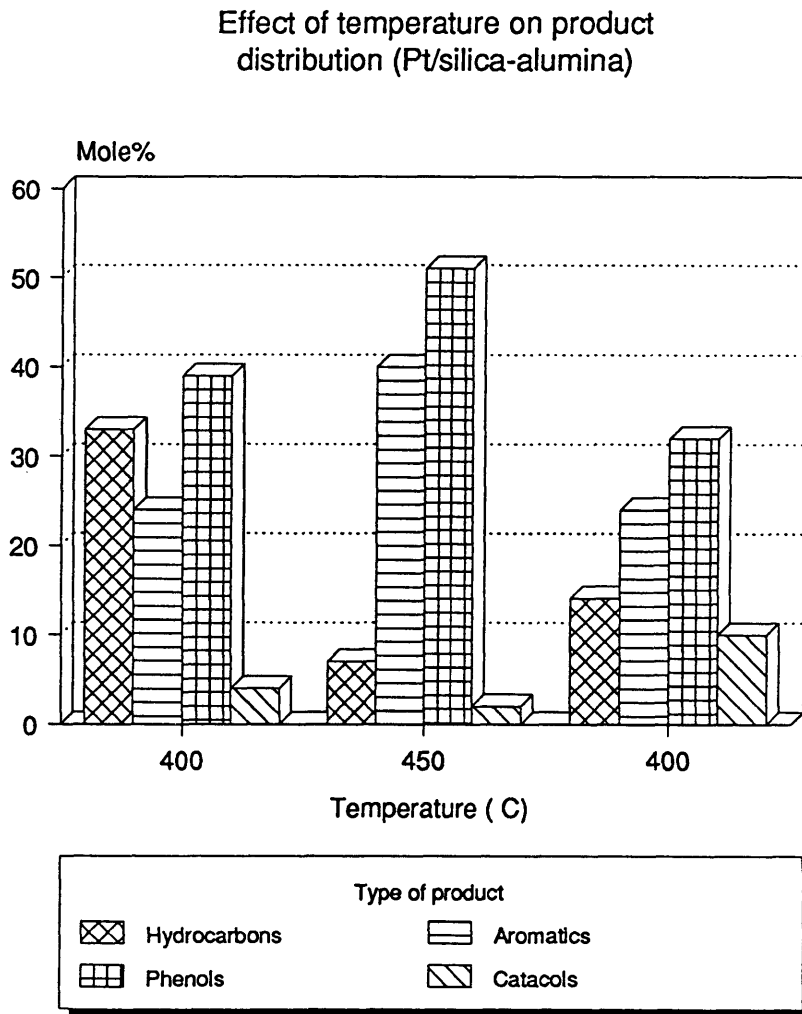
4-propylphenol, Pressure = 200 psig
Fig-20-1 (Table A-15)

4-propylphenol, Pressure = 200 psig
Fig-20-2 (Table A-14)

Figure 20. Comparison of the measured product distribution to the distribution corrected for estimated toluene product.

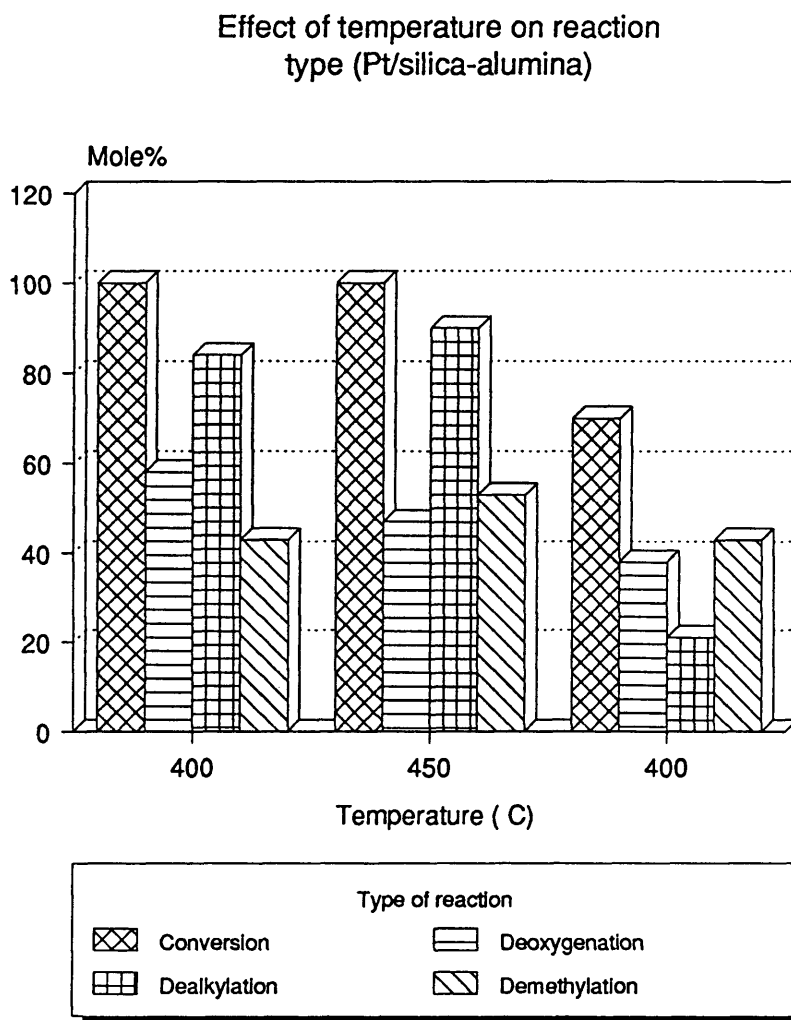
The reaction conditions used were suitable for toluene as a solvent, and for the best selectivity for phenol production based on the study of 4-propylphenol. For one experiment (Run-03-13-91) conditions were 200 psig of hydrogen and a temperature sequence of 400, 450, 400°C and 6 hours total experimental time. For a second experiment (Run-03-17-91) the conditions were 300 psig of hydrogen and a temperature sequence of 400, 450, 400°C and 6 hours. The production (Run-03-13-91) of phenol was 32 mole%, with decreasing amounts of cresol, benzene, and xylene. The conversion of 4-propylguaiacol approached 100 mole% at 4 hours in both runs. The production from toluene in 4-propylguaiacol conversion was assumed to be zero in these analyses, because the production from toluene when using 10 wt% 4-propylguaiacol/hexane as a reactant over the Pt/PAIO₄-Al₂O₃ catalyst at the conditions 350-450°C, 200-500 psig and 12 hours was less than 3 mole% as reported by *Erickson (1990)*.

Increasing the temperature from 400 to 450°C and maintaining the hydrogen pressure at 300 psig resulted in an increase in the aromatic and phenol content (**Figure 21**). The conversion and dealkylation reactions showed a dramatic increase as the temperature was increased, while the selective deoxygenation showed a marked increase and the total deoxygenation showed a marked decrease (**Figure 22**). The results show that these conditions gave maximum phenol production.



4-propylguaiacol, pressure = 300 psig
Fig-21 (Table A-17)

Figure 21. Product types of 4-propylguaiacol as a function of temperature.



4-propylguaiacol, pressure = 300 psig
Fig-22 (Table A-17)

Figure 22. Reaction types of 4-propylguaiacol as a function of temperature.

Based on the observed products the following reaction network for 4-propylguaiacol can be proposed (**Figure 23**). The catalyst functions such as dealkylation (DA), hydrogenation (HA), hydrogenolysis (HO), demethylation (DM) and alkylation (A) are shown in each step. The H° represents a surface proton provided by the $SiO_2-Al_2O_3$ support. The suggested mechanism for the dealkylation reaction is the same as that discussed for 4-propylphenol conversion.

Two proposed heterogeneous surface demethylation mechanisms are shown in **Figures 24** and **25**. For the acid mechanism illustrated in **Figure 24**, a surface proton on the support undergoes electrophilic attack on the oxygen of the methoxy group on the aromatic ring to form an adsorbed σ -complex. The hydroxy group on the benzene ring is formed when CH_3° is transferred from the methoxy group to the surface of the support. The acidic catalyst surface is regenerated when a proton is transferred from the aromatic ring during the electrophilic alkylation reaction with the methyl group on the surface of the support. Such an alkylation reaction mechanism with the methyl group on the surface of the support is proposed in **Figures 26** and **27**. The methyl group on the surface is an electrophilic agent which attacks the aromatic ring on the 4-propylguaiacol to form an adsorbed σ -complex. The aromatic ring is restored when H° is transferred from the ring to the surface of the support.

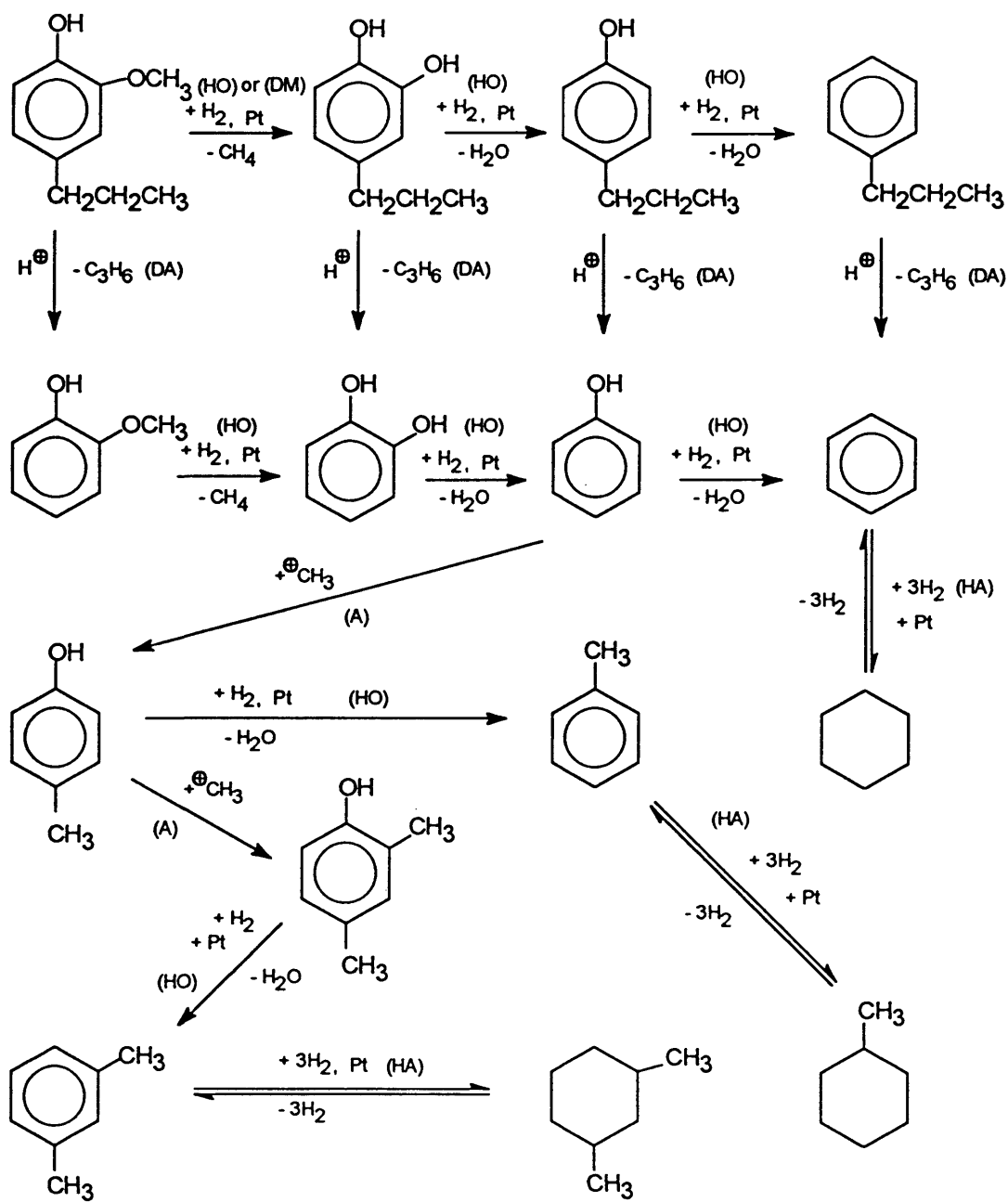


Figure 23. Possible reaction scheme for 4-propylguaiacol conversion.

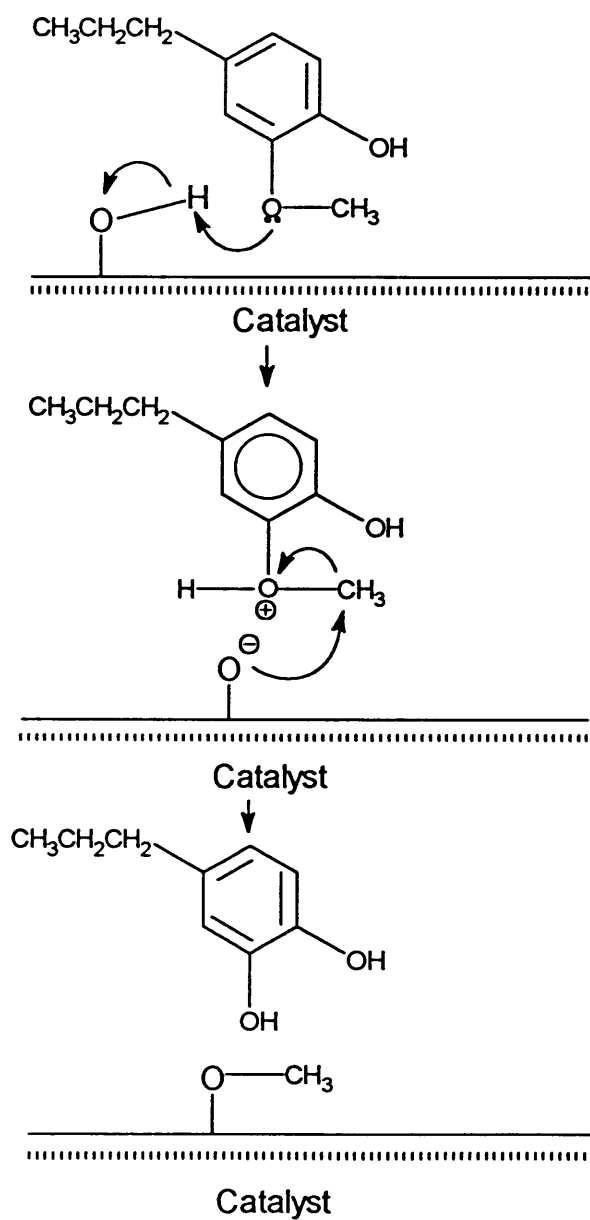


Figure 24. Possible catalyst support demethylation mechanism on an acid site.

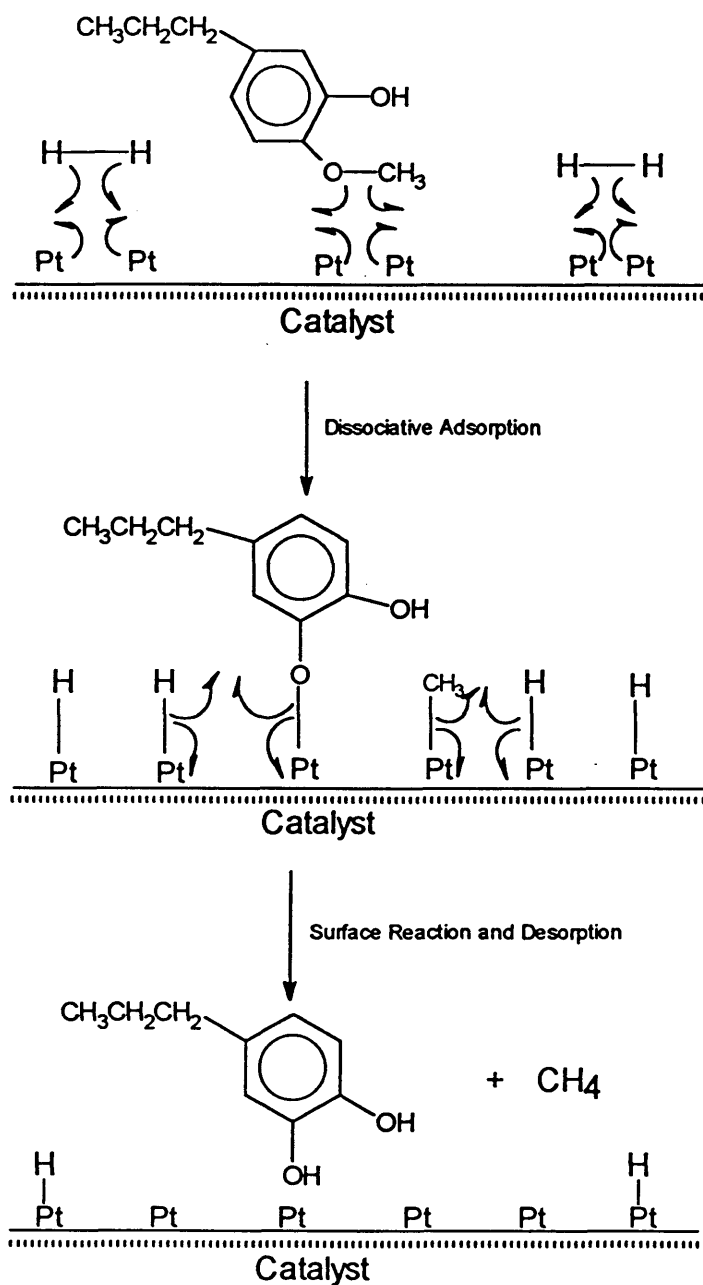


Figure 25. Possible mechanism of metal surface hydrogenolysis for demethylation of 4-propylguaiacol.

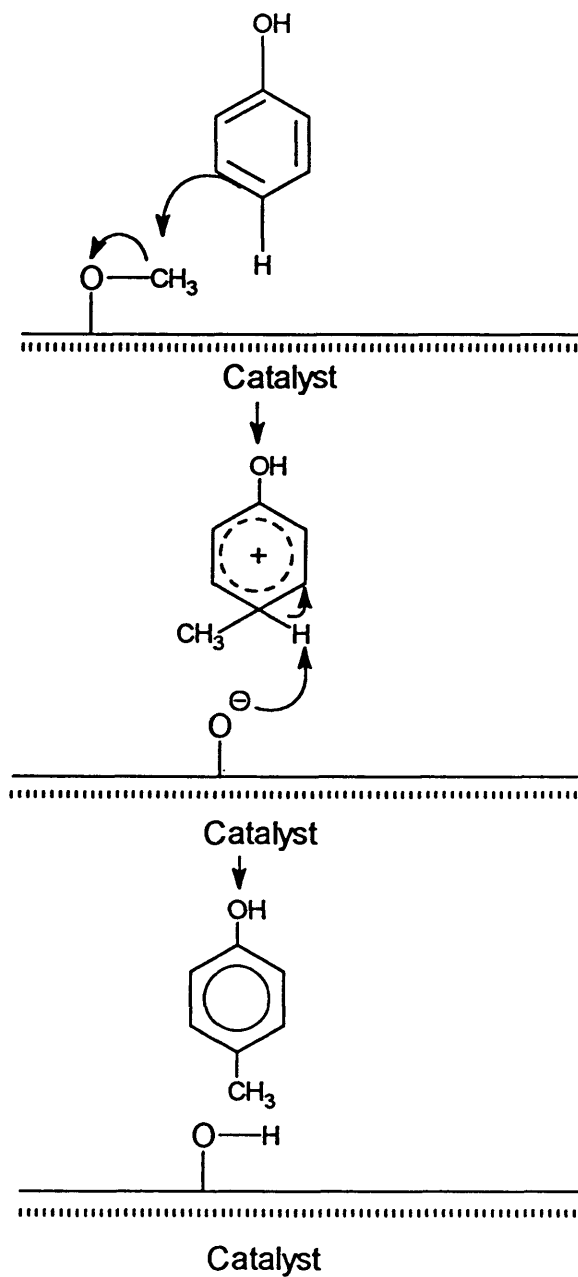


Figure 26. Possible catalyst support alkylation mechanism involving a surface methoxy group.

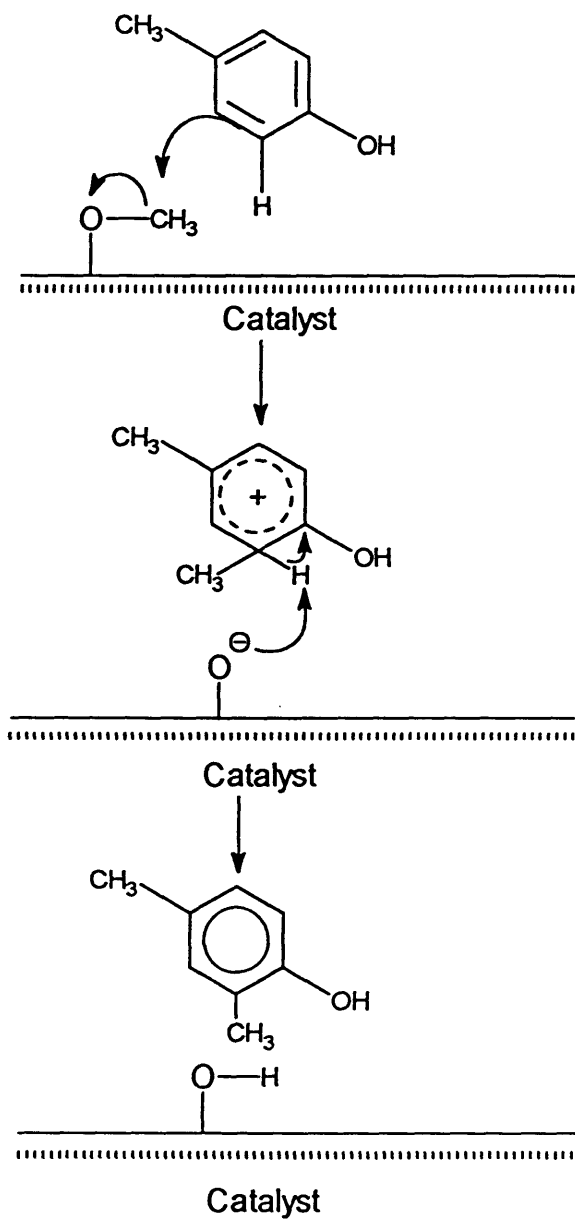


Figure 27. Possible transalkylation mechanism involving a catalyst support acid site.

For the mechanism illustrated in **Figure 25**, the demethylation reaction occurs by the metal function. First, the hydrogen and methoxy groups are dissociatively adsorbed on the metal surface. Then the surface reactions occur between the chemically adsorbed hydrogen atom with the catacol group and the methyl group to form propylcatacol and methane which are desorbed from the metal surface. Based on the production of xylene the heterogeneous demethylation reaction mechanism is more likely to proceed by the acid function than by the metal function. This is because the methyl group chemisorbed on the platinum metal can not undergo the electrophilic alkylation reaction with the benzene.

A proposed heterogeneous surface hydrogenolysis mechanism for dehydroxygenation of the hydroxy group from catacol is shown in **Figure 28**. The catacol adsorbed on the platinum metal forms a π -complex, then forms a σ -complex. The σ -complex is dissociatively adsorbed on the surface of platinum metal, then reacts with the hydrogen atoms to form phenol and water which are desorbed from the metal surface.

Unfortunately, the coking proceeds rapidly. The surface carbon content at 400°C, 200 psig hydrogen and 6 hours was 24%; at 400°C, 300 psig hydrogen and 6 hours was 20%. The coking was less when the experiment started at 300 psig. At the end of the experiment the activity of the catalyst was much lower than at the beginning.

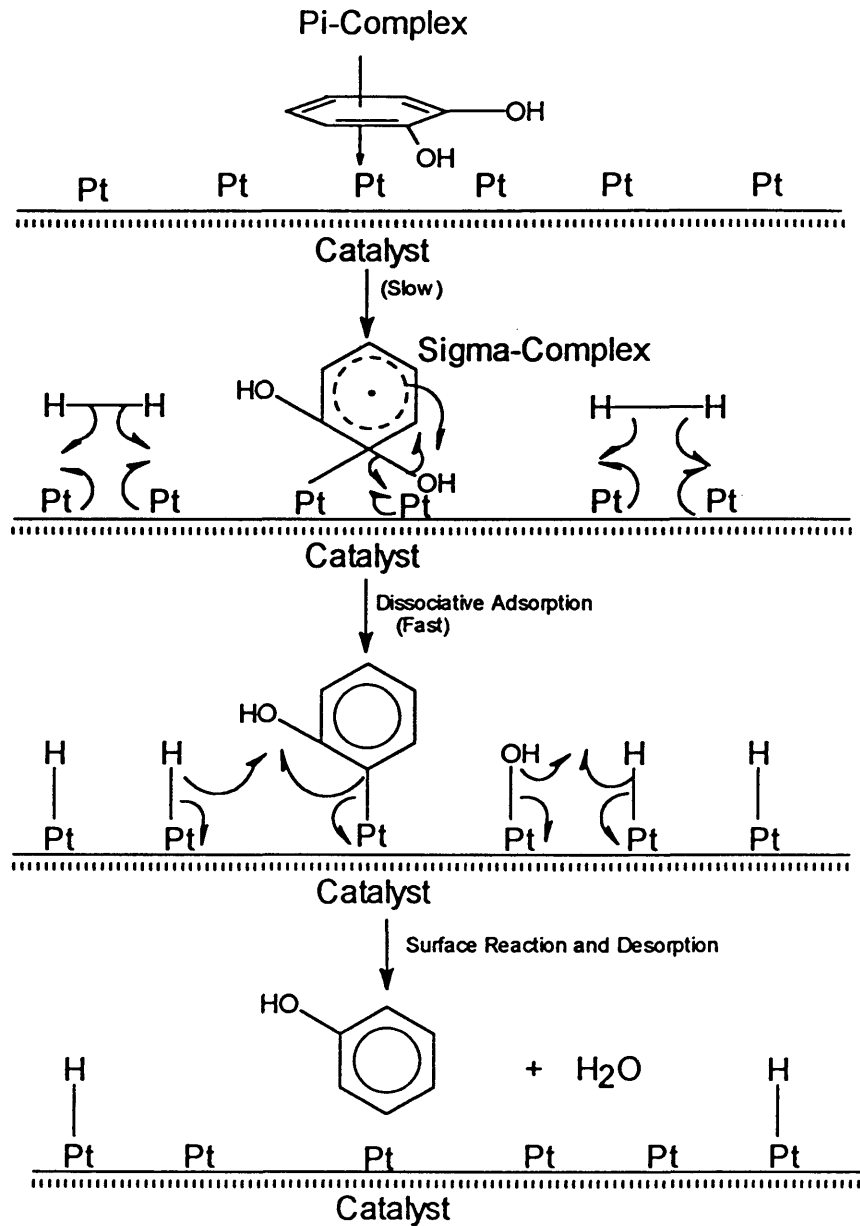


Figure 28. Possible metal surface hydrogenolysis mechanism for the selective dehydroxylation of catacol.

The reactivity of 4-propylguaiacol decreased from 100 mole% to 33 mole% when the experiment was conducted at 200 psig ; it decreased from 100 mole% to 70 mole% when the experiment was conducted at 300 psig with the same temperature range 400, 450 and 400°C.

5.12 Effect of Temperature on Syringol Conversion

In order to evaluate the selective deoxygenation function of the catalyst, syringol was selected as a more realistic model lignin compound than 4-propylphenol or 4-propylguaiacol. A feedstock of 10% syringol (2,6-dimethoxyphenol) in toluene was passed over the 0.3 wt% Pt/SiO₂-Al₂O₃ catalyst at different experimental conditions. The product distributions are given in **Appendix A, Table A-18 and A-19**. The catalyst was shown to have good activity and selectivity for syringol conversion and phenols production. The results showed a good conversion of syringol. The major products included phenol, benzene, xylene, mesitylene, xylenol, and 2-methoxy-4-methylphenol.

In the study of the model lignin compounds such as 4-propylphenol and 4-propylguaiacol, it was concluded that high temperature and low pressure (450°C, and 200 psig) facilitate the production of phenols, but tend

to produce more coke than when with the experiment started at a higher pressure (300 psig).

In order to evaluate the activity and selectivity of the catalyst with a more realistic model lignin compound (syringol) and limit the coke deposits, the conditions for the first experiment (Run-03-07-91) were chosen as 500 and 300 psig of hydrogen, with a temperature sequence of 400, 450, and 400 °C and 8 hours as shown in **Appendix A, Table A-18**. At 450°C, 300 psig hydrogen and 6 hours, the conversion of syringol was 100 mole% and the production of phenols was 39 mole%.

In order to increase the production of phenols another experiment was performed. The reaction conditions (Run-03-11-91) were 200 psig of hydrogen, with a temperature sequence of 400, 450, 400°C and 6 hours as shown in **Appendix A, Table A-19**. At 200 psig, 450°C, and 4 hours, the conversion of syringol approached 100 mole%. The production of phenols was 38 mole%. At 300 psig, 450°C, and 6 hours, the conversion of syringol approached 100 mole% and the production of phenols was 39 mole%.

During each experiment, the activity of the catalyst decreased while coking proceeded. The surface coke content at 400°, 500 psig hydrogen and 8 hours was 17%; at 400°, 200 psig hydrogen and 6 hours it was 22%. The coking was less when the experiment started with high pressure, but the production of phenol decreased.

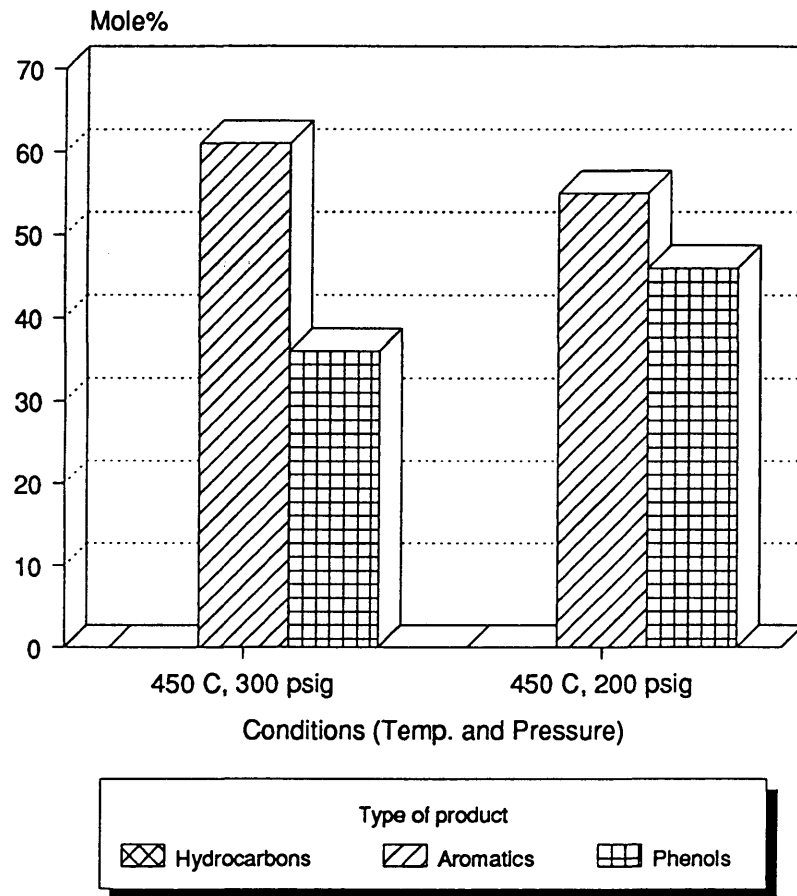
The overall results of these experiments showed that by increasing the temperature from 400 to 450°C (Run-03-07-91) or decreasing the pressure from 300 to 200 psig (Run-03-11-91), the production of phenols increased (**Figure 29** and **30**). The conversion and demethylation reactions increased as the temperature was increased or the pressure decreased.

Based on the products the following reaction sequence for syringol can be proposed (**Figure 31**). The catalyst functions are shown in each step. The mechanisms for the demethylation and dehydroxylation (DH) are the same as discussed for 4-propylguaiacol conversion.

5.13 4-Propylphenol Conversion Over Ni/SiO₂-Al₂O₃

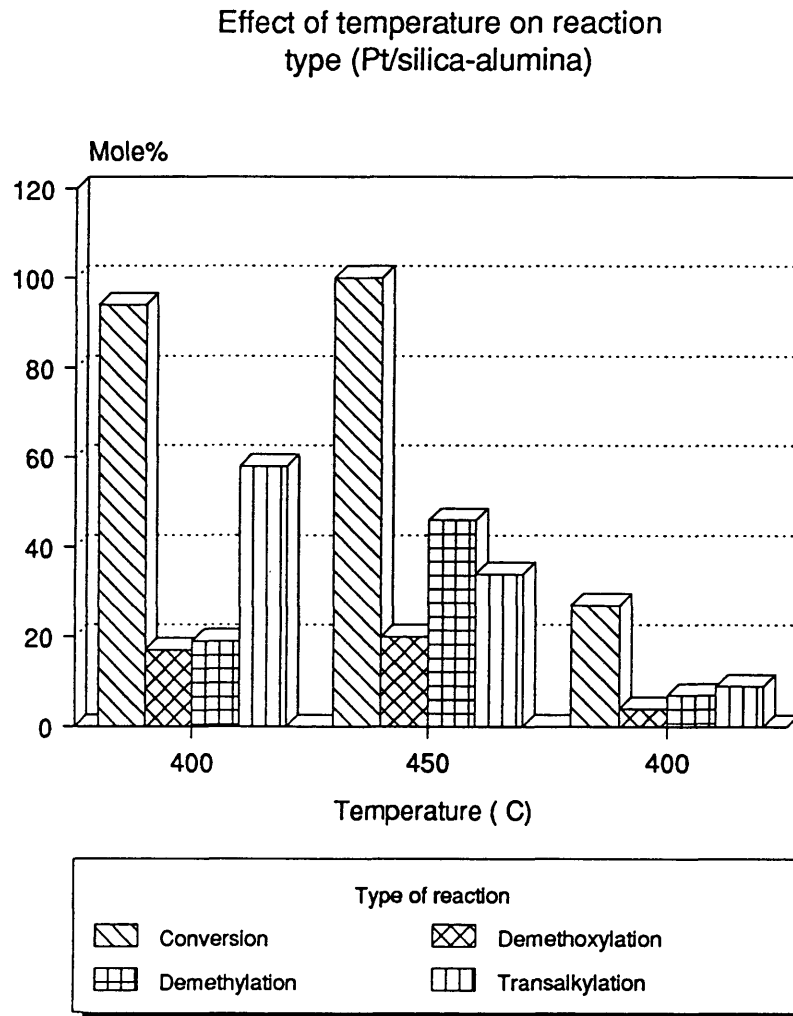
A feedstock of 10 wt% 4-propylphenol in hexane was passed over the 15 wt% Ni/SiO₂-Al₂O₃ catalyst (Run-09-25-92 in **Appendix A, Table A-20**) at the standard condition. At 350°C, 500 psig and 3 hours, the maximum yield of phenol was 15 mole%, the conversion was 54 mole%, the transalkylation products were 5 mole%. Compared to the Pt/SiO₂-Al₂O₃ catalyst, the Ni/SiO₂-Al₂O₃ catalyst was shown to have good selectivity for phenol production, but poor activity for 4-propylphenol conversion, and low hydrocarbon and aromatic production at the same conditions (**Figure 32**).

Effect of pressure on product
distribution (Pt/silica-alumina)



Syringol
Fig-29 (Tables A-18 and A-19)

Figure 29. Effect of pressure on syringol product distribution.



Syringol, pressure = 200 psig
Fig-30 (Table A-19)

Figure 30. Effect of temperature on catalyst function during syringol conversion.

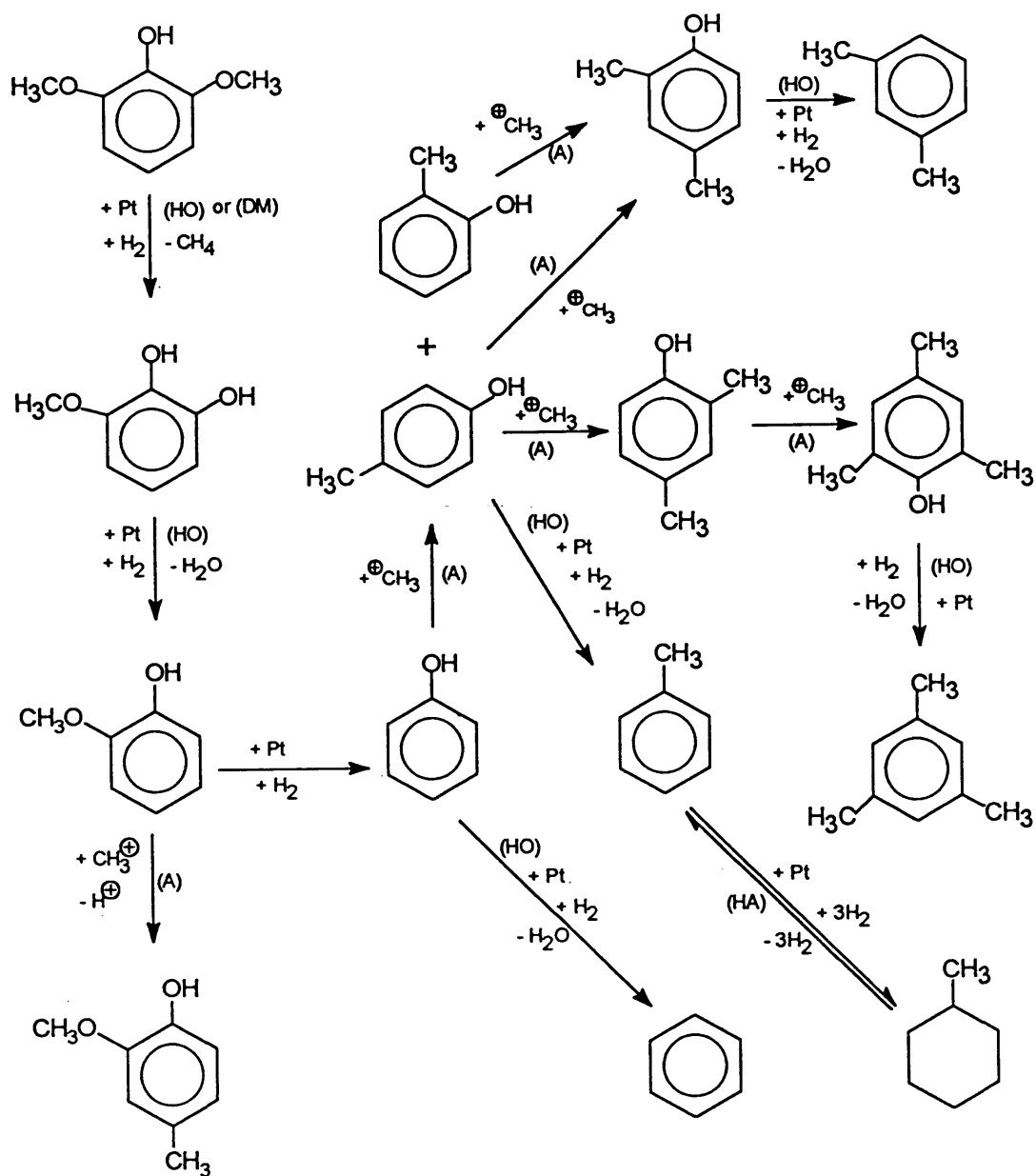
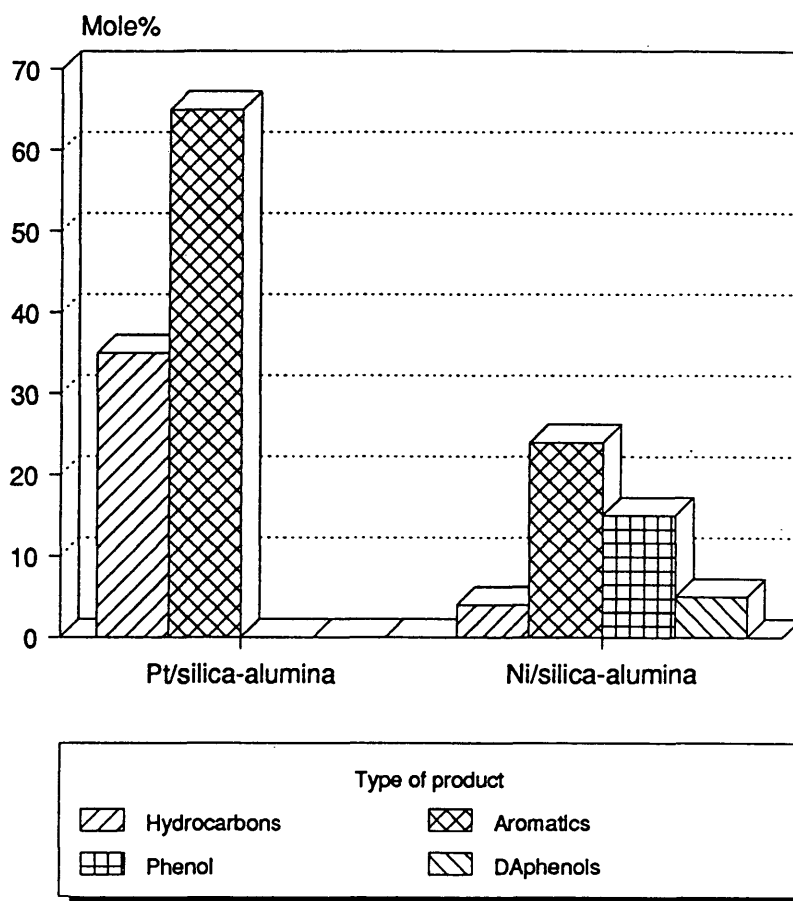


Figure 31. Possible reaction scheme for syringol conversion.

Based on the observed products, the hydrogenation and hydrogenolysis functions of the nickel metal were less active than those for platinum, although the concentration of nickel was fifty times that of platinum. This appears to be because of the active metal loss during the catalyst preparation to form inert nickel aluminate (**Figure 34**) .

Evidence for an nickel aluminate formation was obtained by X-ray diffraction (XRD) analysis. Details of the XRD analysis are discussed later in this thesis. The XRD pattern of the reduced Ni/SiO₂-Al₂O₃ catalyst shows unexpectedly small diffraction peak heights of nickel. Considering the large amount of nickel added to the support, the height of the diffraction lines should have been large and narrow. The most logical explanation of the missing nickel is the formation of a highly dispersed nickel aluminate (NiAl₂O₄). The formation of NiAl₂O₄ on alumina and silica-alumina supports is well known (*Satterfield, 1991*).

Comparison of Activity and Selectivity
of Pt and Ni/silica-alumina Catalysts



4-Propylphenol, 350 C, 500 psig
Fig-32 (Table A-21)

Figure 32. Comparison of activity and selectivity of Ni/SiO₂-Al₂O₃ catalyst with Pt/SiO₂-Al₂O₃ catalyst for 4-propylphenol conversion.

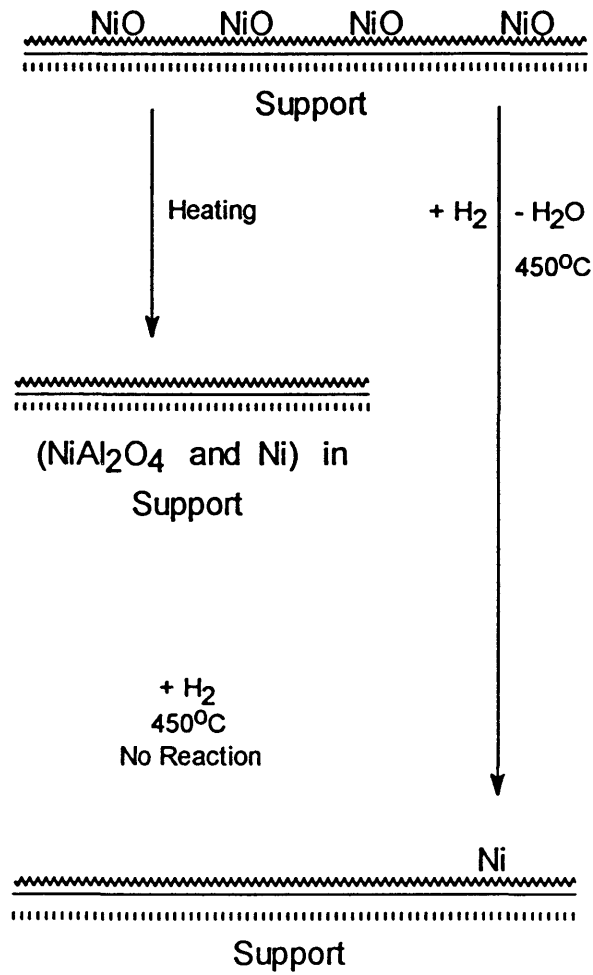


Figure 33. Possible reaction sequence of nickel aluminate formation.

5.14 Activity, Selectivity and Durability of Catalysts

Three kinds of catalysts for the potential conversion of model lignin feedstocks into phenolic products have been developed. The catalysts were designated as Pt/SiO₂-Al₂O₃, Pt/AlPO₄-Al₂O₃ and Ni/SiO₂-Al₂O₃. The catalysts were designed for conversion of the model lignin compounds, 4-propylphenol, 4-propylguaiacol, and syringol. The resulting catalysts were found to be highly active and selective for the production of phenol. The Pt/SiO₂-Al₂O₃ catalyst gives better overall selectivity for phenol production.

The functions incorporated into the catalyst were platinum and nickel metal, containing both hydrogenation and hydrogenolysis activity, and an acidic support to provide dealkylation activity. The supported platinum catalysts were found to be highly active and selective for the production of phenol at 350-450°C and 200-300 psig of hydrogen. Hydrocarbons are the major products at 350°C and 500 psig hydrogen.

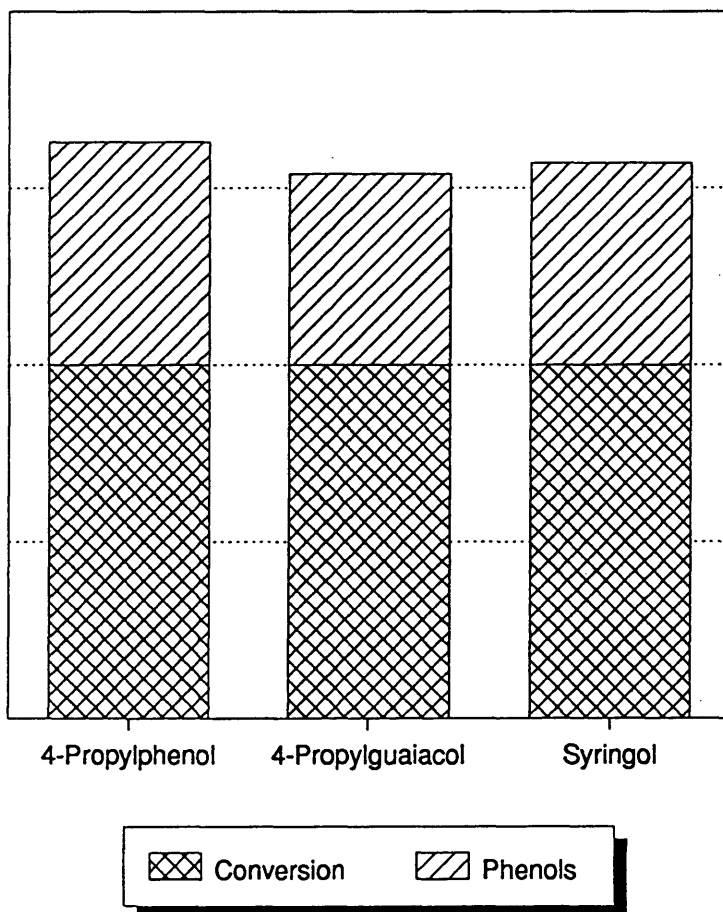
The durability of the catalysts was not very good. The platinum catalysts showed severe signs of coking at the end of the test. The coking was greatest at high temperature (450°C) and low hydrogen pressure (200 psig). The nickel catalyst showed worse coking than platinum at 350°C and 500 psig hydrogen pressure.

5.14.1 Activity, Selectivity, and Durability of Pt/SiO₂-Al₂O₃

The activity, selectivity, and durability of the Pt/SiO₂-Al₂O₃ catalyst was studied using 4-propylphenol as a model lignin compound. The maximum phenol yield with the previous Pt/PAIO₄-Al₂O₃ catalyst was 46% at 450°C and 200 psig of hydrogen (*Erickson, 1990*). The Pt/SiO₂-Al₂O₃ catalyst produced 56% phenol under the same conditions. At the same time the troublesome transalkylation products appear to have been eliminated. The increase in phenol production corresponds directly with the decrease in the transalkylation reaction.

The conversion of 4-propylphenol (4PP), 4-propylguaiacol (4PG), and syringol (SYR) at 450°C and 200 psig over the Pt/SiO₂-Al₂O₃ catalyst are compared in **Figure 34**. The Pt/SiO₂-Al₂O₃ catalyst shows excellent conversion and selectivity at the conditions studied. The total phenolic content ranged from 45 to 67 mole% depending on the model compound studied. The optimum reaction conditions were 450°C and 200 psig for phenol production and 350°C and 500 psig for hydrogen production. The catalyst showed severe signs of coking at the end of the test. The coking is most severe at the high temperature (450°C) and the low hydrogen pressure (200 psig). The tested Pt/SiO₂-Al₂O₃ catalyst can be regenerated in air at about 500 °C. The surface carbon oxidizes to form the volatile carbon oxide gases.

Activity and selectivity for 4PP, 4PG
and SYR conversion (Pt/silica-alumina)



Temp=450 C, Pressure=200 psig
Fig. 34 (Tables A-14, A-16, and A-19)

Figure 34. Comparison of activity and selectivity of Pt/SiO₂-Al₂O₃ catalyst for 4PP, 4PG and SYR conversion.

5.14.2 Activity, Selectivity, and Durability of Pt/AlPO₄-Al₂O₃

The activity, selectivity, and durability of the Pt/AlPO₄-Al₂O₃ catalyst was studied using 10 wt% 4-propylphenol/hexane as the feedstock. A comparison was made with the Pt/SiO₂-Al₂O₃ catalyst using the same feedstock and at the same conditions. At 350°C and 500 psig of hydrogen, the phenol yield with the Pt/SiO₂-Al₂O₃ catalyst was zero mole% and the maximum phenol yield with the Pt/AlPO₄-Al₂O₃ catalyst was 3.5 mole%. The troublesome transalkylation products were 6 mole% with the Pt/SiO₂-Al₂O₃ and 0 mole% with the Pt/AlPO₄-Al₂O₃. The conversion of 4-propylphenol was 93 mole% and 98 mole % (Appendix A, Tables A-4 and A-6).

The Pt/AlPO₄-Al₂O₃ catalyst showed severe signs of coking at the end of the test. The coking was most severe at the high temperature (450°C) and the low hydrogen pressure (200 psig). The surface coke content was 10% with 10 wt% 4-propylphenol/hexane over Pt/AlPO₄-Al₂O₃ catalyst at 350°C, 500 psig and 3 hours.

5.14.3 Activity, Selectivity, and Durability of Ni/SiO₂-Al₂O₃

The activity of the Ni/SiO₂-Al₂O₃ catalyst compared to the Pt/SiO₂-Al₂O₃ and Pt/AlPO₄-Al₂O₃ catalysts was lower and the selectivity of phenol was higher at the same conditions, 350°C, 500 psig and 3 hours.

The durability of the Ni/SiO₂-Al₂O₃ catalyst was very poor. The catalyst showed severe signs of coking at the end of the 3 hour test compared to the Pt/SiO₂-Al₂O₃ and the Pt/AlPO₄-Al₂O₃ catalysts at the same conditions. This is in good agreement with *Corma and Grande (1992)*. When nickel is used as a hydrotreating catalyst, it leads to an increase of coke.

The surface coke content of the Ni/SiO₂-Al₂O₃ catalyst at the end of the three hour test was 9% (**Table 11**). The Pt/SiO₂-Al₂O₃ catalyst was studied at the same standard test conditions at the end of the experiment. Both catalysts apparently had the same surface coke content as evidenced by weight loss during TGA analysis. However, the Ni/SiO₂-Al₂O₃ catalyst was visibly darker than the Pt/SiO₂-Al₂O₃ catalyst, indicating more severe coking. To explain this discrepancy, it is postulated that the nickel oxidized during the TGA analysis. This weight gain decreased the apparent weight loss of surface carbon, and the surface carbon on the Ni/SiO₂-Al₂O₃ catalyst was actually greater.

Although regeneration of tested Pt/SiO₂-Al₂O₃ catalyst is not a serious problem, regeneration of tested Ni/SiO₂-Al₂O₃ catalyst is a serious problem. This is because, during regeneration, the nickel metal would oxidize and tend to form NiAl₂O₄, with loss of the active metal function. Hydrogen reduction is thus a necessary extra step in the regeneration of Ni/SiO₂-Al₂O₃ catalyst.

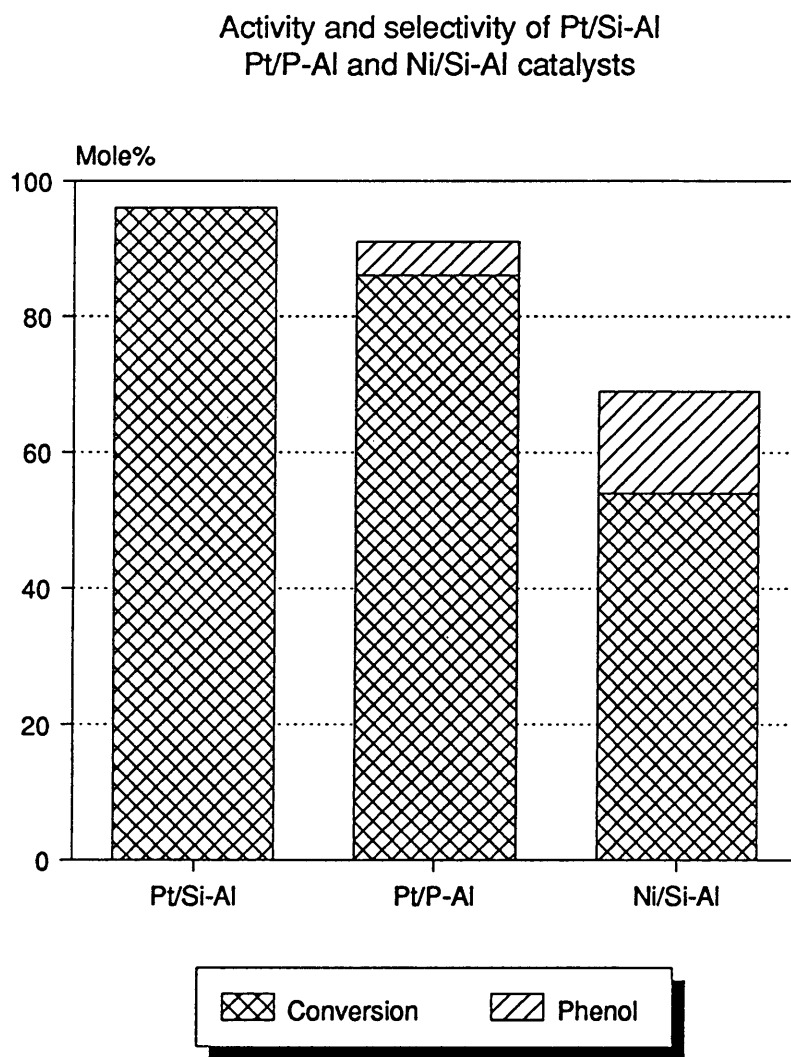
5.14.4 Comparison of the Catalyst Activity and Selectivity

The Pt/SiO₂-Al₂O₃ catalyst gives better overall selectivity for phenol production than Pt/AlPO₄-Al₂O₃ at 450°C and 200 psig hydrogen. The Ni/SiO₂-Al₂O₃ catalyst gives better overall selectivity for phenol production than the Pt/SiO₂-Al₂O₃ or the Pt/AlPO₄-Al₂O₃ catalyst at 350°C and 500 psig hydrogen, but the activity of the Ni/SiO₂-Al₂O₃ catalyst was much lower than that of the Pt/SiO₂-Al₂O₃ or the Pt/AlPO₄-Al₂O₃ catalyst. The comparison of the three catalysts for 4-propylphenol conversion at 350°C, 500 psig and 3 hours experimental time is shown in **Figure 35** and **Appendix A, Table A-21** .

Compared to platinum catalysts, the nickel catalyst has a high selectivity of phenol production at 350°C, 500 psig and 3 hours. Nickel catalyst may have potential as a lignin hydrotreating catalyst; further studies at reaction conditions of 400-450°C and 200-300 psig for Ni/SiO₂-Al₂O₃ catalyst are recommended.

5.15 Activity and Selectivity of Pt/SiO₂-Al₂O₃ for Model Compound Mixtures

Based on the literature, the monomer concentration of the lignin depolymerization product depends on the type of lignin and the depolymerization method applied. None of the available literature gives the



Temp=350 C, Pressure=500 psig
Fig-35 (Table A-21)

Figure 35. Comparison of activity and selectivity of catalysts for 4-propylphenol conversion.

useful quantitative information about lignin depolymerization products. Most studies simply provide qualitative information about the type of the products formed such as guaiacol or syringol.

Lignin is too large a molecule to be converted by a porous supported catalyst to low molecular weight products. Lignin must first be converted into low molecular weight compounds or monomers which can enter the catalyst pores. The depolymerization of lignin subsequent to characterization of the monomer product is a very complicated process. Work by *Frerichs (1984)* has shown that single model compounds are useful in studying the catalyst functions, but they do not successfully predict the behavior of a more complex mixture. For this purpose a model compound mixture was used to evaluate the catalyst performance in the presence of a mixture of low molecular weight compounds or monomers.

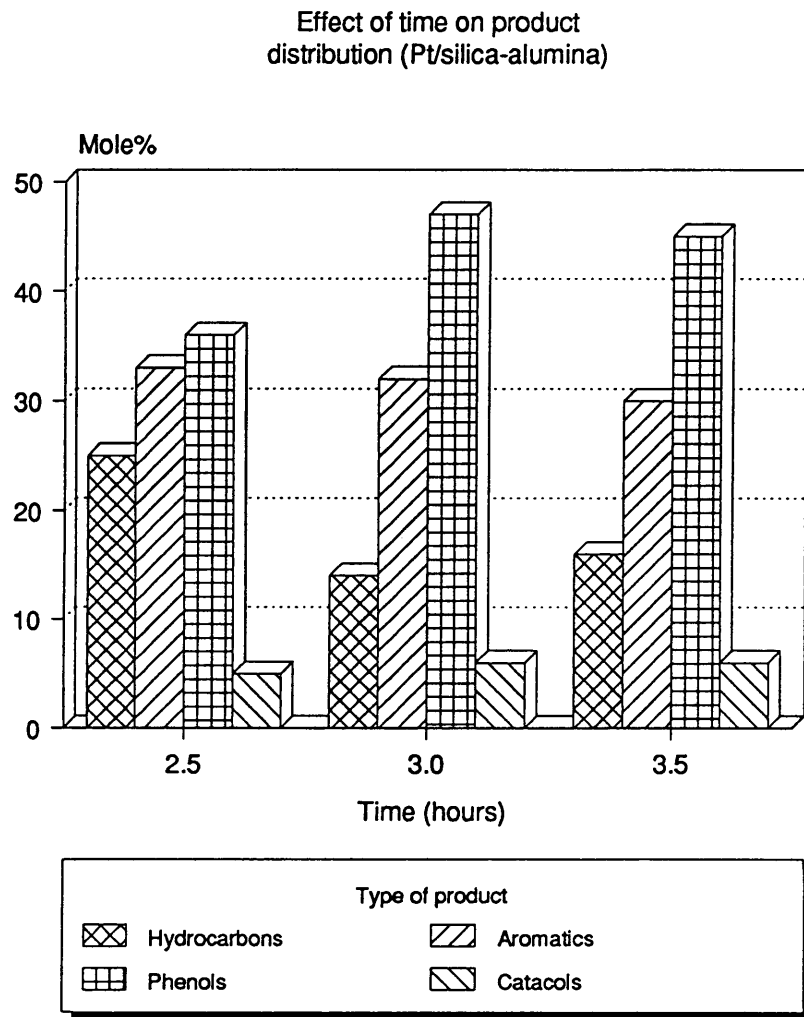
A mixture of 5 wt % 4-propylguaiacol and 5 wt% syringol with 90 wt% toluene over 0.3 wt% Pt/SiO₂-Al₂O₃ catalyst, at 300 psig, 450°C and 2.5, 3.0 and 3.5 hours (Run-04-23-93) has been studied. The results are shown in **Appendix A, Table A-22**. The phenols yield were 36, 46 and 43 mole% respectively. The conversion of 4-propylguaiacol was 100% and the conversion of syringol was 99 mole% to 96 mole%. The catalyst shows excellent selectivity for phenols production and a better activity for 4-propylguaiacol conversion than for syringol. The type of the products

collected as a function of time are shown in **Figure 36**. The results suggest that the system reached the steady state at approximately 3 hours. The Pt/SiO₂-Al₂O₃ catalyst is a potential hydrotreating catalyst for low molecular weight lignin feedstock.

Comparing the product distribution of the mixture to that obtained for pure 4-propylguaiacol and syringol, the kinds of product were the same as kinds from the sum of the pure model compound products. Quantitatively, the mixture of model compounds does not behave as the sum of single compounds, as shown by the increased production of phenol, and decreased production of aromatics and hydrocarbons compared to those of the single compounds at the same conditions. The surface reaction sequence of the mixture must be different from that of each single compound. The mixture is better at predicting the behavior of a mixture of low molecular weight lignin fragments than the single model compounds.

5.16 Blending Ability of Products

In order to use the products for gasoline reformulation, the reaction conditions need to maximize phenol yield and minimize aromatic production. Unfortunately, the conditions favorable to aromatic ring saturation also are favorable to hydrogenolysis of the phenol's carbon-oxygen bond to form



4PP + 4PG, Temp = 450 C, P = 200 psig
Fig-36 (Table A-22)

Figure 36. The mixture of model lignin compounds product as a function of time.

benzene and water. The separation of phenol and aromatic compounds is therefore necessary to use the products to reformulate gasoline.

Like the hydroxyl proton of water, the hydroxyl proton of phenol is weakly acidic. A strong base can remove the hydroxyl proton of phenol to give a phenoxide ion. The resonance stabilization in the phenoxide ion makes phenol an unusually "strong acid" compared to cyclohexanol. The reaction of phenol with sodium hydroxide to form sodium phenoxide is an exothermic reaction, and can be made to go to completion. Sodium phenoxide is a water soluble compound and the aromatic compounds are not. After the separation of phenol from aromatic compounds, the sodium phenoxide can be neutralized by hydrochloric acid to form phenol, which then reacts with methanol to form methylphenyl ether.

5.17 Support and Catalyst Characterization

5.17.1 XRD Analysis

Since the metal function is necessary for the hydrogenation and hydrogenolysis of model lignin compounds to phenol products, the presence of metal is important for catalyst performance. The supported metal catalyst has been made by impregnating the support with the metal salt solution, then

calcining in air at 500°C. Before the catalyst testing sequence the catalyst was reduced in hydrogen flowing about 50 ml/min, at 450°C and atmospheric pressure for two hours. All reduced catalysts were produced by the same procedure used for catalyst testing.

To obtain information about the active metal on the support after the catalyst preparation and pretreatment, the catalysts and the supports were characterized by XRD. XRD is a common method employed to identify and characterize catalytic materials. These catalysts and supports are listed in **Table 9**. The application of XRD to catalyst characterization included correlation of XRD powder diffraction patterns to known crystal diffraction patterns, and determination of crystallite size. The average crystallite diameter of the supported metal crystallite was determined by a line broadening method (*Klug and Alexander, 1959*).

The XRD patterns for a pure platinum metal, a pure nickel metal, a pure nickel oxide (NiO), a prepared $\text{AlPO}_4\text{-Al}_2\text{O}_3$ support and a commercial $\text{SiO}_2\text{-Al}_2\text{O}_3$ support were used as references in this study. The spectrum of the platinum metal reference material is shown in **Figure 37**. It has diffraction lines at 39.8, 46.3, 67.7, 81.6 and 86.1 degrees 2θ . The d-spacing corresponds to the platinum metal. The spectra of the nickel oxide and nickel metal reference materials are shown in **Figures 38-a** and **38-b**. In **Figure 38-a**, the diffraction lines at 37.2, 43.3, 62.9, 75.4, 79.4 and 95.1 degrees 2θ

Table 9. Catalysts characterized by XRD

<u>Material</u>	<u>Metal</u>	<u>Metal wt%</u>	<u>Support</u>
Pt	Pt	100	None
NiO	None	None	None
Ni	Ni	100	None
SiO ₂ -Al ₂ O ₃	None	None	SiO ₂ -Al ₂ O ₃
XZ-AlPO ₄ -Al ₂ O ₃ -Batch#2	None	None	AlPO ₄ -Al ₂ O ₃
XZ-0.3Pt/silica-alumina-28	Pt	0.3	SiO ₂ -Al ₂ O ₃
Re-XZ-0.3Pt/silica-alumina-28	Pt	0.3	SiO ₂ -Al ₂ O ₃
XZ-0.3Pt/aluminophosphate-03A	Pt	0.3	AlPO ₄ -Al ₂ O ₃
Re-XZ-0.3Pt/aluminophosphate	Pt	0.3	AlPO ₄ -Al ₂ O ₃
XZ-1.2Pt/aluminophosphate	Pt	1.2	AlPO ₄ -Al ₂ O ₃
XZ-15Ni/silica-alumina-29	Ni	15	SiO ₂ -Al ₂ O ₃
Re-XZ-15Ni/silica-alumina-29	Ni	15	SiO ₂ -Al ₂ O ₃

[Continued]

Definitions for the above table:

- XZ = Xianghong Zhao (who made this catalyst or support)
- Re = The catalyst which has been reduced in hydrogen flowing about 50 ml/min at 450°C and atmospheric pressure for two hours
- 0.3Pt = 0.3 wt% of platinum
- 1.2Pt = 1.2 wt% of platinum
- 15Ni = 15 wt% of nickel
- A = Weight of catalyst calcined in this experiment (2 grams)
- "03" or
"28" or
"29" = Serial number of catalyst made for this study

correspond to the nickel oxide. In **Figure 38-b**, the diffraction lines at 44.5, 51.8, 76.4, 93.0 and 98.5 degrees 2θ correspond to the nickel metal.

The XRD patterns of the commercial $\text{SiO}_2\text{-Al}_2\text{O}_3$ and the prepared $\text{AlPO}_4\text{-Al}_2\text{O}_3$ supports are shown in **Figure 39-a** and **Figure 39-b**. In **Figure 39-a**, the commercial $\text{SiO}_2\text{-Al}_2\text{O}_3$ support shows a broad diffraction line at 23 degrees 2θ . This suggests that the $\text{SiO}_2\text{-Al}_2\text{O}_3$ support has a crystal structure for only short distances. In **Figure 39-b**, the blank $\text{AlPO}_4\text{-Al}_2\text{O}_3$ support shows a broad diffraction line at 24 degrees 2θ . This suggests that the $\text{AlPO}_4\text{-Al}_2\text{O}_3$ support also has a low order crystal structure.

The spectra of the $\text{SiO}_2\text{-Al}_2\text{O}_3$ supported platinum catalysts are shown in **Figure 40**. The XRD pattern for 0.3 wt% platinum supported on $\text{SiO}_2\text{-Al}_2\text{O}_3$ prepared by impregnation and then calcined in air at 500°C is shown in **Figure 40-a**; the XRD pattern for this catalyst after being reduced in hydrogen is shown in **Figure 40-b**. The two catalysts have the same diffraction lines at 39.7, 46.1 and 67.2 degrees 2θ . The d-spacing of the peaks corresponds to the platinum metal. The results show that both the calcined and the reduced $\text{SiO}_2\text{-Al}_2\text{O}_3$ supported platinum catalysts have platinum in the metal phase. This would suggest that the prereduction step used during the catalyst testing stage was not needed.

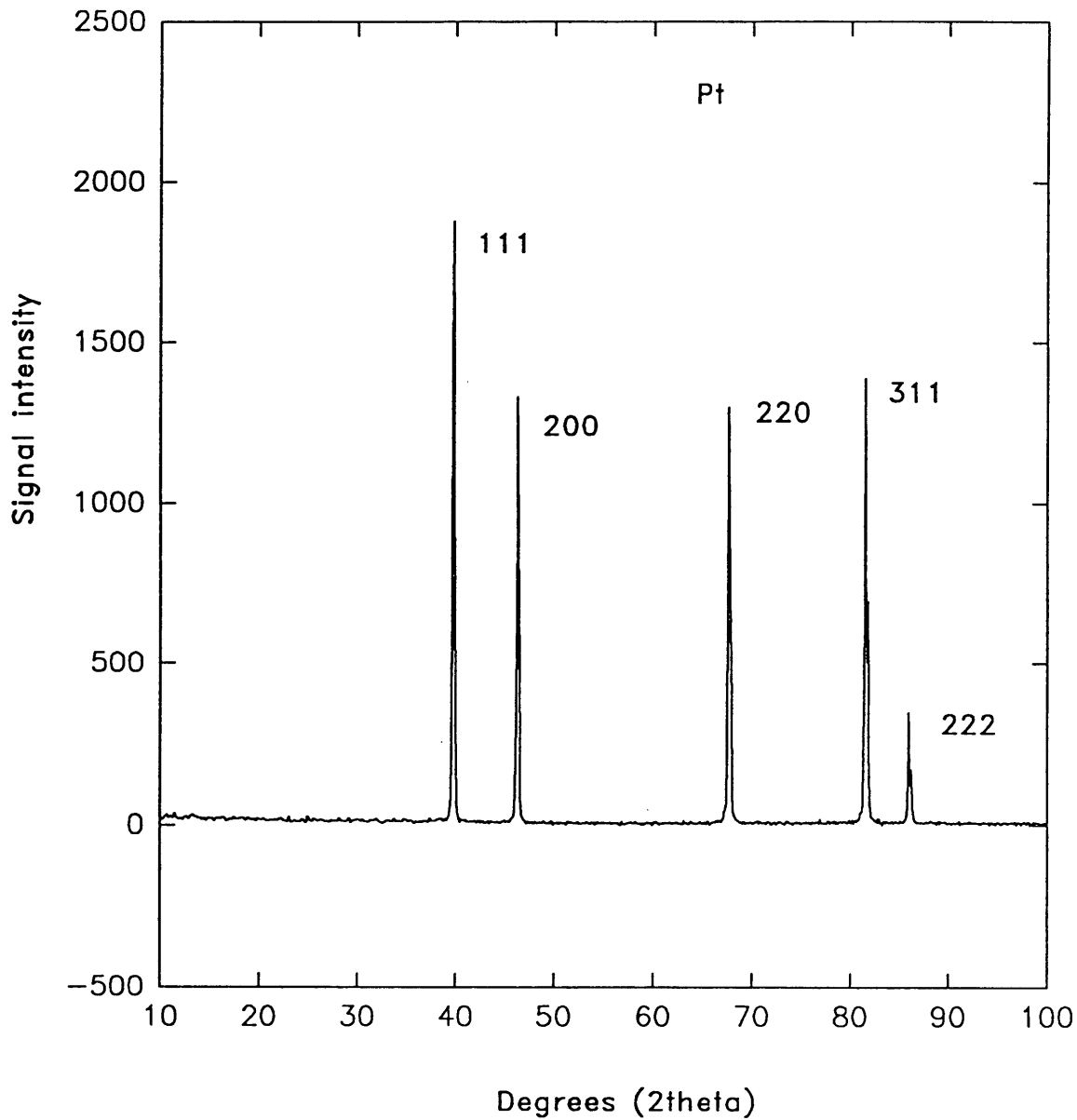


Figure 37. XRD pattern of platinum metal reference.

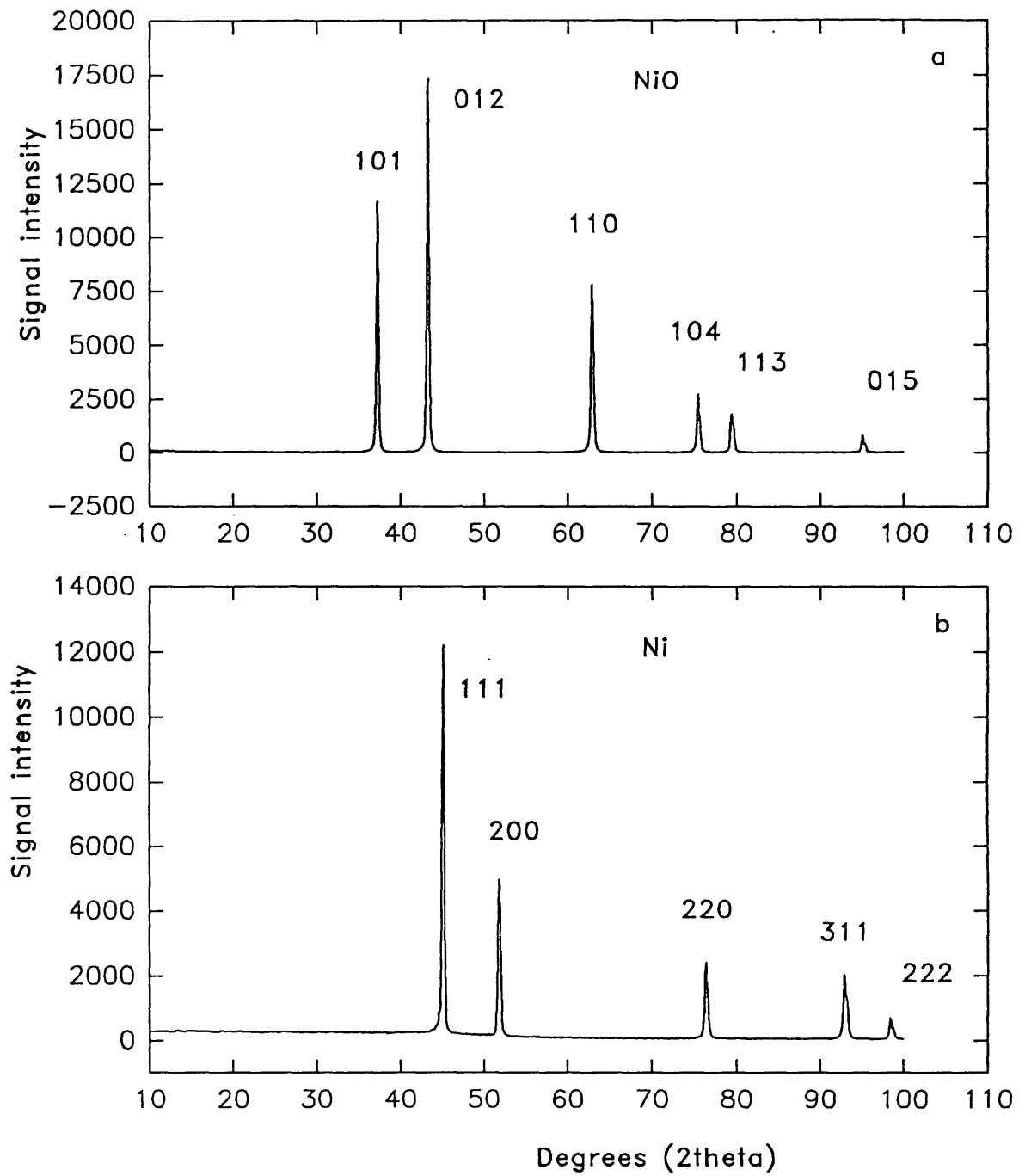


Figure 38. XRD patterns of nickel oxide and nickel metal references.

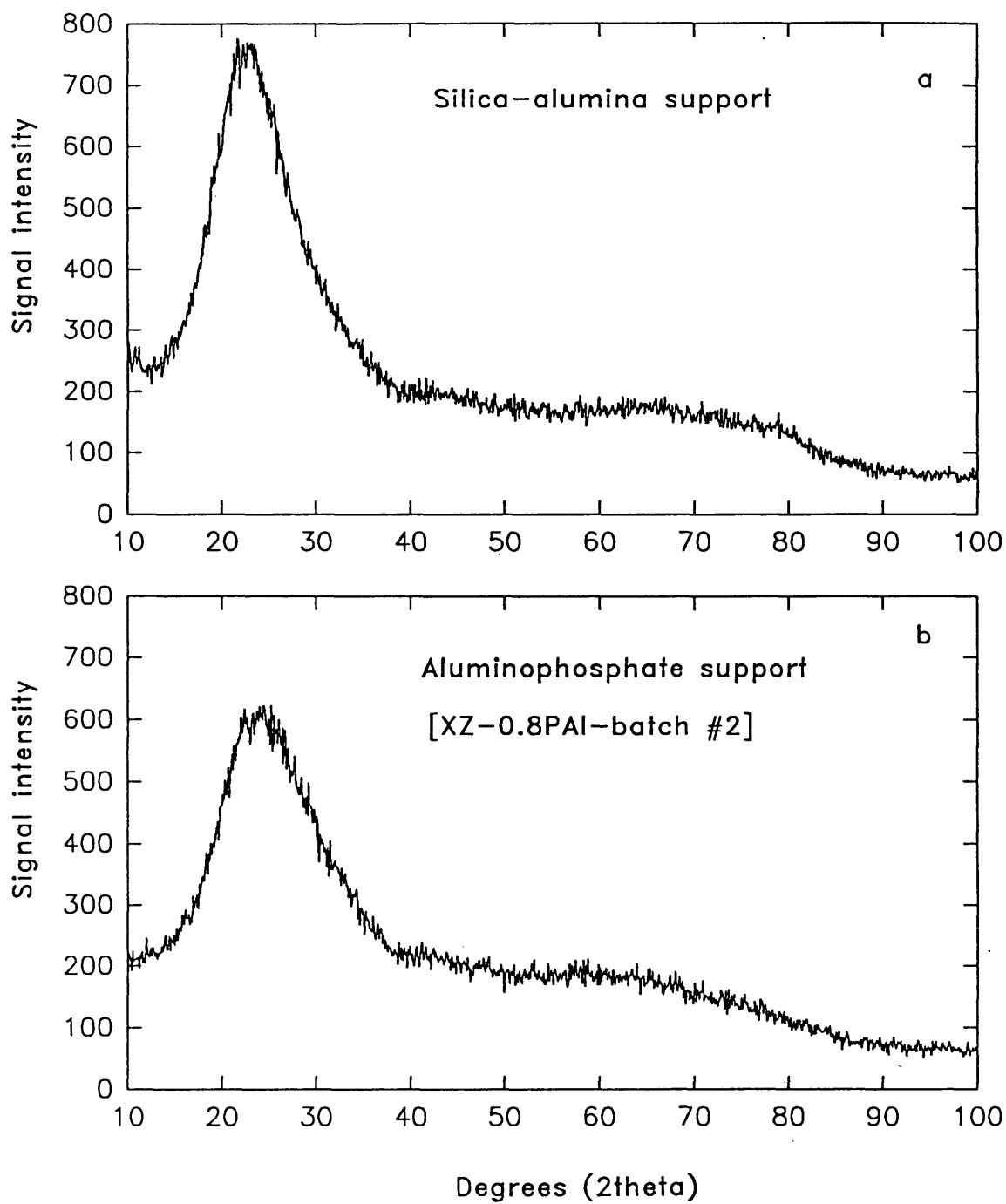


Figure 39. XRD patterns of commercial $\text{SiO}_2\text{-Al}_2\text{O}_3$ and prepared $\text{AlPO}_4\text{-Al}_2\text{O}_3$ supports.

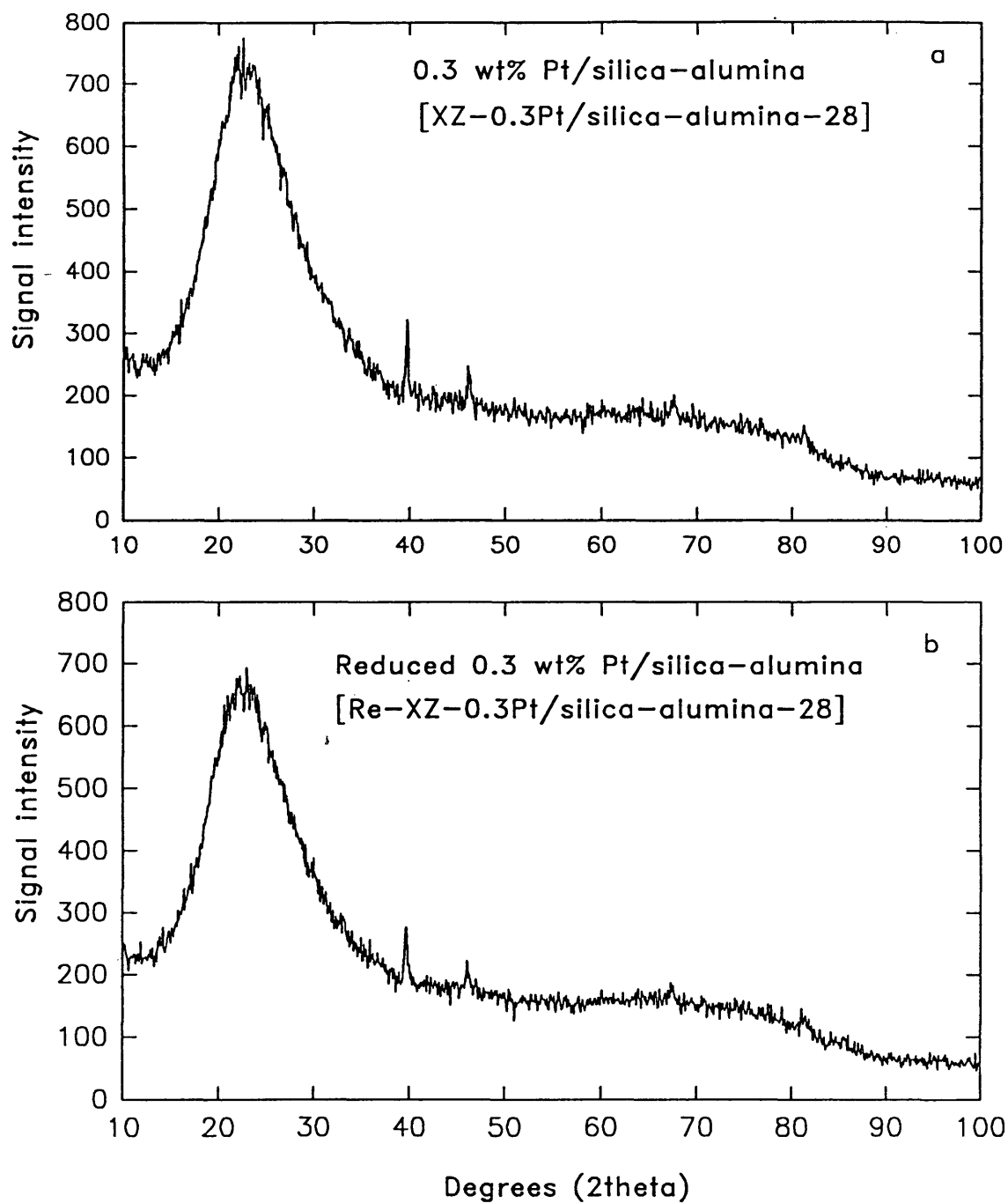


Figure 40. XRD patterns of (a) 0.3 wt% Pt/SiO₂-Al₂O₃ and (b) reduced 0.3 wt% Pt/SiO₂-Al₂O₃ catalysts.

Since the platinum metal function is necessary for the hydrogenation and hydrogenolysis reaction, any heating process may cause sintering of the platinum, which results in decreased activity of the catalyst and more severe coking. The average particle diameter (**Table 10**) of the reduced platinum supported by $\text{SiO}_2\text{-Al}_2\text{O}_3$ is twice that of the unreduced catalyst. In the future, the prereduction step for $\text{Pt/SiO}_2\text{-Al}_2\text{O}_3$ catalyst should be omitted.

The spectra for $\text{AlPO}_4\text{-Al}_2\text{O}_3$ supported platinum are shown in **Figure 41**. **Figure 41-a** shows the XRD pattern for 0.3 wt% platinum supported on $\text{AlPO}_4\text{-Al}_2\text{O}_3$ prepared by impregnation, then calcined at 500°C in air. **Figure 41-b** shows the XRD pattern for this catalyst after being reduced in hydrogen. The two catalysts show identical diffraction lines at 39.7 , 46.1 and 67.5 degrees 2θ . The d-spacing of the peaks correspond to the platinum (111), (200) and (220) lattice planes. The results show that platinum metal, and not platinum oxide, is present on the $\text{AlPO}_4\text{-Al}_2\text{O}_3$ support.

During the calcination at 500°C in air for 16 hours, part of the platinum may oxidize, but platinum oxide is thermodynamically less stable than NiO . The amount of platinum oxide was XRD invisible. As with the $\text{Pt/SiO}_2\text{-Al}_2\text{O}_3$ catalyst, the hydrogen pretreatment step prior to catalyst testing may not have been necessary.

A comparison of the XRD patterns for the platinum supported on $\text{SiO}_2\text{-Al}_2\text{O}_3$ and $\text{AlPO}_4\text{-Al}_2\text{O}_3$ substrates is shown in **Figure 42**. The XRD patterns

for 1.2 wt% of platinum supported on $\text{AlPO}_4\text{-Al}_2\text{O}_3$ prepared by impregnation then calcined in air at 500°C is shown in **Figure 42-a**; the XRD patterns for 0.3 wt% of platinum supported on $\text{AlPO}_4\text{-Al}_2\text{O}_3$ with the same preparation method is shown in **Figure 42-b**, and the XRD patterns for 0.3 wt% of platinum supported on $\text{SiO}_2\text{-Al}_2\text{O}_3$ with the same preparation method is shown in **Figure 42-c**.

In **Figure 42-a**, the catalyst has diffraction lines at 39.7, 46.1, 67.3 and 81.1 degrees 2θ . The d-spacing of the peaks corresponds to the platinum metal. Compared to **Figure 42-b**, increasing the platinum loading on $\text{AlPO}_4\text{-Al}_2\text{O}_3$ support shows a small increase in the peak height (**Tables 10**). The peak height is related to the weight percent loading of platinum, but the diffraction pattern of 1.2 wt% Pt/ $\text{AlPO}_4\text{-Al}_2\text{O}_3$ shows the same peak height for platinum metal. This is in good agreement with the catalyst testing results. The activity of 1.2 wt% Pt/ $\text{AlPO}_4\text{-Al}_2\text{O}_3$ is not greater than that of 0.3 wt% Pt/ $\text{AlPO}_4\text{-Al}_2\text{O}_3$. This indicates that the excess platinum over 0.3 wt% is not in the crystalline metal phase. In **Figure 42-a**, a broad shoulder at approximately 34.3 degrees 2θ and a small broad diffraction line at 55.5 degrees 2θ makes identification of metal oxide uncertain. The broad diffraction lines indicate that the material is relatively highly dispersed on the $\text{AlPO}_4\text{-Al}_2\text{O}_3$ support.

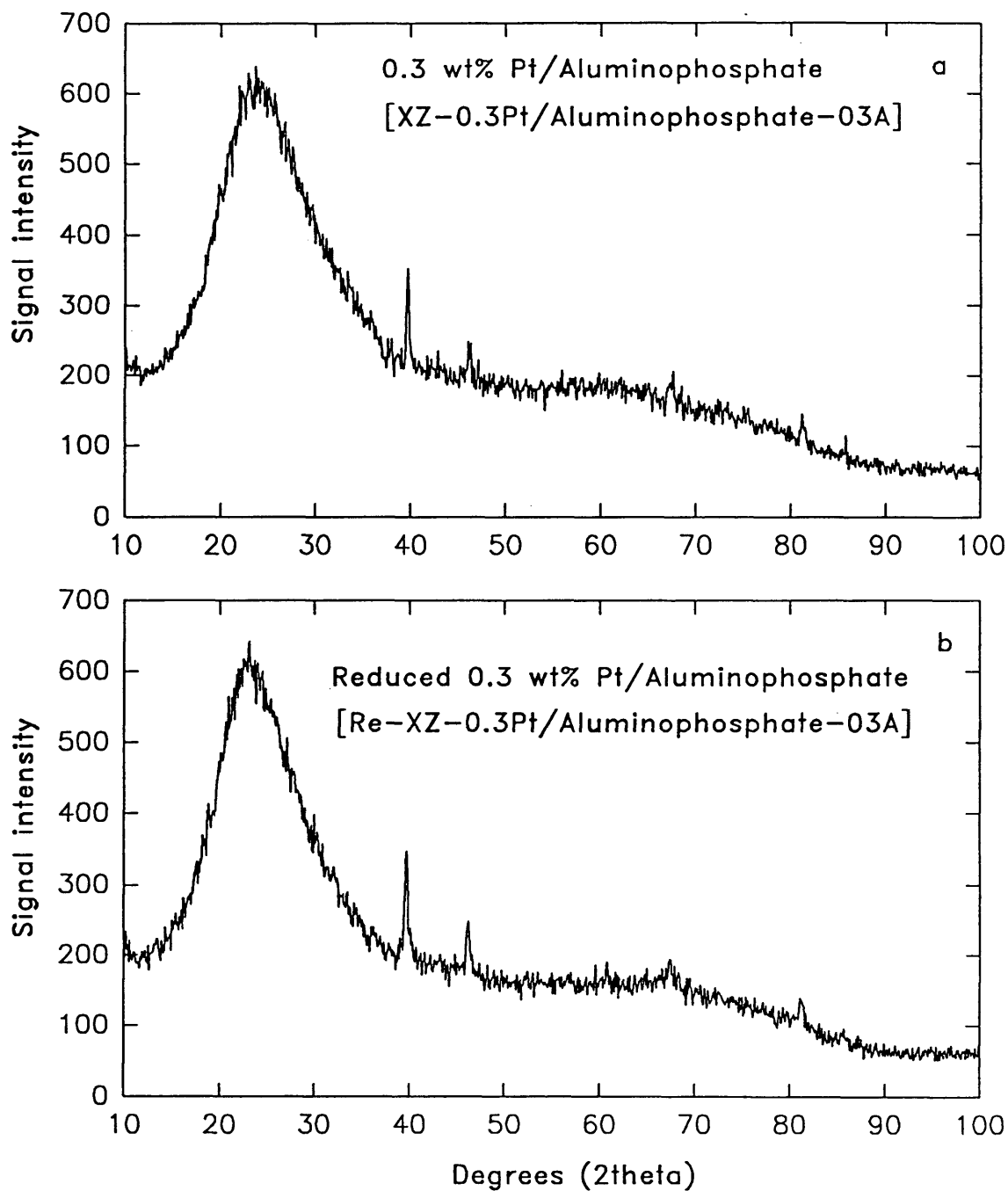


Figure 41. XRD patterns for (a) calcined 0.3 wt% Pt/ $\text{AlPO}_4\text{-Al}_2\text{O}_3$ and (b) reduced 0.3 wt% Pt/ $\text{AlPO}_4\text{-Al}_2\text{O}_3$ catalysts.

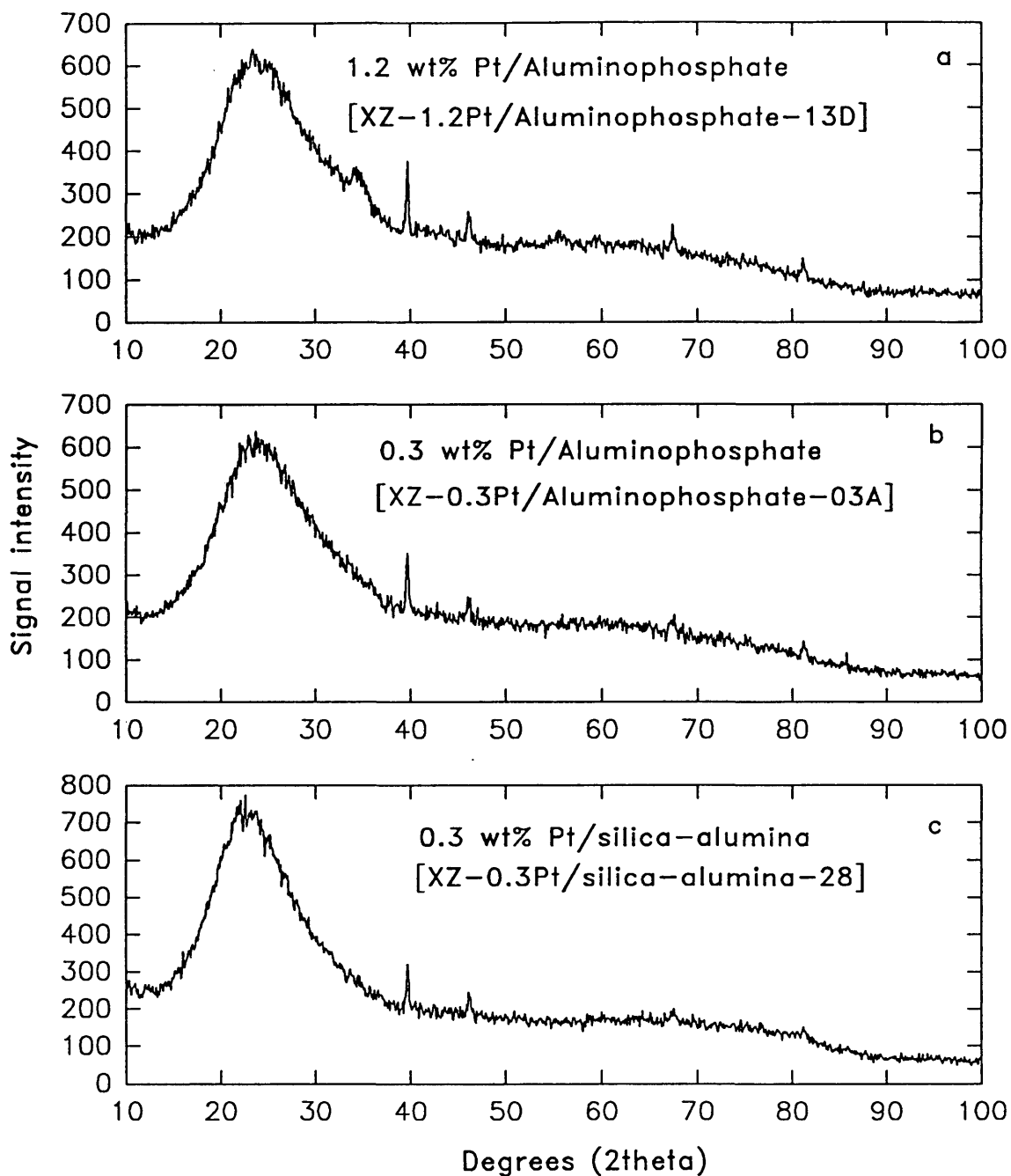


Figure 42. XRD patterns for (a) calcined 1.2 wt% Pt/ $\text{AlPO}_4\text{-Al}_2\text{O}_3$, (b) calcined 0.3 wt% Pt/ $\text{AlPO}_4\text{-Al}_2\text{O}_3$ and (c) calcined 0.3 wt% Pt/ $\text{SiO}_2\text{-Al}_2\text{O}_3$.

In **Table 10**, the peak height and line broadening of each diffraction pattern were calculated by the Rigaku X-ray diffraction computer program. The particle diameters were calculated by the equations (*Klug and Alexander, 1959*) shown in **Appendix B**.

Comparing the spectra in **Figure 42-b** and **Figure 42-c**, platinum supported on $\text{AlPO}_4\text{-Al}_2\text{O}_3$ has a slightly larger particle diameter (**Table 10**). This indicates that the platinum was better dispersed on the $\text{SiO}_2\text{-Al}_2\text{O}_3$ than on the $\text{AlPO}_4\text{-Al}_2\text{O}_3$ support. This is in a good agreement with the catalyst testing results, where the catalyst activity of the same amount of platinum supported on $\text{SiO}_2\text{-Al}_2\text{O}_3$ is higher than that supported on $\text{AlPO}_4\text{-Al}_2\text{O}_3$.

Better dispersion is an important factor since platinum is a noble metal and the metal function is necessary for the hydrogenation and hydrogenolysis reactions. The acidity and the polarity of the supports are important factors in catalytic metal dispersion, and future studies to characterize the acidity and polarity of the support are recommended.

The spectra of $\text{SiO}_2\text{-Al}_2\text{O}_3$ supported nickel catalysts are shown in **Figure 43**. **Figure 43-a** shows the XRD patterns of 15 wt% nickel supported on $\text{SiO}_2\text{-Al}_2\text{O}_3$ prepared by impregnation then calcined at 500°C in air. **Figure 43-b** shows the XRD patterns of this catalyst after being reduced in hydrogen.

Table 10. XRD results and calculated average catalyst particle diameters

Catalyst	Height (111)	Area (111)	B (111)	D(Å) (111)
XZ-0.3Pt/SiO ₂ -Al ₂ O ₃ -28	322	256	0.795	115
Re-XZ-0.3Pt/SiO ₂ -Al ₂ O ₃ -28	278	147	0.528	194
XZ-0.3Pt/AlPO ₄ -Al ₂ O ₃ -03A	353	259	0.940	126
XZ-1.2Pt/AlPO ₄ -Al ₂ O ₃ -13D	377	259	0.688	136
Re-XZ-15Ni/SiO ₂ -Al ₂ O ₃ -29	256	264	1.031	85

Definitions for the above table:

B = experimentally observed breadth

D = mean dimension of the crystallites (particle diameter)

Height = XRD peak height

Area = XRD peak area

Definitions for the catalysts listed in here are the same as in Table 17

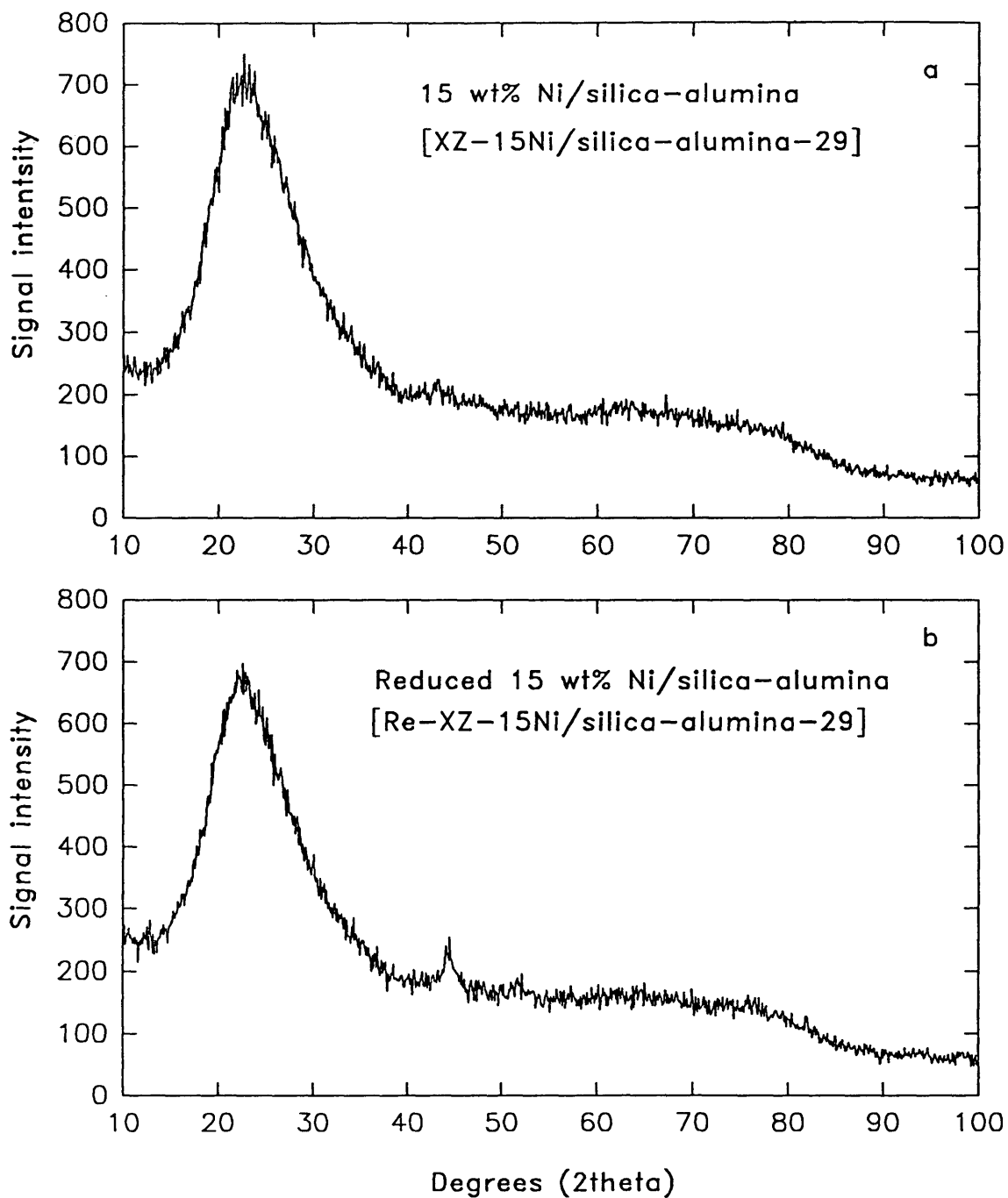


Figure 43. XRD patterns for 15 wt% Ni/SiO₂-Al₂O₃ and reduced 15 wt% Ni/SiO₂-Al₂O₃ catalysts.

In **Figure 43-a**, the spectrum of $\text{SiO}_2\text{-Al}_2\text{O}_3$ supported nickel catalyst shows a small broad diffraction line at 43.3 degrees 2θ . The d-spacing of the peaks corresponds to the nickel oxide (compare **Figures 43-a** and **38**). In **Figure 43-b**, the spectrum of reduced $\text{SiO}_2\text{-Al}_2\text{O}_3$ supported nickel catalyst shows a large broad diffraction line at 44.5 degrees 2θ . The d-spacing of the peaks corresponds to the nickel metal (compare **Figure 43-b** and **38**). The results indicate that nickel oxide is the major crystalline component on the calcined $\text{SiO}_2\text{-Al}_2\text{O}_3$ supported catalyst, and nickel metal is the major crystalline component on the reduced $\text{SiO}_2\text{-Al}_2\text{O}_3$ supported catalyst. The reduction step is necessary for testing the $\text{SiO}_2\text{-Al}_2\text{O}_3$ supported nickel catalyst.

The XRD signal of 15 wt% Ni supported on $\text{SiO}_2\text{-Al}_2\text{O}_3$ was very small for NiO and Ni. These small signals are explained as follows: During the calcination and reduction processes, the NiO monolayer may be reduced to nickel metal or may form nickel aluminate (NiAl_2O_4) (*Satterfield, 1991*) by reacting with the support or may dissolve in the support to form a solid solution [$\text{Al}_2(\text{NiO})_3$] (*Satterfield, 1991*). At the usual calcination temperatures, up to 500 or 600°C, silica does not react appreciably with most metals. Alumina which is a commonly used support can react with a divalent metal oxide to form a metal aluminate (*Satterfield, 1991*).

5.17.2 Surface Carbonaceous Residue (Coke) Content

Typical plots of thermal gravimetric analysis (TGA) and differential thermal analysis (DTA) as shown in **Figure 44**. In **Figure 44-a**, the X axis is temperature and the Y axis is DTA. In **Figure 44-b**, the X axis is also temperature and the Y axis is TG. A positive value of DTA indicates an exothermic reaction. The decrease in TG shows the sample weight loss as surface carbon is oxidized to carbon dioxide .

The thermal analysis results of fourteen tested catalysts and supports are summarized in **Table 11**. The results show that more coke was observed when hexane was used as the solvent as compared to toluene under the same test conditions (compare experimental runs RUN-08-28-90 and RUN-08-31-90). The test conditions (temperature, pressure and experiment time) also affect the amount of coke formation. Low H₂ pressures and high reaction temperatures (see experimental runs RUN-03-13-91 and Run-03-17-91) tend to promote more coke formation. Longer experiment time also promotes more coke.

The amount of coke deposited on both the supported platinum and nickel catalysts was apparently similar (compare experimental runs RUN-06-19-90 and RUN-09-05-92). This was not a true result for the nickel catalyst.

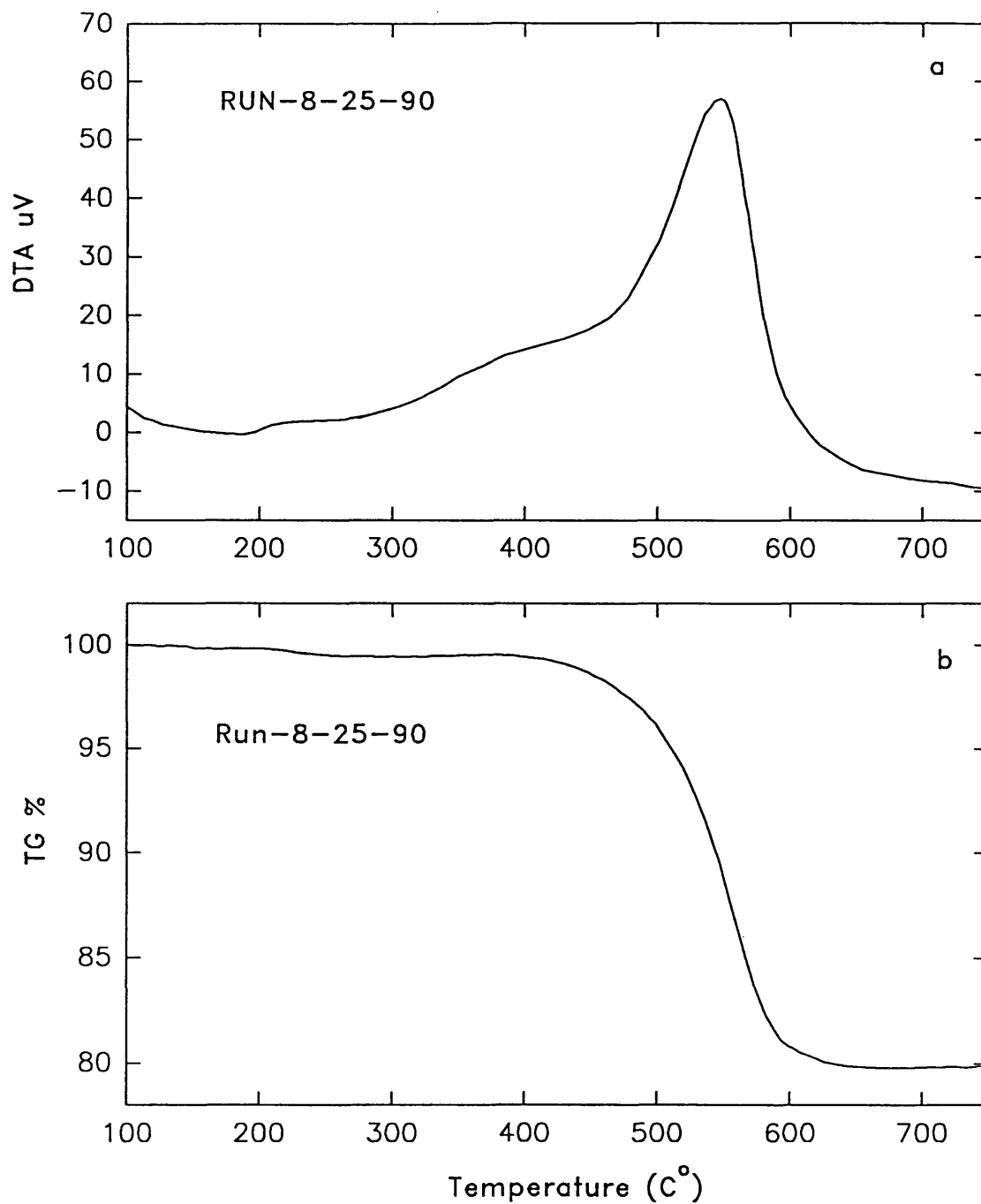


Figure 44. Thermal analysis of tested catalyst (a) DTA and (b) TGA.

Table 11. Apparent surface coke content on the tested catalysts

Catalysts	Run #	Run conditions			React. + Solv.	Weight loss (wt%)
		P (psig)	Temp. (°C)	T (hr.)		
Pt/P-Al	RUN-06-04-90	500	350	3.0	4PP+H	9.8
0.8P:Al	RUN-06-20-90	500	350-450	6.5	4PP+H	28.5
Si-Al	RUN-08-25-90	500	350-450	6.0	4PP+H	20.1
Pt/P-Al	RUN-06-19-90	500	350	3.0	4PP+H	9.9
Pt/Si-Al	RUN-08-28-90	500	350-450	12.5	4PP+H	18.4
Pt/Si-Al	RUN-08-31-90	500	350-450	12.5	4PP+T	12.4
Pt/Si-Al	RUN-03-13-91	200	400-450	6.0	4PG+T	24.3
Pt/Si-Al	RUN-03-17-91	300	400-450	6.0	4PG+T	19.5
Pt/Si-Al	RUN-03-07-90	300-500	400-450	8.0	SYR+T	17.3
Pt/Si-Al	RUN-03-11-90	200	400-450	6.0	SYR+T	22.3
Pt/Si-Al	RUN-09-07-90	200	350-450	9.0	SYR+T	23.0
Pt/Si-Al	RUN-08-27-90	500	350	3.0	SYR+T	13.1
Pt/Si-Al	RUN-04-23-93	300	450	3.5	Mix+T	13.9
Ni/Si-Al	RUN-09-05-92	500	350	3.0	4PP+H	9.2

Definitions for the previous table:

4PP+H = 10 wt% 4-propylphenol + 90 wt% hexane

4PP+T = 10 wt% 4-propylphenol + 90 wt% toluene

4PG+T = 10 wt% 4-propylguaiacol + 90 wt% toluene

SRY+T = 10 wt% syringol + 90 wt% toluene

Mix+T = 5 wt% 4-propylguaiacol + 5 wt% syringol + 90 wt% toluene

Pt/P-Al = 0.3 wt% Pt/ $\text{AlPO}_4\text{-Al}_2\text{O}_3$

Pt/Si-Al = 0.3 wt% Pt/ $\text{SiO}_2\text{-Al}_2\text{O}_3$

Ni/Si-Al = 15 wt% Ni/ $\text{SiO}_2\text{-Al}_2\text{O}_3$

0.8P:Al = Blank aluminophosphate support ($\text{AlPO}_4\text{-Al}_2\text{O}_3$)

Si-Al = Blank silica-alumina support ($\text{SiO}_2\text{-Al}_2\text{O}_3$)

Since the oxidation rate of nickel is much higher than that of platinum at the temperature range as studied, an appreciable amount of nickel oxide can be formed during the TGA analysis. The weight gained by nickel oxidized to form nickel oxide must be added to the gross weight loss to get the true weight loss of coke.

The formation of coke on the tested catalyst is an unwanted side reaction which occurs in all reactions involving hydrocarbons. Normally, coke is defined as the carbonaceous material left on the catalyst after the catalyst testing. The lifetime of the catalyst under the process conditions may be limited due to the coke on the surface. This residue is not pure carbon but is composed of a mixture of highly unsaturated hydrocarbons with the average atomic ratio of hydrogen to carbon of 0.3 to 1.0 (*Pines, 1981*).

Coke formation is a complex reaction. The mechanism of the formation of coke from feed or product molecules is still not completely understood (*Van-Doorn and Moulijn, 1989*). Little fundamental information has been published regarding the steps involved. Coking as a cause of deactivation is also still not fully understood. The amount of coke on the surface may not always have a proportional relationship to the activity loss of the catalyst (*Acharya et al., 1990*).

In summary, the catalyst coke level is determined by the solvent, model

compound, reaction temperature, pressure and experiment time. Since coke is detrimental to the catalyst lifetime, the reaction conditions must be optimized so as to minimize the coking rate. In addition, a process must be adopted which incorporates a catalyst regeneration step to remove the coke deposit.

5.18 Preparation and Characterization of More Realistic Lignin Feedstock

The use of raw lignin as a reactant to evaluate the catalyst was proposed to complete this project, but a problem was found. The raw lignin molecules were too large to enter the pores of the catalyst. Then low molecular weight lignin fragments as reactants were proposed instead of raw lignin to evaluate the potential catalyst. It was found that to obtain these low molecular weight lignin fragments from raw lignin and characterize them would be too complicated and time consuming for this study. Therefore, based on references in the literature a mixture of model lignin compounds was used. This mixture should simulate the chemical reactivity of low molecular weight lignin fragments. Some preliminary work on the solvent extraction of lignin was done and the details are presented in the **Appendix D**. There was no difference in the FTIR spectra of the extract, residue, or raw lignin. This

suggests that the extract may be lower molecular weight segments of the original lignin; however, extensive characterization of the extract is necessary before work on the extracts can continue.

Chapter 6
CONCLUSIONS

6.1 Catalysts

- a. Three kinds of catalyst were prepared and tested to determine which type of catalytic functions they contained. The results show that individual model lignin compounds and a mixture of model lignin compounds were successfully converted into phenolic products using a Pt/SiO₂-Al₂O₃ or Pt/AlPO₄-Al₂O₃ catalyst.
- b. The AlPO₄-Al₂O₃ or SiO₂-Al₂O₃ supports provide a good acidity function, which is necessary for dealkylation. High reaction temperature also assists dealkylation.
- c. Platinum has a good hydrogenation function which reduces transalkylation. The Pt/SiO₂-Al₂O₃ catalyst shows the best phenol yields and lowest transalkylation products.

- d. Platinum exhibits a good hydrogenolysis activity which is necessary to cleave C-O bonds. High pressure (500 psig) favors complete deoxygenation while lower pressure (200-300 psig) favors phenol production. The platinum-based catalysts are much more active and selective than the molybdenum-based catalysts used in petroleum refining. In addition, the platinum-based catalysts do not require the addition of sulfur compounds to the feedstock in order to maintain their activity.
- e. The $\text{SiO}_2\text{-Al}_2\text{O}_3$ supported platinum catalyst is a potential hydrotreating catalyst for low molecular weight lignin fragments.

6.2 Physical and Chemical Properties of Catalysts

XRD was used to determine the presence of active metals in the catalyst. The crystal size of the active metals on the support was determined by the breadth of the metal peak.

- a. The XRD results show that platinum metal is the predominant crystal structure on the calcined $\text{SiO}_2\text{-Al}_2\text{O}_3$ and $\text{AlPO}_4\text{-Al}_2\text{O}_3$ supported catalysts. The calcined and reduced $\text{SiO}_2\text{-Al}_2\text{O}_3$ and

$\text{AlPO}_4\text{-Al}_2\text{O}_3$ supported platinum catalysts had the same platinum metal crystal pattern. Therefore the prereduction step may not be needed for the catalyst testing.

- b. The XRD results indicate that nickel oxide is the major component on the calcined $\text{SiO}_2\text{-Al}_2\text{O}_3$ supported catalyst and that nickel metal is the major component on the reduced $\text{SiO}_2\text{-Al}_2\text{O}_3$ supported catalyst. The reduction step is necessary for testing the $\text{SiO}_2\text{-Al}_2\text{O}_3$ supported nickel catalyst.
- c. The average particle diameter of the reduced platinum supported by $\text{SiO}_2\text{-Al}_2\text{O}_3$ is twice that of the unreduced catalyst. In the future the prereduction step for $\text{Pt/SiO}_2\text{-Al}_2\text{O}_3$ catalyst should be omitted.
- d. The average particle diameter of the active metal was determined by the line broadening method. The results indicate that platinum has better dispersion on the $\text{SiO}_2\text{-Al}_2\text{O}_3$ than on the $\text{AlPO}_4\text{-Al}_2\text{O}_3$ support.

The surface coke content of various catalysts tested in this study was characterized by thermal gravimetric analysis (TGA).

- a. The TGA results indicate that hexane as a solvent produces more

coke on the tested catalysts than toluene does at the same conditions.

- b. The test conditions (temperature, pressure and experiment time) also affect the amount of coke formation. Low H_2 pressure and high reaction temperature tend to promote more coke formation. Longer experiment time also promotes more coke.

Chapter 7

RECOMMENDATIONS FOR FUTURE STUDIES

Recommendations for further study in conversion of lignin to phenols are:

1. The direct conversion of lignin into usable products such as phenol is severely limited by poor access of the high molecular weight lignin materials to the internal pore structure of the catalyst. The depolymerization of the lignin into lower molecular weight fragments is highly recommended prior to any catalytic operation. Acid and base catalyzed depolymerization methods are fraught with problems. Biodegradation, pyrolysis, thermal degradation in a hydrodonor solvent or steam reforming are more acceptable. Biodegradation, however may be too slow for commercial applications. A proposed schematic of a combined thermal conversion and catalytic conversion system is shown in **Appendix C, Figure C-1.**

2. The pyrolysis of lignin into low molecular weight oils has been studied extensively at NREL. It is recommended that the catalytic conversion of pyrolysis oils into phenolic products be investigated using the catalysts developed in this study. A major drawback to using this feedstock, however, it is high olefin content. A high olefin content makes the catalyst much more susceptible to coking.

3. Catalyst coking appears to be a major problem in this process and alternative methods of lignin degradation should be investigated. The non-catalytic and catalytic steam reforming of lignin into a low molecular weight feedstock should be investigated, because the steam can help reduce the amount of coke formation by forming carbon monoxide and carbon dioxide. High temperature steam may cause the catalyst to degenerate; catalyst stability must also be monitored during this study. The selection of appropriate steam reforming conditions should favor the production of aromatic hydrocarbons, phenols, and synthesis gas.

Typically high temperatures (600-1000°C) are required for the steam reforming of hydrocarbons into synthesis gas. These

temperatures exceed those recommended for high surface area alumina or silica. Special refractory low surface area supports are required. However, oxygenated compounds have a much faster reforming rate and thus require a much lower reaction temperature and the reaction temperature should be maintained so as to promote steam induced dealkylation of aromatics without destruction of the aromatic ring. Temperatures as low as 430-500°C may be effective. Such low temperatures may permit the use of high surface area supports.

The $\text{AlPO}_4\text{-Al}_2\text{O}_3$ support has good thermal stability in the presence of steam and a large average pore diameter. A $\text{Ni/AlPO}_4\text{-Al}_2\text{O}_3$ catalyst would be a good potential catalysts for this process. In addition, the problems associated with catalyst coking may be substantially reduced in the presence of excess steam.

REFERENCES CITED

- Acharya, D. R., M. R. Ghassemi and R. Hughes. 1990. Coking and Regeneration of Zeolite Catalysts in Fixed Beds During Cumene Cracking. Applied Catalysis 58: 53-67.
- Agblevor, F. A. and D. G. B. Boocock. 1989. The Origins of Phenol Produced in the Rapid Hydrothermolysis and Alkaline Hydrolysis of Hybrid Poplar Lignins. Journal of Wood Chemistry and Technology 9 (2): 167-188.
- Anderson, J. R. 1975. Structure of Metallic Catalysts. Academic, New York.
- Assafi, M. and D. Duprez. 1992. Steam-Dealkylation and Hydrodealkylation of Meta-Cresol on Potassium-Promoted Rhodium and Nickel Catalysts. Applied Catalysis A: General 80: 23-39.
- Avni, E. and R. Coughlin. 1985. Kinetic Analysis of Lignin Pyrolysis Using Non-Isothermal TGA data. Thermochemica Acta 90: 157-167.
- Boorman, P.M., R. A. Kydd, Z. Sarbak and A. Somogyvari. 1985. Surface Acidity and Cumene Conversion. I. A Study of γ -Alumina Containing Fluoride, Cobalt, and Molybdenum Additives. Journal of Catalysis 96: 115-121.
- Brauns, F.E. 1948. The Proven Chemistry of Lignin. Journal of the Technical Association of the Pulp and Paper Industry (TAPPI) Monograph Ser. 6: 108-129.
- Chen, D., S. Sharma, N. Cardona-Martinez, J. A. Dumesic, V. A. Bell, G. D. Hodge and R. J. Madon. 1992. Acidity Studies of Fluid Catalytic Cracking Catalysts by Microcalorimetry and Infrared Spectroscopy. Journal of Catalysis 136: 392-402.
- Chum, H. L., D. K. Johnson, S. Black, M. Ratcliff and D. W. Goheen. 1987. Lignin Hydrotreatment to Low-Molecular-Weight Compounds. In Advances in Solar Energy: Annual Review of Research and Development. K. W. Boer (editor). American Chemical Society, Boulder, CO. 1987. 4: 92-171.

Clark, Ira T. and J. Green. 1968. Production of Phenols by Cooking Kraft Lignin in Alkaline Solutions. Journal of the Technical Association of the Pulp and Paper Industry (TAPPI) 51 (1): 44-48.

Corma, A. and M. S. Grande. 1992. Nickel Passivation on Fluidized Cracking Catalysts with Different Antimony Complexes. Applied Catalysis A: General 85: 61-71.

Davoudzadeh, F., B. Smith, E. Avni and R. W. Coughlin. 1985. Depolymerization of Lignin at Low Pressure Using Lewis Acid Catalysts and Under High Pressure Using Hydrogen Donor Solvents. Holzforschung 39: 159-166.

Dietz, W.A. 1967. Response Factors for Gas Chromatographic Analysis. Journal of Gas Chromatography Feb. 68-71.

Edelman, M. C., M. K. Maholland, R. M. Baldwin and S. W. Cowley. 1988. Vapor-Phase Catalytic Hydrodeoxygenation of Benzofuran. Journal of Catalysis 111: 243-252.

Elder, T. J. and E. J. Soltes. 1980. Pyrolysis of Lignocellulosic Materials. Wood and Fiber 12(4): 217-226.

Eltzner, W., M. Breyse, M. Lacroix, C. Leclercq and M. Vrinat. 1988. A New Highly Active Hydrotreating Catalyst Prepared by the Decomposition of Thiotungstato-nickelate and Characterized by High Resolution Electron Microscopy. Polyhedron 7(22/23): 2405-2409.

Erickson, Dee A. 1990. The Hydrodeoxygenation and Dealkylation of Model Lignin Compounds. Thesis, Colorado School of Mines.

Frerichs, Scott R. 1984. The Characterization of Pt/Al₂O₃ and Pt-Re/Al₂O₃ Reforming Catalysts and Their Evaluation Using a Model Naphtha Feedstock. Dissertation, Colorado School of Mines.

Freudenberg, Karl. 1939. Polysaccharides and Lignin. Annual Review of Biochemistry 8: 81-107.

Freudenberg, K. 1965. Lignin: Its Constitution and Formation From p-Hydroxycinnamyl Alcohols. Science 148: 595-600.

Funaoka, M., M. Shibata and I. Abe. 1990. Structure and Depolymerization of Acid-Condensed Lignin. Holzforschung 44: 357-366.

Furimsky, E. 1983. Chemistry of Catalytic Hydrodeoxygenation. Catalysis Reviews: Science and Engineering 25(3): 421-458.

Glasser, W. G.(editor). 1988. Lignin Properties and Materials. American Chemical Society, Washington DC.

Goheen, D. W. 1971. Low Molecular Weight Chemicals. Lignins, Occurrence, Formation, Structure, and Reactions. Edited by K. V. Sarkanen and C. H. Ludwig. Wiley-Interscience, New York. Chap.19: 797-831.

Goldstein, Irving S. 1975. Perspectives on Production of Phenols and Phenolic Acids from Lignin and Bark. Applied Polymer Symposium 28: 259-267.

Grange, P. 1980. Catalytic Hydrodesulfurization. Catalysis Reviews: Science and Engineering 21: 135-182.

Hadsell, K. J. 1985. The Effect of Coking and Sulfur Poisoning on Pt/Al₂O₃ and Pt-Re/Al₂O₃ Reforming Catalysts Using a Model Naphtha Feedstock. Thesis, Colorado School of Mines.

Hammel, E. Kenneth and Mark A. Moen. 1991. Depolymerization of a Synthetic Lignin in Vitro by Lignin Peroxidase. Enzyme Microbiology Technology 13 (January): 15-18.

Houalla, M., C. L. Kibby, L. Petrakis and D. M. Hercules. 1983. Effects of Impregnation pH on the Surface Structure and Hydrodesulfurization Activity of Mo/Al₂O₃ Catalysts. Journal of Catalysis 83: 50-60.

Hurff, S. J. and M. T. Klein. 1983. Reaction Pathway Analysis of Thermal and Catalytic Lignin Fragmentation by Use of Model Compounds. Industrial & Engineering Chemistry Fundamentals 22: 426-429.

Ichimura, K., Y. Inoue and I. Yasumori. 1992. Hydrogenation and Hydrogenolysis of Hydrocarbons on Perovskite Oxides. Catalysis Reviews: Science and Engineering 34(4): 301-320.

Kallury, R.K.M.R., W. M. Restivo, T. T. Tidwell, D. G. B. Boocock, A. Crimi and

J. Douglas. 1985. Hydrodeoxygenation of Hydroxy, Methoxy, and Methyl Phenols with Molybdenum Oxide/Nickel Oxide/Alumina Catalyst. Journal of Catalysis 96: 535-543.

Kirk, T. K. and R. L. Farrell. 1987. Enzymatic "Combustion": The Microbial Degradation of Lignin. Annual Review of Microbiology 41: 465-505.

Klug, H. P. and L. E. Alexander. 1959. X-ray Diffraction Procedures. New York, John Wiley & sons, INC. 491-538.

Kuroda, Ken-ichi and Y. Inoue. 1990. Analysis of Lignin by Pyrolysis-Gas Chromatography. Journal of Analytical and Applied Pyrolysis 18: 59-69.

Maholland, M. K. 1987. Synthesis, Characterization, and Activity Evaluation of Phosphate-Modified Hydroprocessing Catalysts for Benzofuran Hydrodeoxygenation. Dissertation, Colorado School of Mines.

March, Jerry (editor). 1985. Advanced Organic Chemistry: Reactions, Mechanisms, and Structure. John Wiley & Sons, New York. P. 505.

Muralidar, G., F. E. Mossoth and J. Shabtai. 1984. Catalytic Functionalities of Supported Sulfides. I. Effect of Support and Additives on the CoMo Catalyst. Journal of Catalysis 85: 44-52.

Obst, John R. 1983. Analytical Pyrolysis of Hardwood and Soft Wood Lignins and Its Use in Lignin-Type Determination of Hardwood Vessel Elements. Journal of Wood Chemistry and Technology 3(4): 377-397.

Ohtsuka, T. 1977. Catalyst for Hydrodesulfurization of Petroleum Residua. Catalysis Reviews: Science and Engineering 16: 291-325.

Owen, N. L. and Thomas, D. W. 1989. Infrared Studies of Hard and Soft Woods. Applied Spectroscopy 43(3): 451-455.

Panasyuk, L.V., L. V. Travleeva and V. G. Panasyuk. 1970. National Lending Library for Science and Technology. Boston Spa, Yorkshire, England. P.59.

Pepper, J. M. and R. W. Fleming. 1978. Lignin and Related Compounds. V. The Hydrogenolysis of Aspen Wood Lignin Using Rhodium/Charcoal as Catalyst. Canadian Journal of Chemistry 56: 896-912.

Pepper, J. M. and D.C. Hagerman. 1954. The Isolation and Oxidation of Aspen Lignins. Canadian Journal of Chemistry 32: 614-627.

Piel, W.J. and R. X. Thomas. 1988. Oxygenates for Reformulated Gasoline. Process Technology 69 (7): 68-73.

Pines, H. (editor). 1981. The Chemistry of Catalytic Hydrocarbon Conversions. Academic Press Inc. New York. P. 80.

Ramirez de Agudelo, M. M., L. G. Reyes and N. Do Campo. 1987. The Role of Transition Metal Sulfides in Hydrotreatment. III. Acidity, XPS, and Catalytic Activity. Applied Catalysis 31: 1-12.

Ratcliff, M. A., D. K. Johnson, F. L. Posey, M. K. Maholland, S. W. Cowley and H. L. Chum. 1988. Hydrodeoxygenation of Lignin Model Compounds. Presented at the IEA international conference on research in thermochemical biomass conversion. Phoenix, Arizona, 2-6 May 1988, Elsevier Applied Science Publishers, London.

Ratnasamy, P. and H. Knozinger. 1978. Infrared and Optical Spectroscopic Study of Co-Mo-Al₂O₃ Catalysis. Journal of Catalysis 54: 155-165.

Riddick, J. A., W. B. Bunger, and T. K. Sakano. 1986. Organic Solvents: Physical Properties and Methods of Purification. John Wiley & Sons. New York.

Rohrbaugh, Wayne J. and Ellen L. Wu. 1989. Factors Affecting X-ray Diffraction Characteristics of Catalyst Materials. Characterization and Catalyst Development: An Interactive Approach. Edited by Steven A. Bradley, Mark J. Gattuso, and Ralph J. Bertolacini. American Chemical Society, Washington, DC.

Sarkanen, K. V. and C. H. Ludwing (editors). 1971. Lignin Occurrence, Formation, Structure and Reactions. Wiley-Interscience, New York.

Satterfield, C. N. (editor). 1991. Heterogeneous Catalysis in Industrial Practice. Second edition, McGraw-Hill, Inc. New York.

Stanislaus, A., M. Absi-Halabi, and K. Al-Dolama. 1989. Effect of Nickel on the Surface Acidity of γ -Alumina and Alumina-Supported Nickel-Molybdenum Hydrotreating Catalysts. Applied Catalysis 50: 237-245.

Stiles, A. B. 1987. Catalyst Supports and Supported Catalysts: Theoretical and Applied Concepts 11-86.

Tai, Die-sheng and M. Terazawa. 1990. Lignin Biodegradation Products from Birch Wood Decayed by Phanerochaete Chrysosporium. Holzforschung 44: 257-262.

Thakur, D. S., P. Grange and B. Delmon. 1985. The Role of Group VIII Metal Promoter in MoS₂ and WS₂ Hydrotreating Catalysis. II. Catalytic and Physicochemical Properties of Nickel-Promoted Catalysis. Journal of Catalysis 91: 318-326.

Thompson, S. C. and J. F. Mathews. 1989. Characterization of Hydro-Cracking Catalysts by Acidity Measurement. Applied Catalysis 47: 45-57.

Thring, R. W., E. Chornet, J. Bouchard, P. F. Vidal and R. P. Overend. 1990. Characterization of Lignin Residues Derived from the Alkaline Hydrolysis of Glycol Lignin. Canadian Journal of Chemistry 68: 82-114.

Thring, R. W., E. Chornet, J. Bouchard, P. F. Vidal and R. P. Overend. 1991. Evidence for the Heterogeneity of Glycol Lignin. Industrial & Engineering Chemistry Research 30: 232-240.

Train, P. M. and M. T. Klein. 1987. Chemical Modeling of Lignin. Pyrolysis Oils from Biomass (Edited by E.J.Soltes and T.A.Milne) 241-263.

Valyon, J., R. L. Schneider and W. K. Hall. 1984. Site Selective Chemisorption on Sulfided Molybdena-Alumina Catalysis. Journal of Catalysis 85: 277-283.

Van Doorn, J. and J. A. Moulijn. 1989. Characterization of Carbon Deposits on Used Hydrotreating Catalysts by Curie-Point Pyrolysis. Journal of Analytical and Applied Pyrolysis 15: 333-345.

Venuto, P. B. and Habib, E. T. (editors) 1979. Fluid Catalytic Cracking With Zeolite Catalysts. Dekker, New York.

Ware, R. A. and J. Wei. 1985. Catalytic Hydrodemetallation of Nickel Porphyrins. III. Acid-Base Modification of Selectivity. Journal of Catalysis 93: 135-151.

Wariishi, H., K. Valli, and N. H. Gold. 1991. In Vitro Depolymerization of Lignin by Manganese Peroxidase. Biochemical and Biophysical Research Communications 176 (1) 169-275.

Wyman, C. E. 1990. The DOE/SERI Ethanol From Biomass Program. Ethanol From Biomass Annual Review Meeting, September 12-13, Lincoln, Nebraska.

Zhao, X., D. A. Erickson and S. W. Cowley. 1990. The Conversion of Lignin Model Compounds Into Phenolic Products Using MoS₂ and Pt on Acidic Support. Ethanol From Biomass Annual Review Meeting, September 12-13, Lincoln, Nebraska.

APPENDIX A
TABLES

Table A-1. Activity and selectivity of α -Al₂O₃ for conversion of 4-propylphenol to phenol

Run#	06-21-90	
Tested Material	Blank α -Al ₂ O ₃ only	
Feed Composition	10 wt% 4-propylphenol + 90 wt% hexane	
Space Velocity	0.12 gram 4-propylphenol/hour-gram-catalyst	
Liquid Recovery (%)	93	
Time on Stream (hr)	3	6
Pressure (psig)	500	500
Temperature (°C)	350	450
Component	Mole Percent %	
Methylcyclohexane	4.6	0.0
Propylcyclohexane	0.0	6.1
Propylbenzene	2.0	3.2
Dipropylbenzene	8.2	0.0
Phenol	0.0	22.0
2,6-Dipropylphenol	0.0	2.3
2-Propylphenol	0.0	12.1
4-Propylphenol	85.2	36.0
Dipropylphenol (1)	0.0	11.2
Dipropylphenol (2)	0.0	4.6
Dipropylphenol (3)	0.0	2.5

Dipropylphenol(1), dipropylphenol(2) and dipropylphenol(3) are isomers

Table A-2. Effect of temperature on liquid products distribution for 4-propylphenol conversion over pure quartz

Run#	07-30-90			
Tested Material	Blank quartz only			
Feed Composition	10 wt% 4-propylphenol + 90 wt% hexane			
Space Velocity	0.12 gram 4-propylphenol/hour-gram-catalyst			
Liquid Recovery (%)	90			
Time on Stream (hr)	3.0	5.0	5.5	6.0
Pressure (psig)	500	500	500	500
Temperature (°C)	350	450	450	450
Component	Mole Percent %			
4-Propylphenol	100	100	100	100

Table A-3. Catalysts used with preparation conditions

Catalyst Identification	Support*	Weight % Platinum	Wetting Volume (ml)	Initial Weight (g)	Calcining Time (hr)
XZ-01A	DE-4	0.5	1.5	5	24
DE-01A	DE-3	0.3	0.9	5	24
XZ-05A	DE-4	0.3	1.5	5	24
XZ-03A	DE-4	0.3	0.9	2	24
XZ-13D	XZ-2	1.2	1.5	2	24
XZ-15D	XZ-2	1.2	1.5	2	18
XZ-16D	XZ-2	0.5	1.5	2	18
XZ-07B	DE-2	0.5	1.5	25	24
XZ-09A	DE-2	0.5	1.5	5	24
XZ-10A	DE-2	0.5	1.5	5	24

All supports contain a phosphorous-to-aluminum atomic ratio (P:Al) of 0.8.

XZ = Xianghong Zhao (who made this catalyst or support)

DE = Dee Erickson (who made this catalyst or support)

Table A-4. Effect of catalyst on product distribution

Run #	6-4-90	6-19-90	6-5-90	6-15-90	6-11-90	6-18-90
Tested Material	DE-01A	XZ-03A	XZ-01A	XZ-16D	XZ-13D	XZ-15D
Feed Composition	10 wt% 4-propylphenol + 90 wt% hexane					
Space Velocity	1 gram 4-propylphenol/hour-gram-catalyst					
Liquid Recovery (%)	88	88	87	84	89	88
Time on Stream (hr)	3.0	3.0	3.0	3.0	3.0	3.0
Pressure (Psig)	500	500	500	500	500	500
Temperature (C°)	350	350	350	350	350	350
Component	Mole Percent					
Cyclohexane	8.2	8.5	5.5	6.1	7.1	7.5
Methylcyclohexane	0.0	2.6	3.0	5.6	3.1	3.9
Ethylcyclohexane	0.9	0.0	0.9	0.0	0.0	0.0
Benzene	2.3	3.4	2.3	2.8	3.2	3.5
Propylcyclohexane	51.6	38.3	32.5	26.8	31.5	31.6
Propylbenzene	27.7	22.1	13.6	13.3	17.2	16.2
Dipropylbenzene	4.5	3.9	4.5	3.9	2.5	2.5
Phenol	1.1	3.5	5.3	5.6	5.0	4.9
2,6-Dipropylphenol	0.7	0.0	1.3	0.0	0.0	0.0
2-Propylphenol	0.8	4.4	5.8	6.3	5.4	5.4
4-Propylphenol	1.7	7.3	13.7	13.7	13.1	13.4
Dipropylphenol(1)	0.0	2.9	4.2	6.5	3.9	3.6
Dipropylphenol(2)	0.5	3.1	4.3	4.7	4.2	3.8
Dipropylphenol(3)	0.0	0.0	3.1	4.7	3.8	3.7

Table A-5. Comparison of the effect of quartz and α -Al₂O₃ on liquid product distribution for 4-propylphenol conversion over Pt/AlPO₄-Al₂O₃

Run#	08-23-90	06-04-90
Tested Material	DE-01 + α -Al ₂ O ₃	DE-01 + Quartz
Feed Composition	10 wt% 4-propylphenol + 90 wt% hexane	
Space Velocity	1 gram 4-propylphenol/hour-gram-catalyst	
Liquid Recovery (%)	89	
Time on Stream (hr)	3	3
Pressure (psig)	500	500
Temperature (°C)	350	350
Component	Mole Percent	
Cyclohexane	14.6	8.2
Methylcyclohexane	5.2	0.0
Ethylcyclohexane	0.0	0.9
Benzene	2.3	2.3
Propylcyclohexane	46.2	51.6
Propylbenzene	12.7	27.7
Dipropylbenzene	2.8	4.6
Phenol	3.2	1.1
2,6-Dipropylphenol	0.0	0.7
2-Propylphenol	2.3	0.8
4-Propylphenol	7.0	1.7
Dipropylphenol (1)	1.6	0.0
Dipropylphenol (2)	1.3	0.4
Dipropylphenol (3)	0.8	0.0

Table A-6. Effect of temperature and pressure on liquid product distribution for 4-propylphenol conversion over Pt/SiO₂-Al₂O₃

Run#	08-28-90				
Tested Material	XZ-0.3Pt/SiO ₂ -Al ₂ O ₃ -20D + Quartz				
Feed Composition	10 wt% 4-propylphenol + 90 wt% hexane				
Space Velocity	1 gram 4-propylphenol/hour-gram-catalyst				
Liquid Recovery (%)	96				
Time on Stream (hr)	3.0	6.5	9.0	11.0	12.5
Pressure (psig)	500	200	200	200	500
Temperature (°C)	350	350	400	450	350
Component	Mole Percent				
Cyclohexane	4.5	0.0	0.0	0.0	0.0
Trimethylcyclohexane (1)	2.9	0.0	0.0	0.0	0.0
Trimethylcyclohexane (2)	3.6	0.0	0.0	0.0	0.0
Ethylcyclohexane	4.7	0.0	0.0	0.0	0.0
Ethylmethylcyclohexane (1)	7.2	0.0	0.0	0.0	0.0
Benzene	13.0	0.0	10.2	17.3	3.5
Ethylmethylcyclohexane (2)	4.5	0.0	0.0	0.0	0.0
Propylcyclohexane	40.7	4.7	0.0	0.0	14.8
Toluene	0.0	0.0	0.0	3.6	0.0
Propylbenzene	11.5	11.5	15.6	8.0	12.8
Phenol	0.0	17.7	42.5	53.8	12.0
2,6-Dipropylphenol	0.0	0.0	2.1	4.2	0.0
2-Propylphenol	0.0	9.5	7.3	2.7	2.3
4-Propylphenol	7.4	52.0	22.2	10.4	54.7
Dipropylphenol (1)	0.0	2.1	0.0	0.0	0.0
Dipropylphenol (2)	0.0	2.5	0.0	0.0	0.0

* Trimethylcyclohexane(1) and trimethylcyclohexane(2) are isomers

* Ethylmethylcyclohexane(1) and ethylmethylcyclohexane (2) are isomers

Table A-7. Duplicate runs to test experimental reproducibility at fixed temperature and pressure

Run#	06-05-90	06-07-90	05-21-90
Tested Material	XZ-0.5Pt/AlPO ₄ -Al ₂ O ₃ -01A + α -Al ₂ O ₃		
Feed Composition	10 wt% 4-propylphenol + 90 wt% hexane		
Space Velocity	1 gram toluene/hour-gram-catalyst		
Liquid Recovery (%)	87	85	94
Time on Stream (hr)	3.0	3.0	3.0
Pressure (psig)	500	500	500
Temperature (°C)	350	350	350
Component	Mole Percent		
Cyclohexane	5.5	5.7	6.3
Methylcyclohexane	3.0	2.3	2.6
Ethylcyclohexane	0.9	0.8	0.7
Benzene	2.3	3.0	3.4
Propylcyclohexane	32.4	32.9	28.5
Propylbenzene	13.6	16.2	14.2
Dipropylbenzene	4.5	2.4	3.6
Phenol	5.3	4.6	6.0
2,6-Dipropylphenol	1.3	1.3	1.4
2-Propylphenol	5.7	5.6	6.2
4-Propylphenol	13.9	12.7	14.3
Dipropylphenol(1)	4.2	4.1	4.1
Dipropylphenol(2)	4.3	4.2	4.2
Dipropylphenol(3)	3.1	4.2	4.5

Table A-8. Duplicate runs to test experimental reproducibility at fixed temperature and pressure

Run#	08-27-90	08-28-90
Tested Material	XZ-0.3Pt/SiO ₂ -Al ₂ O ₃ -2D + Quartz	
Feed Composition	10 wt% 4-propylphenol + 90 wt% hexane	
Space Velocity	1 gram 4-propylphenol/hour-gram-catalyst	
Liquid Recovery (%)	93	96
Time on Stream (hr)	3	3
Pressure (psig)	500	500
Temperature (°C)	350	350
Component	Mole Percent	
Cyclohexane	4.9	4.6
Methylcyclohexane	6.0	5.7
Trimethylcyclohexane (1)	3.2	3.0
Trimethylcyclohexane (2)	3.8	3.6
Ethylcyclohexane	4.6	4.5
Ethylmethylcyclohexane (1)	6.7	7.0
Benzene	13.8	13.8
Ethylmethylcyclohexane (2)	4.3	4.5
Propylcyclohexane	35.7	37.9
Propylbenzene	11.4	9.8
4-Propylphenol	5.7	5.6

Table A-9. Effect of temperature on liquid product distribution for 4-propylphenol conversion over $\text{AlPO}_4\text{-Al}_2\text{O}_3$ blank support

Run#	06-20-90	
Tested Material	Blank $\text{AlPO}_4\text{-Al}_2\text{O}_3$ support + $\alpha\text{-Al}_2\text{O}_3$	
Feed Composition	10 wt% 4-propylphenol + 90 wt% hexane	
Space Velocity	1 gram 4-propylphenol/hour-gram-catalyst	
Liquid Recovery (%)	93	
Time on Stream (hr)	3.5	6.5
Pressure (psig)	500	500
Temperature ($^{\circ}\text{C}$)	350	450
Component	Mole Percent	
Methylcyclohexane	5.8	0.0
Propylbenzene	0.0	5.7
Phenol	22.3	54.6
2,6-Dipropylphenol	3.0	19.8
2-Propylphenol	15.5	6.8
4-Propylphenol	32.8	13.1
Dipropylphenol (1)	7.3	0.0
Dipropylphenol (2)	7.1	0.0
Dipropylphenol (3)	6.2	0.0

Table A-10. Effect of temperature on liquid product distribution for 4-propylphenol conversion over $\text{SiO}_2\text{-Al}_2\text{O}_3$ blank support

Run#	08-25-90			
Tested Material	Blank $\text{SiO}_2\text{-Al}_2\text{O}_3$ support + Quartz			
Feed Composition	10 wt% 4-propylphenol + 90 wt% hexane			
Space Velocity	1 gram 4-propylphenol/hour-gram-catalyst			
Liquid Recovery (%)	92			
Time on Stream (hr)	3.0	5.0	5.5	6
Pressure (psig)	500	500	500	500
Temperature ($^{\circ}\text{C}$)	350	450	450	450
Component	Mole Percent			
Methylcyclohexane	6.0	0.0	0.0	0.0
Phenol	16.8	59.1	55.7	52.8
2,6-Dipropylphenol	0.0	4.0	3.6	3.1
2-Propylphenol	4.7	7.5	8.2	8.8
4-Propylphenol	66.3	29.4	32.5	35.3
Dipropylphenol (1)	3.8	0.0	0.0	0.0
Dipropylphenol (2)	2.4	0.0	0.0	0.0

Table A-11. Effect of temperature and pressure on liquid product distribution of pure toluene over Pt/SiO₂-Al₂O₃

Run#	09-04-90	
Tested Material	XZ-0.3Pt/SiO ₂ -Al ₂ O ₃ + Quartz	
Feed Composition	Pure toluene	
Space Velocity	12 gram toluene/hour-gram-catalyst	
Liquid Recovery (%)	100	
Time on Stream (hr)	3.5	6.5
Pressure (psig)	500	200
Temperature (°C)	350	450
Component	Mole Percent	
Hexane	0.3	0.0
Cyclohexane	26.7	0.6
Methylcyclohexane	49.8	0.8
Trimethylcyclohexane (1)	0.2	0.0
Toluene	23.0	98.6

Table A-12. Effect of temperature and pressure on liquid product distribution for pure toluene over Pt/SiO₂-Al₂O₃

Run#	11-12-90				
Tested Material	XZ-0.3Pt/SiO ₂ -Al ₂ O ₃ -28 + Quartz				
Feed Composition	Pure toluene				
Space Velocity	14 gram toluene/hour-gram-catalyst				
Liquid Recovery (%)	100				
Time on Stream (hr)	3.5	6.5	9.0	11.0	12.5
Pressure (psig)	500	200	200	200	500
Temperature (°C)	350	350	400	450	350
Component	Mole Percent				
Hexane	1.5	0.5	0.4	0.0	0.0
Cyclohexane	22.9	4.7	2.6	1.2	6.5
Methylcyclohexane	49.9	12.7	4.8	1.0	17.7
Benzene	0.0	0.0	0.0	0.0	3.5
Toluene	25.7	82.1	92.3	97.9	75.8

Table A-13. Effect of pressure and time on liquid product distribution for pure toluene over Pt/SiO₂-Al₂O₃

Run#	11-19-90			
Tested Material	XZ-0.3Pt/SiO ₂ -Al ₂ O ₃ -28 + Quartz			
Feed Composition	Pure toluene			
Space Velocity	14 gram toluene/hour-gram-catalyst			
Liquid Recovery (%)	100			
Time on Stream (hr)	3.0	5.0	7.0	9.0
Pressure (psig)	350	300	250	200
Temperature (°C)	450	450	450	450
Component	Mole Percent			
Hexane	3.2	1.6	0.0	0.0
Cyclohexane	3.0	1.7	1.3	0.4
Methylcyclohexane	1.0	0.9	0.7	0.4
Benzene	0.6	0.5	0.3	0.3
Toluene	91.0	94.8	97.4	98.7
Dimethylbenzene	1.2	0.5	0.3	0.2

Table A-14. Effect of temperature and pressure on liquid product distribution for 4-propylphenol conversion over Pt/SiO₂-Al₂O₃

Run#	08-31-90				
Tested Material	XZ-0.3Pt/SiO ₂ -Al ₂ O ₃ -20D + Quartz				
Feed Composition	10 wt% 4-propylphenol + 90 wt% toluene				
Space Velocity	1 gram 4-propylphenol/hour-gram-catalyst				
Liquid Recovery (%)	99				
Time on Stream (hr)	3.5	6.5	9.0	11.0	12.5
Pressure (psig)	500	200	200	200	500
Temperature (°C)	350	350	400	450	350
Component	Mole Percent				
Hexane	2.2	0.0	0.0	0.0	0.0
Cyclohexane	23.4	5.5	0.0	0.0	5.7
Methylcyclohexane	59.7	14.3	3.8	0.0	41.2
Ethylcyclohexane	1.0	0.0	0.0	0.0	0.0
Benzene	2.1	0.0	6.3	24.8	3.0
Propylcyclohexane	5.3	3.8	0.0	0.0	9.9
Propylbenzene	2.3	5.2	7.8	4.9	5.3
Dipropylbenzene (1)	1.3	4.8	7.1	7.2	0.0
Phenol	0.8	18.7	44.7	63.1	4.8
2-Propylphenol	0.0	7.9	7.5	0.0	0.0
4-Propylphenol	1.9	39.9	23.0	0.0	30.3

Table A-15. Effect of temperature and pressure on liquid product distribution for 4-propylphenol conversion over Pt/SiO₂-Al₂O₃ (The estimated contribution of toluene products is subtracted)

Run#	08-31-90				
Tested Material	XZ-0.3Pt/SiO ₂ -Al ₂ O ₃ -20D + Quartz				
Feed Composition	10 wt% 4-propylphenol + 90 wt% toluene				
Space Velocity	1 gram 4-propylphenol/hour-gram-catalyst				
Liquid Recovery (%)	99				
Time on Stream (hr)	3.5	6.5	9.0	11.0	12.5
Pressure (psig)	500	200	200	200	500
Temperature (°C)	350	350	400	450	350
Component	Mole Percent				
Benzene	15.6	0.0	6.5	24.8	5.5
Propylcyclohexane	36.2	4.7	0.0	0.0	18.5
Propylbenzene	15.8	6.5	8.1	4.9	10.0
Dipropylbenzene (1)	9.1	6.1	7.4	7.2	0.0
Phenol	6.3	23.1	46.4	63.1	9.0
2-Propylphenol	0.0	9.9	7.7	0.0	0.0
4-Propylphenol	17.0	49.7	23.9	0.0	57.0

Table A-16. Effect of temperature on liquid product distribution 4-propylguaiacol over Pt/SiO₂-Al₂O₃ at 200 psig

Run#	03-13-91		
Tested Material	XZ-0.3Pt/SiO ₂ -Al ₂ O ₃ -28 + Quartz		
Feed Composition	10 wt% 4-propylguaiacol + 90 wt% toluene		
Space Velocity	1 gram 4-propylguaiacol/hour-gram-catalyst		
Liquid Recovery (%)	89		
Time on Stream (hr)	2	4	6
Pressure (psig)	200	200	200
Temperature (°C)	400	450	400
Component	Mole Percent		
Cyclohexane	8.6	0.0	0.0
Methylcyclohexane	12.5	0.0	0.0
Dimethylcyclohexane	11.7	8.4	9.0
Benzene	7.2	13.9	3.3
Xylene	13.6	10.6	2.3
Propylbenzene	7.3	7.8	3.0
Phenol	16.8	31.9	4.6
Cresol	13.3	14.2	1.6
4-Propylguaiacol	0.0	0.0	67.1
2-Methoxyphenol	0.0	2.9	0.0
Propylcatacol	0.0	2.5	3.8
4-propylphenol	9.0	7.8	5.3

Table A-17. Effect of temperature on liquid product distribution 4-propylguaiacol over Pt/SiO₂-Al₂O₃ at 300 psig

Run#	03-17-91		
Tested Material	XZ-0.3Pt/SiO ₂ -Al ₂ O ₃ -28 + Quartz		
Feed Composition	10 wt% 4-propylguaiacol + 90 wt% toluene		
Space Velocity	1 gram 4-propylguaiacol/hour-gram-catalyst		
Liquid Recovery (%)	92		
Time on Stream (hr)	2	4	6
Pressure (psig)	300	300	300
Temperature (°C)	400	450	400
Component	Mole Percent		
Hexane	3.9	0.0	0.0
Cyclohexane	9.1	0.0	0.0
Methylcyclohexane	11.2	0.0	0.0
Dimethylcyclohexane	8.1	7.0	14.1
Benzene	5.4	15.4	1.0
Xylene	10.8	18.3	16.1
Propylbenzene	8.1	6.0	6.6
Phenol	17.7	31.9	11.9
Methylphenol	13.5	15.2	6.3
4-Propylguaiacol	0.0	0.0	29.5
2-Methoxyphenol	4.4	2.2	3.9
Propylcatacol	0.0	0.0	6.9
4-propylphenol	7.8	4.0	13.7

Table A-18. Effect of temperature and pressure on liquid product distribution for syringol over Pt/SiO₂-Al₂O₃

Run#	03-07-91			
Tested Material	XZ-0.3Pt/SiO ₂ -Al ₂ O ₃ -28 + Quartz			
Feed Composition	10 wt% syringol + 90 wt% toluene			
Space Velocity	1 gram toluene/hour-gram-catalyst			
Liquid Recovery (%)	87			
Time on Stream (hr)	2.0	4.0	6.0	8.0
Pressure (psig)	500	300	300	500
Temperature (°C)	400	400	450	400
Component	Mole Percent			
Benzene	11.9	8.3	21.6	8.8
Xylene	65.9	44.2	39.4	15.1
Mesitylene	14.9	9.2	0.0	11.9
Phenol	0.0	12.9	21.4	9.7
Xylenol	0.0	11.4	17.6	6.5
Syringol	7.3	14.0	0.0	48.0

Table A-19. Effect of temperature on liquid product distribution for syringol over Pt/SiO₂-Al₂O₃

Run#	03-11-91		
Tested Material	XZ-0.3Pt/SiO ₂ -Al ₂ O ₃ -28 + Quartz		
Feed Composition	10 wt% syringol + 90 wt% toluene		
Space Velocity	1 gram toluene/hour-gram-catalyst		
Liquid Recovery (%)	92		
Time on Stream (hr)	2.0	4.0	6.0
Pressure (psig)	200	200	200
Temperature (°C)	400	450	400
Component	Mole Percent		
Cyclohexane	10.6	0.0	0.0
Methylcyclohexane	15.4	0.0	0.0
Benzene	6.7	20.0	3.8
Xylene	31.5	26.5	4.9
Mesitylene	10.5	7.7	13.0
Phenol	12.2	23.0	3.3
Xylenol	6.9	15.0	1.4
2-Methoxy-4-methylphenol	0.0	7.8	1.5
Syringol	6.1	0.0	72.1

Table A-20. Liquid product distribution for 4-propylphenol over Ni/SiO₂-Al₂O₃

Run#	09-05-92
Tested Material	15Ni/SiO ₂ -Al ₂ O ₃
Feed Composition	10 wt% 4-propylphenol + 90 wt% hexane
Space Velocity	1 gram 4-propylphenol/hour-gram-catalyst
Liquid Recovery (%)	65
Time on Stream (hr)	3
Pressure (psig)	500
Temperature (°C)	350
Component	Mole Percent
Cyclohexane	0.6
Methylcyclohexane	0.9
Trimethylcyclohexane (1)	0.8
Trimethylcyclohexane (2)	0.5
Ethylcyclohexane	0.8
Benzene	0.6
Propylcyclohexane	9.4
Propylbenzene	12.4
Dipropylbenzene (1)	1.1
Phenol	15.1
2,6-Dipropylphenol	0.9
2-Propylphenol	5.9
4-Propylphenol	45.8
Dipropylphenol (1)	2.1
Dipropylphenol (2)	2.1
Dipropylphenol (3)	0.8

Table A-21. Comparison of selectivity and activity of the platinum catalysts and the nickel catalyst

Run#	10-25-90	06-18-90	09-05-92
Tested Material	0.3Pt/SiO ₂ - Al ₂ O ₃	0.3Pt/AlPO ₄ - Al ₂ O ₃	15Ni/SiO ₂ - Al ₂ O ₃
Feed Composition	10 wt% 4-propylphenol + 90 wt% hexane		
Space Velocity	1 gram 4-propylphenol/hour-gram-catalyst		
Liquid Recovery (%)	87	88	65
Time on Stream (hr)	3	3	3
Pressure (psig)	500	500	500
Temperature (°C)	350	350	350
Component	Mole Percent		
Cyclohexane	5.9	7.5	0.6
Methylcyclohexane	6.0	3.9	0.9
Trimethylcyclohexane (1)	4.0	0.0	0.8
Trimethylcyclohexane (2)	3.8	0.0	0.5
Ethylcyclohexane	4.9	0.0	0.8
Ethylmethylcyclohexane (1)	6.7	0.0	0.0
Benzene	15.3	3.5	0.6
Ethylmethylcyclohexane (2)	4.6	0.0	0.0
Propylcyclohexane	40.0	31.7	9.4
Propylbenzene	4.8	16.3	12.4
Dipropylbenzene (1)	0.0	2.5	1.1
Phenol	0.0	4.9	15.1
2,6-Dipropylphenol	0.0	0.0	0.9
2-Propylphenol	0.0	5.4	5.9
4-Propylphenol	4.0	13.3	45.8
Dipropylphenol (1)	0.0	3.6	2.1
Dipropylphenol (2)	0.0	3.8	2.1
Dipropylphenol (3)	0.0	3.6	0.8

Table A-22. Liquid product distribution for mixture of 4-propylguaiacol and syringol over Pt/SiO₂-Al₂O₃

Run#	04-23-93		
Tested Material	XZ-0.3Pt/SiO ₂ -Al ₂ O ₃ -28 + Quartz		
Feed Composition	5 wt% 4-PG + 5 wt% SYR + 90 wt% toluene		
Space Velocity	1 gram toluene/hour-gram-catalyst		
Liquid Recovery (%)	92		
Time on Stream (hr)	2.5	3.0	3.5
Pressure (psig)	300	300	300
Temperature (°C)	450	450	450
Component	Mole Percent		
Hexane	3.7	2.7	3.0
Cyclohexane	3.0	2.4	2.4
Methylcyclohexane	3.3	1.8	1.8
Dimethylcyclohexane	14.6	7.3	10.8
Benzene	10.9	10.3	11.0
Xylene(1)	12.0	11.7	9.5
Xylene(2)	3.7	3.6	3.2
Xylene(3)	3.5	3.2	2.7
Propylbenzene	3.1	3.0	2.9
Phenol	21.0	26.4	24.6
Cresol	15.3	20.1	18.4
2-Methoxyphenol	1.9	1.0	2.0
2-Methoxy-4-methylphenol	1.6	2.5	2.0
Propylcatacol	1.4	1.9	2.1
Syringol	1.0	2.1	3.6

Table A-23. Comparison of PE Sigma-3B GC TCD relative response weight factors to references

Compound	PE SIGMA-3B Weight Factors (Zhao, 1991)	HP-5840A Weight Factors (Erickson, 1990)	Weight Factors (Dietz, 1967)
Hexane	0.70	0.70	0.7
Heptane	0.70	0.70	0.7
Cyclohexane	0.81	0.73	0.735
Methylcyclohexane	0.89	0.82	0.82
Ethylcyclohexane	0.86	0.82	0.775
Benzene	0.78	0.78	0.78
Propylcyclohexane	0.92	0.81	0.8
Toluene	0.80	0.76	0.8
Ethylbenzene	0.85	0.75	0.818
Propylbenzene	0.83	0.73	0.826
Dipropylbenzene	0.84(?)	----	----
Phenol	0.87	0.58	----
2,6-Dipropylphenol	0.96(?)	----	----
2-Propylphenol	0.93	0.69	----
4-Propylphenol	0.95	0.63	----
Dipropylphenol (1)	0.97(?)	----	----
Dipropylphenol (2)	0.97(?)	----	----
Dipropylphenol (3)	0.96(?)	----	----
Diisopropylphenol	0.82	----	----
3-Methyl,4-isopropylphenol	0.74(?)	----	----
Xylene	0.82	----	----
Mesitylene	0.83	----	----
m-Cresol	0.88	----	----
p-Cresol	0.87	----	----
4-Propylguaiacol	0.95	----	----
Syringol	0.94	----	----
2-Methoxy,4-methylphenol	0.95(?)	----	----
Xylenol	0.88(?)	----	----
Propylcatacol	0.94(?)		

Table A-24. Retention times (PE Sigma-3B)

(4-Propylphenol as a reactant)

<u>Name of compound</u>	<u>Retention time (min.)</u>
Cyclohexane	1.81
Methylcyclohexane	2.75
Ethylcyclohexane	3.82
Benzene	4.59
Propylcyclohexane	5.13
Toluene	5.84
Ethylbenzene	6.67
Propylbenzene	7.31
Dipropylbenzene	8.91
Phenol	13.92
2,6-Dipropylphenol	15.48
2-Propylphenol	16.37
4-Propylphenol	20.17
Dipropylphenol (1)	22.83
Dipropylphenol (2)	24.13
Dipropylphenol (3)	30.15

Table A-25. Retention times (PE Sigma-3B)

(4-Propylguaicol as a reactant)

<u>Name of compound</u>	<u>Retention time (min.)</u>
Hexane	1.44
Cyclohexane	1.67
Methylcyclohexane	2.11
Dimethylcyclohexane	2.32
Benzene	4.43
Xylene	6.70
Propylbenzene	8.00
Phenol	14.14
Methylphenol	15.67
4-Propylguaicol	16.77
2-Methoxyphenol	17.92
Propylcatacol	19.95
4-Propylphenol	20.74

Table A-26. Retention times (PE Sigma-3B)

(Syringol as a reactant)

<u>Name of compound</u>	<u>Retention time (min.)</u>
Cyclohexane	1.6
Methylcyclohexane	2.1
Benzene	4.4
Xylene	6.7
Mesitylene	12.9
Phenol	14.1
Xylenol	15.8
2-methoxy,4-methylphenol	17.9
Syringol	21.9

Table A-27. PE Sigma-3B GC Operation conditions

Initial temperature (°C)	60
Final temperature (°C)	220
Initial time (minutes)	3
Final time (minutes)	30-60
Rate (°C/minute)	30
Carrier gas flowrate (cc/min.)	30
Injection temperature (°C)	235
TCD temperature (°C)	250
Chart speed (in/min.)	0.5
Attenuation	4

Table A-28. HP-5890 GC Run parameters.

Initial Temp.(°C)	Initial Time (min)	Rate (°C/min)	Final Temp.(°C)	Final Time (min)	Total Time(min)
60	3.0	30.0	220	30.0	40.33
		20.0	220	30.0	44.00
		10.0	220	30.0	55.00
Injection Port (°C)		235			
Transfer Line (°C)		280			

Table A-29. MSD Acquisition parameters

Start Time (Min)	Low Mass	High Mass	Scans Per Second
1.0	50.0	500.0	0.86
10.0	50.0	500.0	0.86

APPENDIX B
LIST OF EQUATIONS

Equations B-1. For calculating the relative weight response factor (RRF)

Equation 1:

$$\text{Weight Factor} = \frac{\text{Mole Weight}}{\text{Thermal Response}}$$

Equation 2:

$$\text{Thermal Response} = \text{Relating Response Factor} * 100$$

Equation 3:

$$\text{Relating Response Factor} = \frac{\left[\frac{\text{Component peak Area}}{\text{Component Mole Percent}} \right]}{\left[\frac{\text{Reference Peak Area}}{\text{Reference Mole Percent}} \right]}$$

Equation 4 :

$$\text{Mole\% of Product (i)} = \frac{N(i)}{\sum_{i=1}^n N(i)}$$

Equation 5:

$$N(i) = \frac{\text{Peak Area of Product (i)} * \text{Weight Factor of Product (i)}}{\text{Mole Weight of Product (i)}}$$

Equations B-2. For calculating the mean dimension of crystallites (particle diameter)

The mean dimension of the crystallites (particle diameter), D , composing a powder is related to the pure x-ray diffraction broadening, β , by the equation,

$$D = \frac{K \lambda}{\beta \cos \theta}$$

$$\beta^2 = B^2 - b^2$$

- D: mean dimension of the crystallites or particle diameter (Å).
- K: a constant related to the crystallite shape (taken as 0.9).
- λ : wavelength of x-ray diffraction peak (1.5418 Å for Cu K_{α}).
- β : pure breadth of a powder reflection (the width at half-maximum intensity of the reflection).
- θ : glancing angle of the x-ray diffraction peak.
- B: experimentally observed breadth of a powder reflection
- b: experimentally observed breadth of a material with a crystallite size well in excess of 1000 Å under similar geometrical conditions

The b is 0.3 for this study. This was obtained with pure platinum, assuming a platinum particle size in excess of 1000 Å.

APPENDIX C
FIGURES

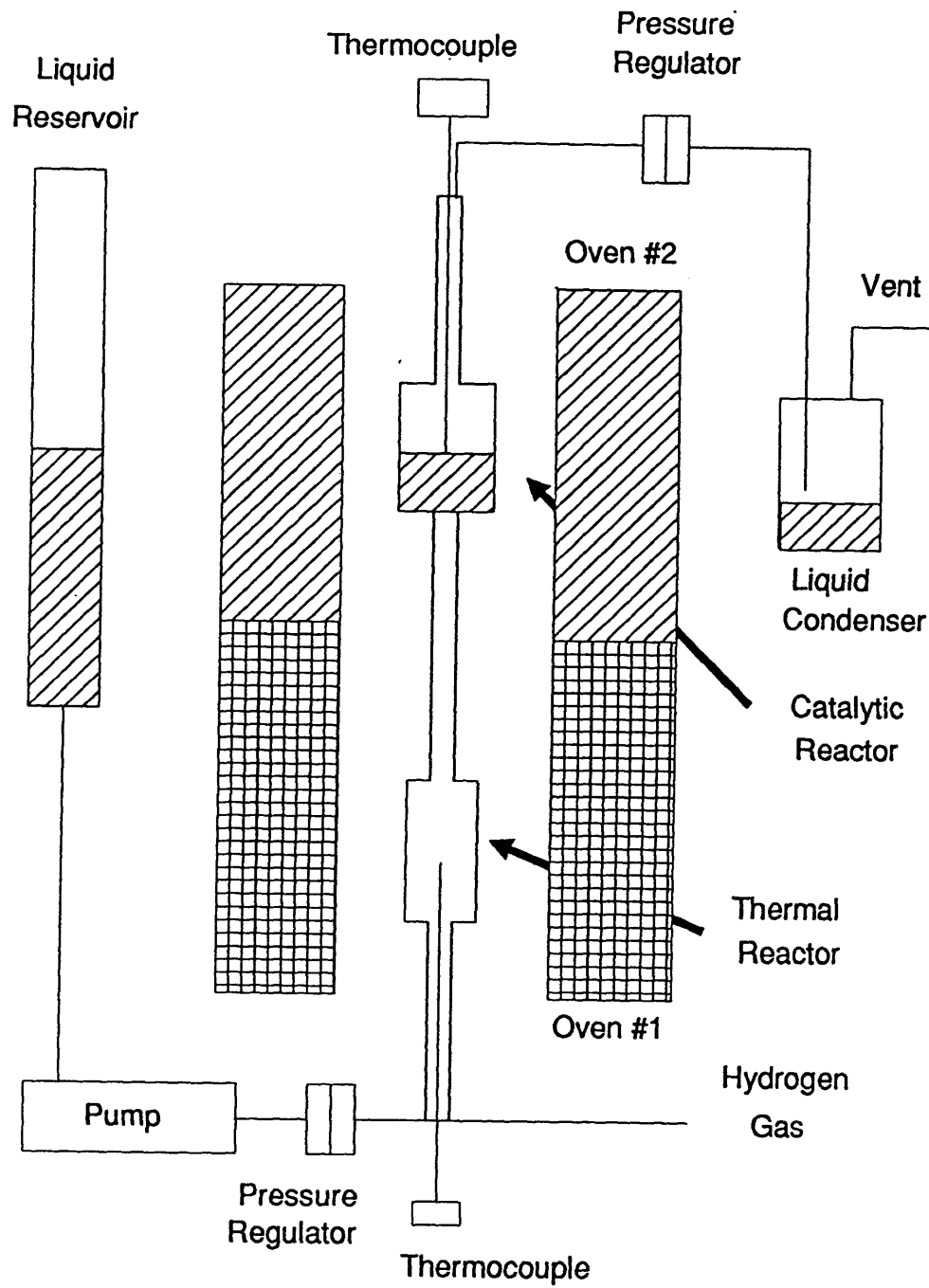
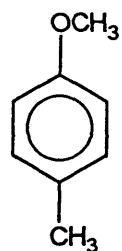
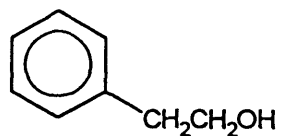


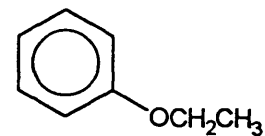
Figure C-1. Schematic of two-stage catalytic reactor system.



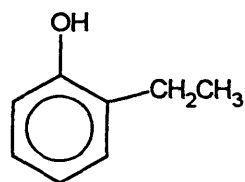
Benzyl Methyl Ether or
Methoxymethylbenzene



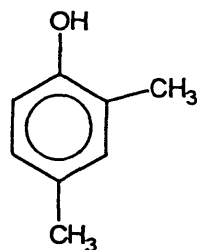
Phenethyl Alcohol



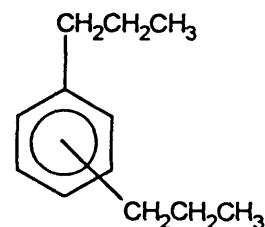
Phenetole



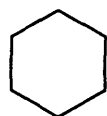
Phlorol



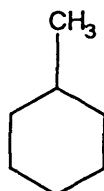
Xylenol



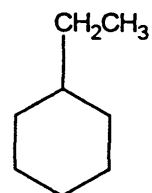
Dipropylbenzene



Cyclohexane

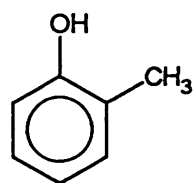


Methylcyclohexane

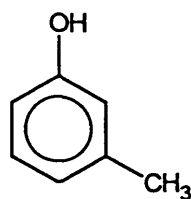


Ethylcyclohexane

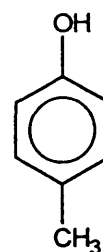
Figure C-2. Structural formulae of the products (1).



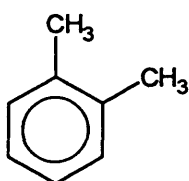
o-Cresol



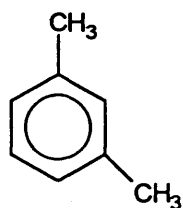
m-Cresol



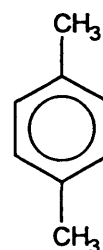
p-Cresol



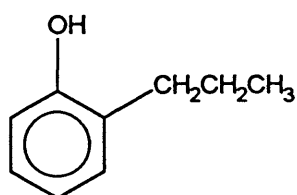
o-Xylene



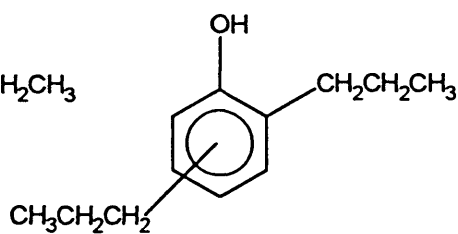
m-Xylene



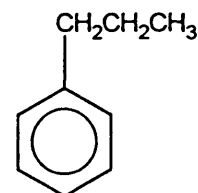
p-Xylene



2-Propylphenol



Dipropylphenol



Propylbenzene

Figure C-3. Structural formulae of the products (2).

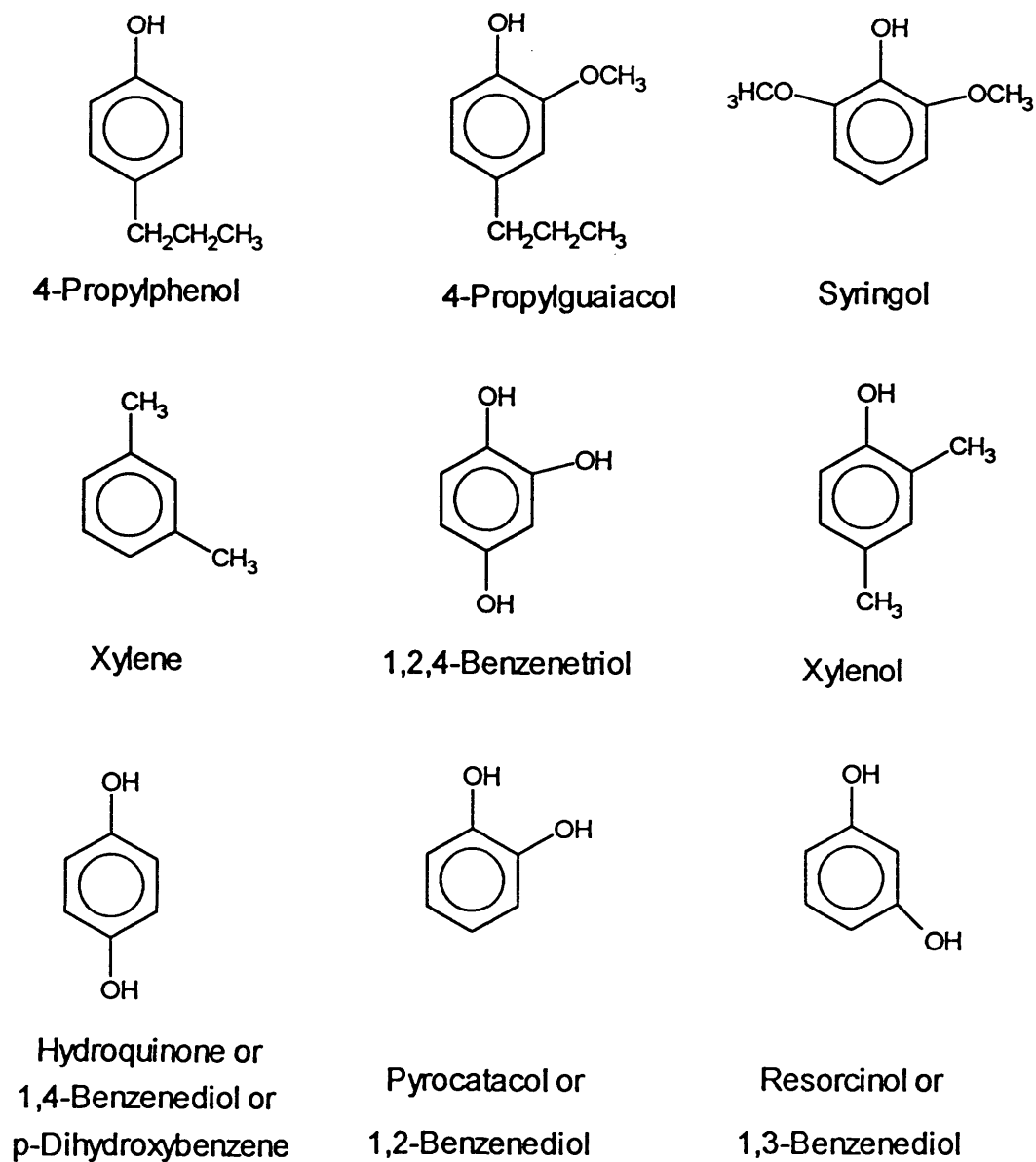


Figure C-4. Structural formulae of the products (3).

APPENDIX D

Preparation and Characterization of More Realistic Lignin Feedstock

Potential Solvents for Lignin Studies

Since the solubility of the raw lignin in hexane and toluene were very low, a better solvent for the catalyst/lignin system than hexane or toluene was desired. The solvent candidate must exhibit good solubility for the reactants, and show little reactivity over the catalyst. The solvent and its potential reaction products must not interfere or overlap with the analysis of reaction products of the lignin model compounds or the low molecular weight lignin feedstocks.

A search was made for a satisfactory solvent for lignin by selecting solvent properties such as dipole moment, dielectric constant and solubility parameter to study the solubility of ROSL and SEL. The solvents were studied and their properties are listed in **Tables D-1** and **D-2** (*Riddick et al, 1986*).

The dipole moment (μ) is an important factor for studying the structure of compounds. Also many physical properties such as solubility can be quantitatively interpreted more readily if the dipole moments are known. The unit of dipole moment is the Debye. If the solubility of a solute is known in a solvent of known dielectric constant (ϵ), its solubility in other solvents can often be roughly estimated from their dielectric constants. The solubility parameter (δ) is a physical constant used to describe the relationship between the physical properties of the solvent and its effectiveness in dissolving specific

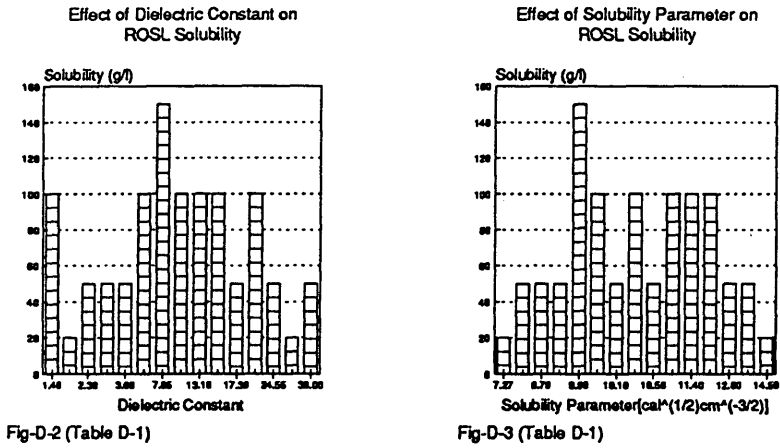
solutes.

Tetrahydrofuran gives the highest solubility for ROSL; it is over 15 wt%. The solubility of ROSL in 2,6-xyleneol, m-cresol, benzylalcohol, cyclohexanol, 2-heptanone or acetone was over 5 wt% and less than 10 wt%. ROSL was poorly dissolved by hexane, toluene, ethylbenzene, phenylether, ethanol, acetophenone or γ -butyrolacetone, giving a solubility less than 5 wt%.

The solubility of SEL in toluene, acetone, tetrahydrofuran, and water was less than 5 wt%. The results are shown in **Table D-2**.

The solubility of ROSL and SEL was determined by adding small amounts of the solute to the solvent until the solvent would not dissolve any more at room temperature. The polarity of the solvent apparently influences the solubility of ROSL (**Figure D-1**).

Solvents with dipole moment between 1.5 to 2.7 Debyes are better solvents for raw ROSL. The dipole moment of 1.75 Debyes gave the highest solubility. In general, ROSL has a good solubility in solvents with dielectric constant between 4.90 and 20.90, except in acetophenone whose dielectric constant is 17.39. ROSL has a good solubility with solubility parameter about $10 \text{ cal}^{1/2}\text{cm}^{-3/2}$. SEL had low solubility in general, and the effect of dipole moment, dielectric constant and solubility parameter could not be determined.



Effect of Dipole Moment on ROSL Solubility

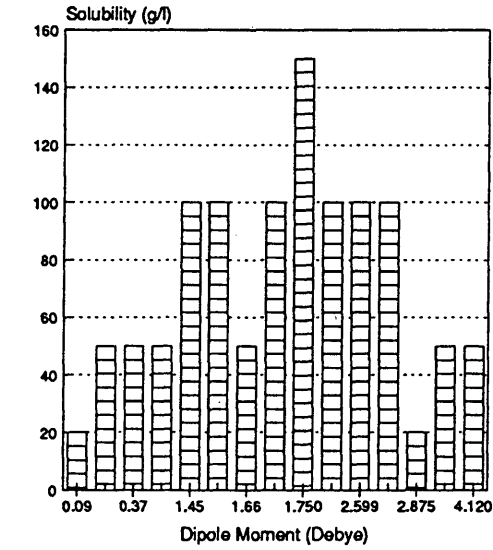


Fig-D-1 (Table D-1)

Figure D-1. Effect of solvent properties on ROSL solubility.

Soxhlet Extraction of Repap Organosolve Lignin (ROSL)

A Soxhlet extractor was employed, in order to get a low molecular weight lignin feedstock for the catalyst studied. The soxhlet extractor was heated up to the boiling point. Ceramic chips were added to the solvents to prevent bumping. The ROSL was extracted in separate experiments by tetrahydrofuran, γ -butyrolacetone, acetone, 2-heptanone, toluene and acetophenone. The results are shown in **Table D-3**.

The initial weight of the ROSL sample for each experiment was 10 grams. The solvent volume for each experiment was 80, 100 or 200 ml. The total experiment time was 20 hours for each sample. The low boiling point solvents gave good extraction results as shown by the fact that the final weight of the ROSL was less than 1 gram. Over 90% of the ROSL was extracted by tetrahydrofuran, γ -butyrolacetone and acetone. The extracted production and the ROSL residue from each solvent were characterized by FTIR and NMR as discussed below.

Table D-1. Properties of the solvents and the solubility of ROSL

Solvent	μ , dipole moment (Debye)	ϵ , dielectric constant (Dimensionless)	δ , solubility parameter ((cal ^{1/2} cm ^{-3/2})	Solubility	
				g/l	wt%
Hexane	0.09	1.89	7.27	<20	<2
Toluene	0.31	2.38	8.91	<50	<5
Ethylbenzene	0.37	2.40	8.79	<50	<5
Phenylether	1.16	3.60	10.10	<50	<5
2,6-Xylenol	1.45	4.90	10.50	>50 (<100)	>5 (<10)
m-Cresol	1.48	1.48	10.80	>50 (<100)	>5 (<10)
Ethanol	1.66	24.55	12.78	>20 (<50)	>2 (<5)
Benzylalcohol	1.66	13.10	12.10	>50 (<100)	>5 (<10)
Tetrahydrofuran	1.75	7.85	9.90	>150	>15
Cyclohexanol	1.86	15.00	11.40	>50 (<100)	>5 (<10)
2-Heptanone	2.59	11.98	8.50	>50 (<100)	>5 (<10)
Acetone	2.69	20.90	10.00	>50 (<100)	>5 (<10)
Methanol	2.87	32.66	14.50	<20	<2
Acetophenone	2.95	17.39	10.58	<50	<5
γ -Butyrolactone	4.12	39.00	12.60	<50	<5

Table D-2. Properties of the solvents and the solubility of Repap SEL

Solvent	μ , dipole moment (Debye)	ϵ , dielectric constant (Dimensionless)	δ , solubility parameter ($\text{cal}^{1/2}\text{cm}^{-3/2}$)	Solubility (25°C)	
				g/l	wt%
Toluene	0.31	2.30	8.91	<50	<5
Tetrahydrofuran	1.75	7.58	9.90	<50	<5
Water	1.82	80.16	23.53	<50	<5
Acetone	2.69	20.90	10.00	<50	<5

Table D-3. Results of ROSL Soxhlet extraction by different solvents

Solvent	B.P. (°C)	Initial weight (g)	Final weight (g)	Volume of sol- vent used (ml)	Extraction time (hr)
Tetrahydrofuran	66.0	10	0.10	100	20
γ -butyrolactone	91.0	10	0.34	100	20
Acetone	56.1	10	0.46	200	20
2-heptanone	151.1	10	3.67	80	20
Toluene	110.6	10	9.86	100	20
Acetophenone	202.0	10	9.93	100	20

Characterization of SEL, ROSL and ROSL Extractions by FTIR

The SEL, ROSL, ROSL solvent extracts and residue were characterized by FTIR. The spectra of untreated SEL and ROSL, and the solvent extracted ROSL fractions are shown in **Figures D-2, D-3, D-4, D-5 and D-6**.

Assignments of the absorption bands listed in **Table D-4** were based on information obtained from work of others (*Owen and Thomas, 1989; Sarkanen and Ludwing, 1971; Glasser, 1988; Thring, 1991*).

The raw solid SEL and ROSL lignin samples were prepared as KBr disks. The two spectra (**Figures D-2 and D-3**) are nearly identical with the exception of a lower carbonyl (C=O) stretch at 1705-1706 cm^{-1} . The smaller magnitude of the carbonyl function in SEL relative to ROSL may reflect the different methods in which the raw lignin was obtained.

The raw solid SEL and ROSL lignin samples were obtained from the National Renewable Energy Laboratory (NREL), but all characteristics such as experimental conditions, procedure, carbon, hydrogen, oxygen, methyl group and hydroxyl group etc. content of these two lignins were unknown.

The raw ROSL lignin was extracted with toluene, THF, acetone, and 2-heptanone solvents having dipole moments of 0.31, 1.75, 2.69, and 2.97 Debyes respectively. FTIR spectra of the undissolved ROSL residue extracted by 2-heptanone, acetone and toluene are shown in **Figure D-4**. For the most

part, the FTIR spectra of the extracted ROSL residues closely resemble that of the raw ROSL lignin.

The one exception is the acetone extracted residue which shows a significant increase in intensity at approximately 1604 and a decrease in intensity at approximately 1706 cm^{-1} . The increase in intensity at 1604 cm^{-1} suggests a larger aromatic C-O contribution to the residue's spectrum. The decrease in intensity at 1706 cm^{-1} suggests a small C=O carbonyl and ketone contribution to the residue's spectrum.

The reason for these changes remains unclear. The other exception is that the acetone and toluene extracted residues both show a small peak at approximately 760 cm^{-1} . These small peaks suggest that =CH and aromatic C-H out-of-plane deformations exist. This may be caused by the solvent during the extraction.

The low boiling point solvent ROSL extracts were selected. The solvent was evaporated using a rotary evaporator. The extracts were analyzed by FTIR, and the spectra are shown in **Figure D-5**. The ROSL extract by acetone in **Figure D-5-a** has a shoulder at approximately 2840 cm^{-1} the same as raw lignin, compared to no shoulder in the ROSL extracted by THF **Figure D-5-b**. This suggests that the population of symmetric C-H bonds in methyl and methylene groups was decreased for ROSL extracted by THF, compared to raw ROSL.

In **Figure D-5-a** and **b**, the peaks are at approximately 1706 cm^{-1} , but the intensities were different. Compared to raw ROSL, intensities of the extracts at 1706 cm^{-1} were increased. This suggests that the relatively large number of carbonyl groups contribute to the extract's spectrum.

Since the residues and extracts may be contaminated by the solvent, in order to study the spectrum of the residues and extracts, pure solvents were characterized by FTIR (**Figure D-6**) as a reference.

Overall the spectra of the extract and the residue are very similar to that of the raw lignin. This suggests that the extracted portion of the lignin contains identical functionality of the raw lignin.

Table D-4. Assignments of absorption bands in the infrared spectra of lignins

Wavenumber (cm ⁻¹)	Assignment
3437-3427	O-H stretching (phenols)
2940-2930	C-H stretching in methyl and methylene groups (asymmetric)
2850-2840	C-H stretching in methyl and methylene groups (symmetric)
1730-1700	C=O stretching (carbonyl stretching-unconjugated ketone and carbonyl groups)
1610-1590	aromatic skeletal vibration; intensity proportional to aromatic C-O stretching mode
1510-1500	aromatic skeletal vibrations coupled with C-H in-plane deformation
1460-1450	C-H deformations (asymmetric) in methyl, methylene, and methoxyl group
1430-1420	aromatic skeletal vibrations coupled with C-H in-plane deformations; affected by nature of ring substituents
1330-1325	syringol ring breathing with C-O stretching
1273-1267	guaiacol ring breathing with C-O stretching
1222-1215	syringol and guaiacol ring breathing with C-O stretching
1120-1110	aromatic C-H in-plane deformation, syringol type
970-950	=CH out-of-plane deformation (trans) aromatic C-H out-of-plane deformations
860-855	same as above
835-815	same as above
770-750	same as above

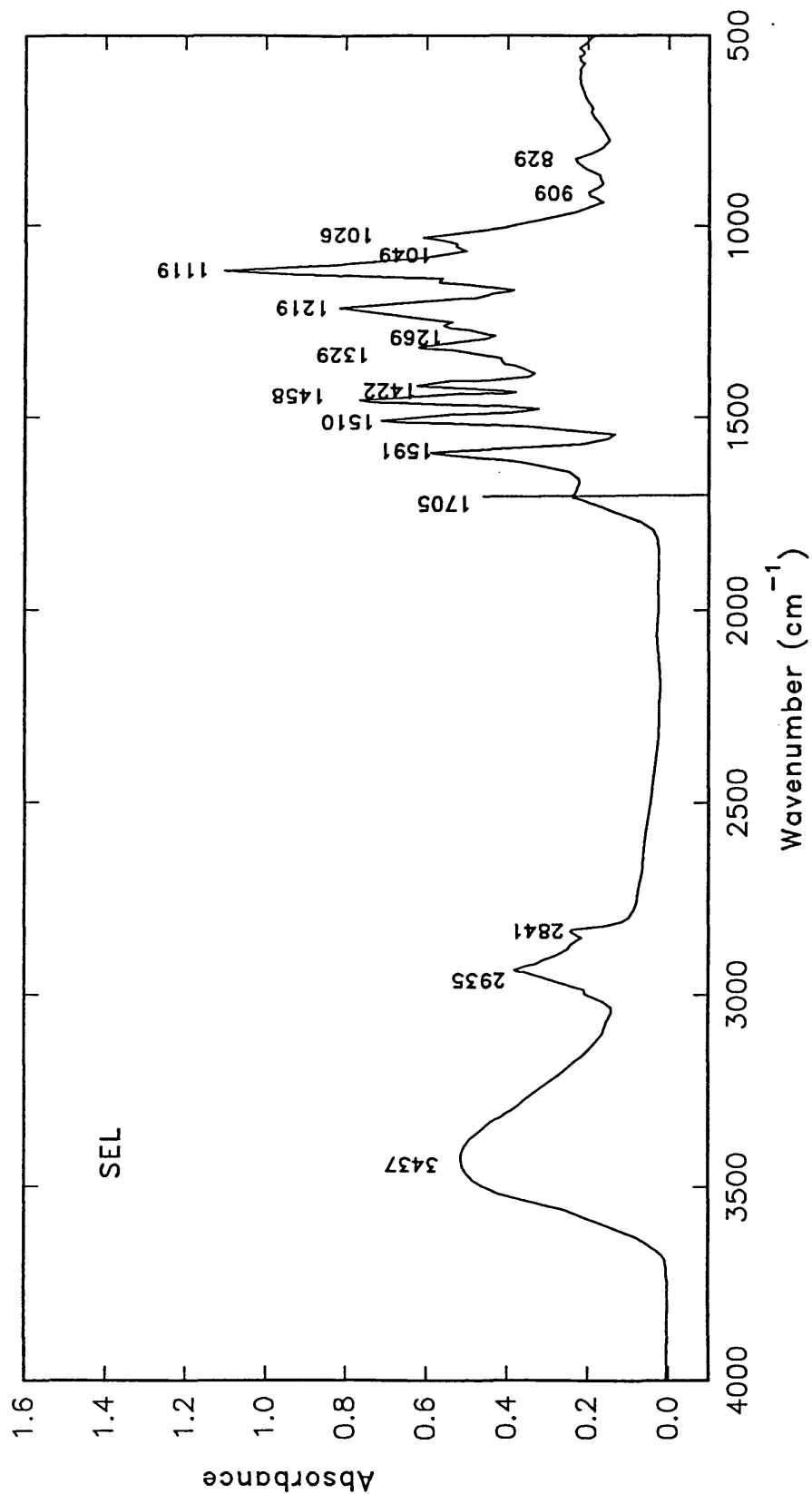


Figure D-2. IR-spectra of the steam exploded lignin.

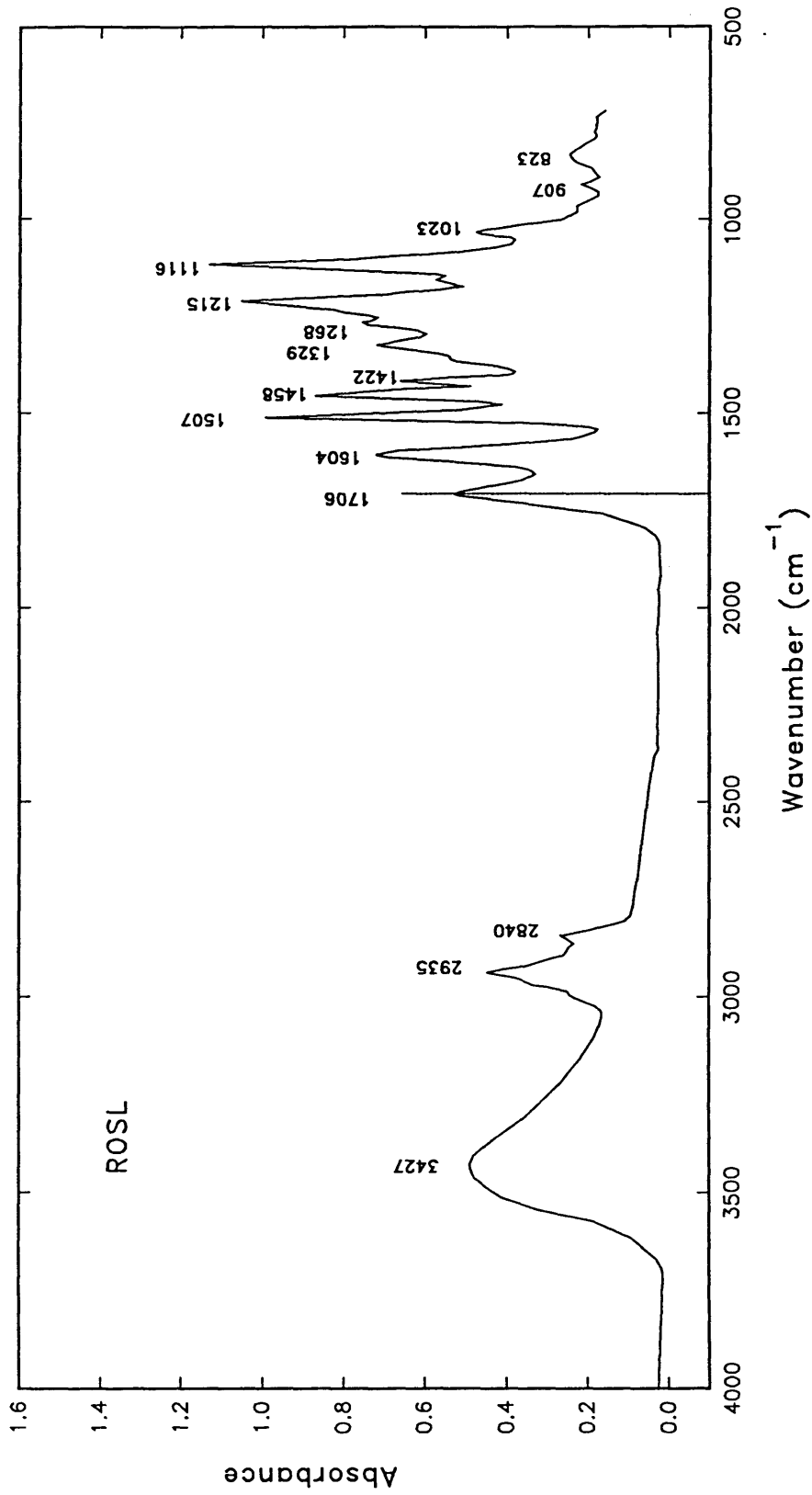


Figure D-3. IR-spectra of the repap organosolve lignin.

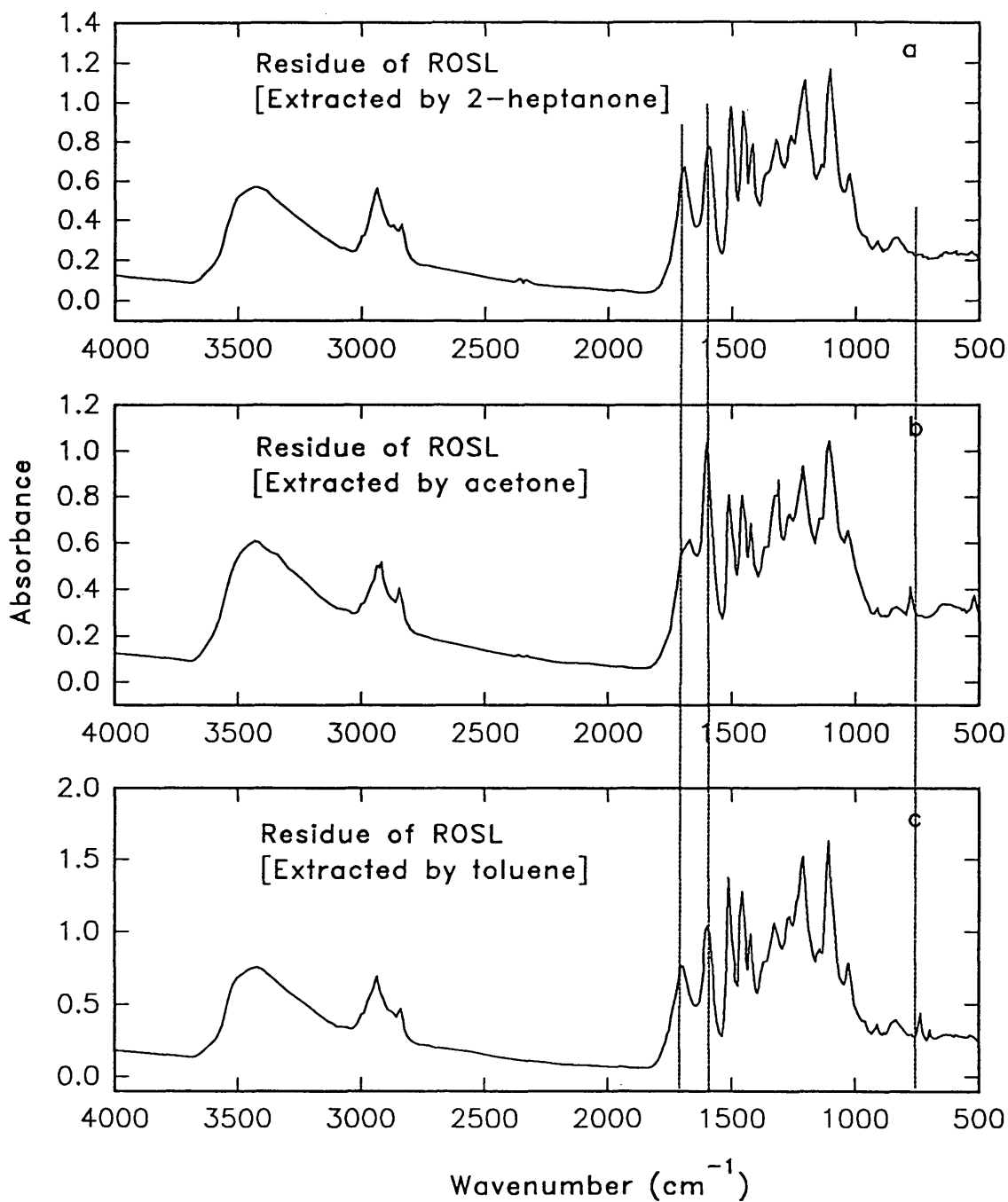


Figure D-4. IR-spectra of the repap organosolve lignin residue after extraction by (a) 2-heptanone, (b) acetone, and (c) toluene.

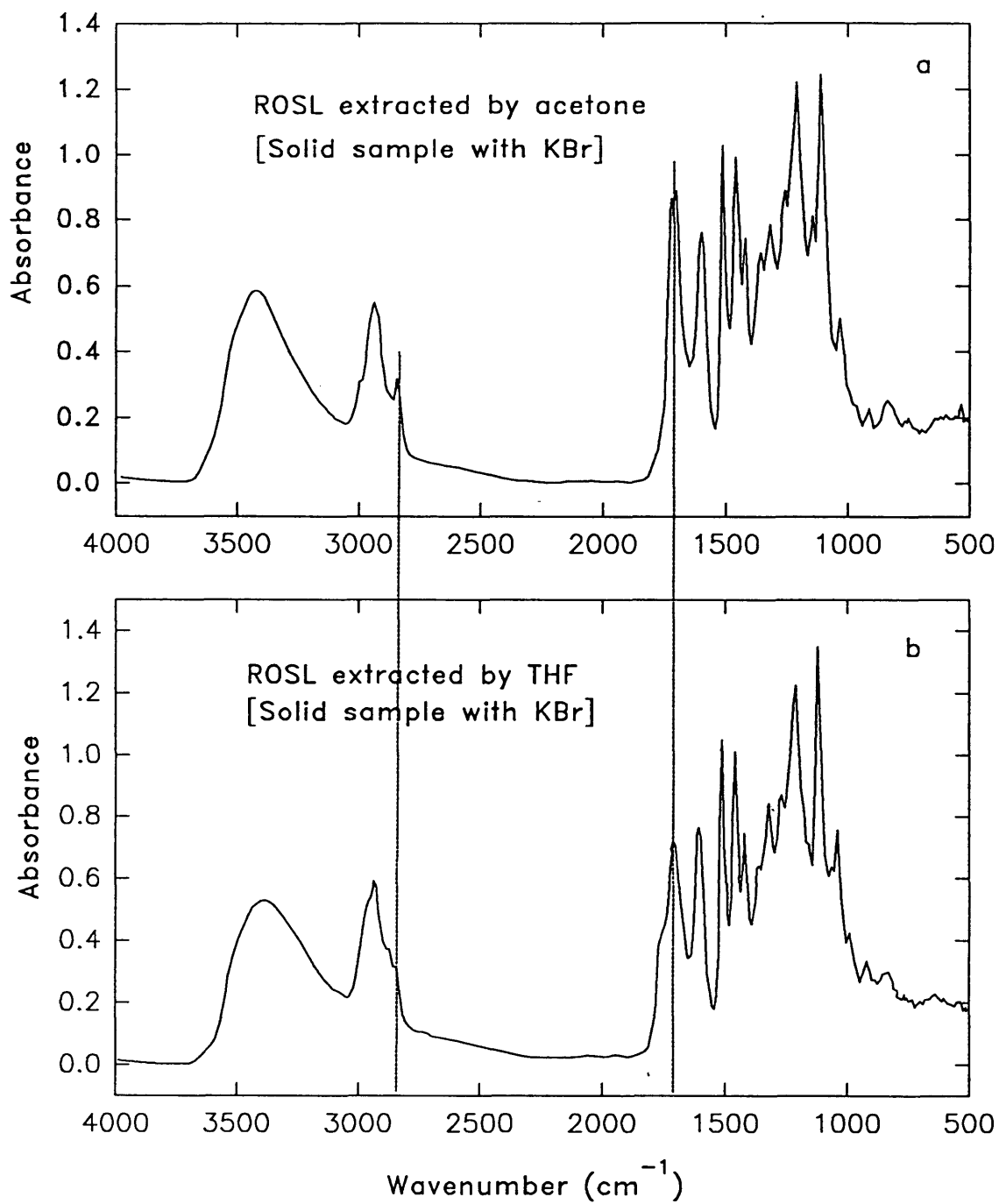


Figure D-5. IR-spectra of the solid repap organosolve lignin (a) extracted by acetone with acetone then evaporated, and (b) extracted by THF with THF then evaporated.

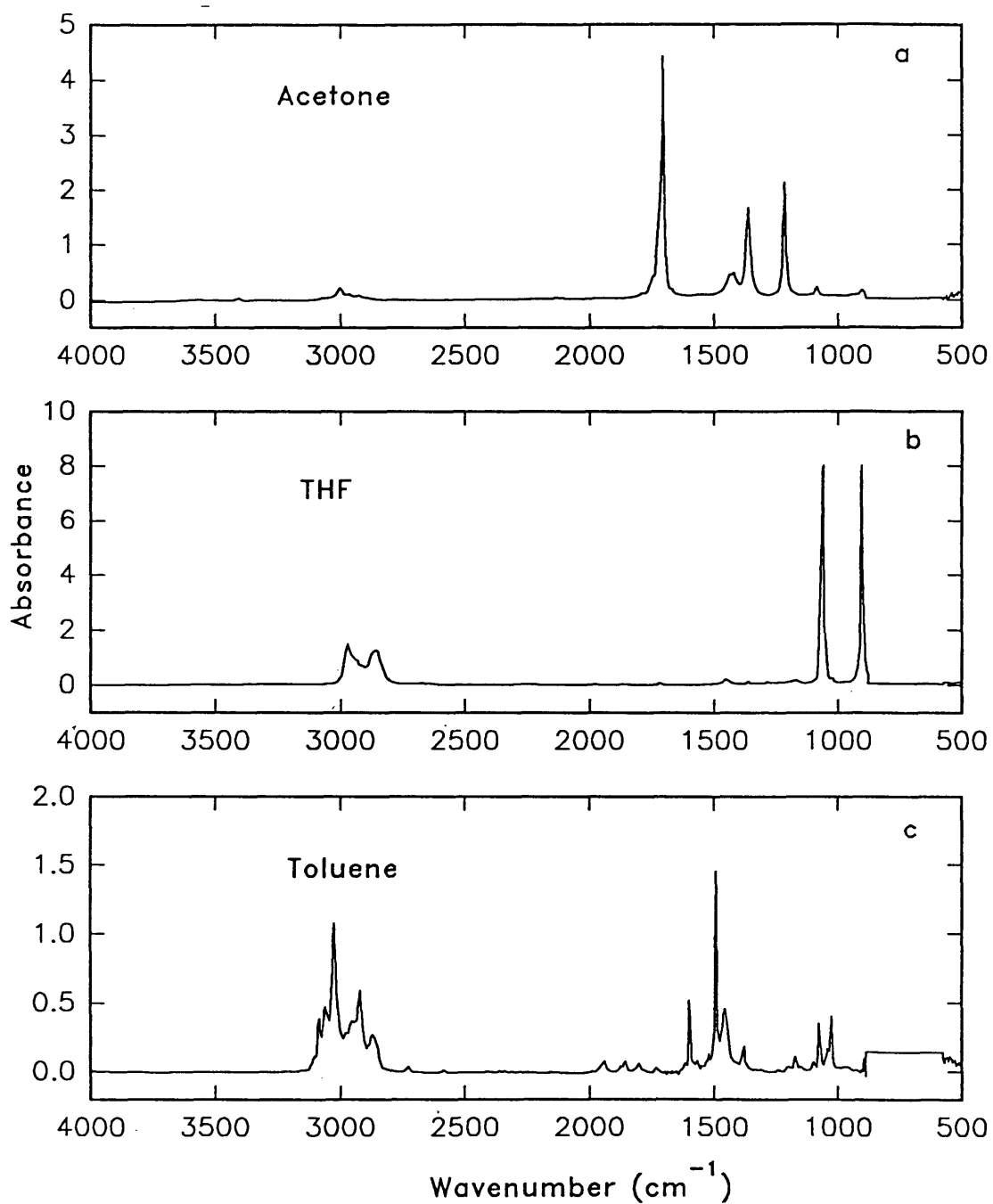


Figure D-6. IR-spectra of (a) acetone, (b) THF, and (c) toluene.